Doctoral Dissertation

Effects of pore void saturation degree on nondestructive tests for durability assessment of concrete structures

(コンクリート構造物の耐久性評価のための非破壊試験に及ぼす空隙中の飽和度の影響)

by

Uwazuruonye Raphael Nnodim

A dissertation submitted to

Graduate School of Urban Innovation
Yokohama National University, Japan

In partial fulfillment of the requirements for the degree of

Doctor of Philosophy in Engineering

supervised by

Akira Hosoda

Professor, Faculty of Urban Innovation

September 2020

The academic adviser and dissertation committee members hereby accept and recommend to the Graduate School of Urban Innovation for acceptance, the dissertation entitled:

Effects of pore void saturation degree on nondestructive tests for durability assessment of concrete structures

submitted by **Uwazuruonye Raphael Nnodim** in partial fulfilment of the requirements for the degree of **Doctor of Philosophy in Engineering**

in **Urban Innovation (Concrete Engineering)**

Academic Adviser

Professor Akira HOSODA

Examining Committee:

Professor Koichi MAEKAWA

Professor Kimitoshi HAYANO

Associate Prof. Chikako FUJIYAMA

Associate Prof. Sai EI (Ying CUI)

Abstract

This research aims to clarify the effects of pore void saturation degree on nondestructive test (NDT) assessment for durability of in-situ concrete structures. And this research also aims to propose a threshold for the saturation degree of pore voids before water absorption NDT assessment is conducted utilizing Surface Water Absorption Test (SWAT).

Percentage saturation degree of permeable pore voids (PSD) that is directly related to the volume of pore voids of concrete is proposed as a new form of measuring moisture content of concrete. And the effects of PSD on surface water absorption and electrical resistivity are investigated. Ordinary Portland cement concrete samples (w/c ratios: 0.40, 0.50 and 0.60; age at the beginning of tests: 510 days) were preconditioned to moisture equilibrium and tested at several PSDs to study the combined influence of pore void saturation degree and pore size distribution on surface water absorption. All samples exhibited the same trend in the relationship between surface water absorption rate and PSD. Between 26% - 45% PSD, no apparent effect of PSD (showed the existence of plateau) on the rate of surface water absorption was observed. It led to the conclusion that 45% of PSD should be the upper threshold for appropriate evaluation of covercrete quality by Surface Water Absorption Test (SWAT). Investigation using numerical simulation by DuCOM showed a similar trend and further revealed that the plateau depends on empty capillary pore diameters between 10^{-8} m (10 nm) and 10^{-7} m (100 nm). The range of plateau depends on the volume of capillary pore diameters in this range. Meanwhile, the investigation of the relationship between PSD and electrical resistivity showed that resistivity increases with a decrease in PSD but by no means linear.

To verify the application of the threshold value and the existence of plateau on in-situ concretes, further investigations were conducted on concretes produced with ordinary Portland cement (w/c ratios: 0.40, 0.50 and 0.60; age at the beginning of tests: 90 days) and ground granulated blast furnace slag cement- JIS type B slag cement, (w/c

ratio: 0.50; age at the beginning of tests: 90 days). The influences of different environmental exposures on pore void saturation degrees and internal moisture gradients were simulated by exposing the concrete blocks to 60%, 80% and 90% R.H. for different durations. Many kinds of PSDs (measured by three different moisture meters, HI-100, HI-520-2 and CMEX II) and internal moisture gradients for the different kinds of concretes were obtained. Relationships between PSDs and surface water absorption rates were investigated to verify the proposed upper threshold and to establish the appropriate surface moisture meter for SWAT. The results showed plateau zone in in-situ concretes. Also, the proposed upper threshold (45% PSD) was found to be appropriate for the initial moisture content of concrete before SWAT. Only HI-100 surface moisture meter is effective in detecting PSDs of in-situ concrete.

Moreover, the correlation between the SWAT (tested within the proposed threshold PSD) and JSCE sorptivity test was evaluated. Concretes made of ordinary Portland cement (w/c ratios: 0.40, 0.50 and 0.60; age at the beginning of tests: 60 days), ground granulated blast furnace slag cement- JIS type B slag cement, (w/c ratio: 0.50; age at the beginning of tests: 60 days) and JIS type II fly as 20% by weight of OPC replacing fine aggregate (w/b ratio: 0.41; age at the beginning of tests: 60 days) were utilized. A new SWAT index (coefficient of surface water absorption-*CSWA*) was introduced and the result was found to be correlated with JSCE sorptivity index. This validates the use of SWAT as a good device both for quality control (in durability design) and for in-situ covercrete evaluation (in durability assessment) to water penetration.

Meanwhile, the influence of hysteresis on the resistance to surface water absorption, air permeability and surface moisture contents were investigated. Concretes were preconditioned to moisture equilibrium through desorption and absorption processes and tested at several PSDs. The results revealed that hysteresis does not influence the rate of surface water absorption (p_{600}) by SWAT, air permeability coefficient (kT) by double chamber air permeability test and the surface moisture contents by three different moisture meters.

Table of Contents

List of Tables

List of Figures

Acknowledgement

All Glory be to God the Father, God the Son and God the Holy Spirit- the Trinity, for favouring me with countless blessings, good health and the persevering grace to get thus far. All honour be to the Blessed Virgin Mary, the Mother of God for Her constant intercession.

I would like to express my immense gratitude to my academic adviser, Professor Akira Hosoda, for his supports, patience and kind guidance throughout the programme. My appreciation goes to Professor Koichi Maekawa and Associate Professor Chikako Fujiyama for their advice and kind supports. The inspirations from them all have helped me to develop various competencies to tackle challenging problems holistically.

I also wish to appreciate the supports from Dr. Satoshi Komatsu, Dr. Arifa Iffat Zerin, Ms. Natsumi Ishibashi, Mr. Takayuki Sogawa, Mr. Yuto Yamanoi, other concrete laboratory members, faculty and staff members of the Institute of Urban Innovation during my research and stay in Japan.

I gratefully acknowledge the funding from the Ministry of Education, Culture, Sports, Science and Technology (MEXT Japan) through the Monbukagakushō Scholarship, for my entire academic fees and living costs for the whole duration of this study. I thank the Yokohama National University for funding my international conferences. I also would like to appreciate The Ministry of Land, Infrastructure, Transport and Tourism- MLIT, Japan for funding my research activities under "Research development on quality and durability attainment system for concrete structures in various regions utilizing curing techniques and admixtures", the commissioned research of "National Institute for Land and Infrastructure Management" under technology research and development system of "The Committee on Advanced Road Technology".

Last but not the least, I appreciate the love and supports from my beloved family- mother, brothers, sisters, sisters-in-law, in-laws, relatives and friends. Special thanks to my dear wife Chidinma Adaoha, son and daughter for their love and sacrifices at all times.

Dedication

I dedicate this work to the memory of my loving father, Late Mr. Godwin Uzoma Uwazuruonye.

Chapter 1

Introduction

1.1 Background of the Research

Concrete is the most commonly used construction material in the world, twice as in today's construction as all other building materials combined and the second most consumed material after water. The demand for concrete is continually on the increase, which undoubtedly will remain the same in the future, particularly in developing countries [1]. In developed countries like Japan, not a few reinforced concrete structures that were constructed in the last 50 years are under severe deterioration due to loading and environmental actions[2] and a considerable fraction of construction budget is spent on repair and replacement of aging concrete infrastructures. It is imperative, therefore that concrete structures remain as durable as possible to serve the designed service life. The durability of concrete has been a major concern in the recent past. "The durability of concrete is defined as its ability to resist weathering action, chemical attack, abrasion, or any other deterioration process to retain its original form, quality and serviceability when exposed to harsh environment"[3]. Furthermore, a very essential aspect of this durability is the assessment, quality evaluation and the prediction of the residual life of concrete structures that are in-service.

The resistance of concrete to the ingress of deleterious substances, liquid and gaseous, is a very important property regarding the quality assurance and service life prediction of concrete structures. Notwithstanding that there is no universally accepted quantifier for the general durability performance of concrete, permeability and electrical resistivity are undoubtedly the most commonly applied indices for evaluating the durability of concrete structures regardless of the deteriorating mechanisms. Reinforcement corrosion, carbonation, freezing/thawing, alkali-silica reaction, etc., have a strong dependency on the moisture condition of concrete [4], which is a function of its

permeability. The ‘near-surface’, ‘concrete cover’, ‘skin of concrete’ or ‘covercrete’ exhibits different characteristics and properties from the ‘inner’ or ‘heart’ of the concrete [5] resulting from the influence of concreting works. The quality of these few centimeters of concrete- the covercrete, determines the rate at which deteriorating substances gain access to the inner part of the concrete.

Furthermore, in the assessment of the quality of covercrete and its resistance to the ingress of deteriorating substances, surface water absorption and air permeability are commonly applied. Also, the electrical resistivity of concrete is among the most applied durability index nowadays. In general, the two permeability indices and electrical resistivity depend on several factors relating to concrete properties that could be summarized into a capillary pore system (pore diameters, connectivity, etc.) and moisture content. The former has received widespread attention in concrete durability and nondestructive test assessment-related researches. To eliminate the influence of moisture content on quality evaluation of concrete, in most laboratory-based sorptivity tests, concrete specimens are dried to steady weight before testing. On the other hand, laboratory-based electrical resistivity tests require the saturation of the specimens before testing. However, these are not practical in non-destructive tests (NDT) assessment. In this regard, a thorough understanding of the moisture content of concrete as it affects durability assessment and quality classification of concrete is needed since variations in the amount of moisture content both surface and internal are constant factors that cannot be eliminated.

In recent years, a considerable number of simplified test methods have been developed such as Surface Water absorption Test (SWAT) [6]–[9], Water Intentional Spraying Test (WIST)[10], etc. to measure surface water absorption of concrete and evaluate the durability through resistance to water penetration. Due to the complexity of the effects of moisture content on surface water absorption tests as [11] observed in the ambiguity on the interpretations SWAT results, few available texts of literature have addressed it but without thorough analysis. Ngo [11] proposed a threshold value for surface moisture content before starting SWAT for appropriate durability assessment and

quality classification (using a commercially available surface moisture meter). The threshold surface moisture content proposed by Ngo might have a meaning that relates to the finding by Shirakawa et al [12]. In the study of the relationship between the degree of drying and gas diffusion coefficient in hardened cement paste, Shirakawa [12] revealed that when the relative humidity of cement paste was between 12%RH to 47%RH, the gas diffusion coefficient- D_e (in m^2/s) remained constant. Above and below this RH range, D_e decreased with an increase in RH. However, the mechanism governing Shirakawa's finding was not detailed. The proposed threshold by Ngo [11] can neither be directly related to the capillary pore system nor expressed in absolute values relating to the volume of pore voids and the saturated amount. Also, an in-depth explanation of the mechanism and reason behind the threshold value is lacking.

1.2 Research Objectives

To clarify the effects of moisture content of concrete on durability assessment and quality evaluation by detailed analysis of the 'threshold value' of moisture content, this research aims (shown in flow schematic -Figure 1-1) to provide an in-depth investigation on the mechanism and the clear meaning of the threshold for utilizing surface water absorption.

From an engineering point, moisture content of concrete must be expressed in a clear and absolute term related to the saturation of volume of permeable pore voids, hence, the first objective of this study is to propose an absolute way to measure and express moisture content of concrete related to the volume of permeable pore voids and evaluate its effect on SWAT and electrical resistivity. Besides, propose a threshold initial surface moisture content before water absorption test for appropriate durability assessment.

To achieve the first objective above, the influence of internal moisture gradient on surface water absorption must first be eliminated by ensuring moisture equilibrium

throughout the volume of the experimental specimen. Therefore, this study will establish a simple method to obtain moisture equilibrium throughout the volume of a specimen.

Furthermore, the third and fourth objectives center on the verification of the application of a proposed threshold in in-situ concrete durability assessment. The third objective attempts to propose the appropriate surface moisture meter when utilizing SWAT. The fourth is to establish a new SWAT index that is equivalent to the sorptivity index through the investigation of the correlation between SWAT results and JSCE-G 582 sorptivity test results.

Lastly, the fifth objective of this study is to appraise the influence of moisture transport hysteresis on SWAT, air permeability and moisture content.

Research Objectives

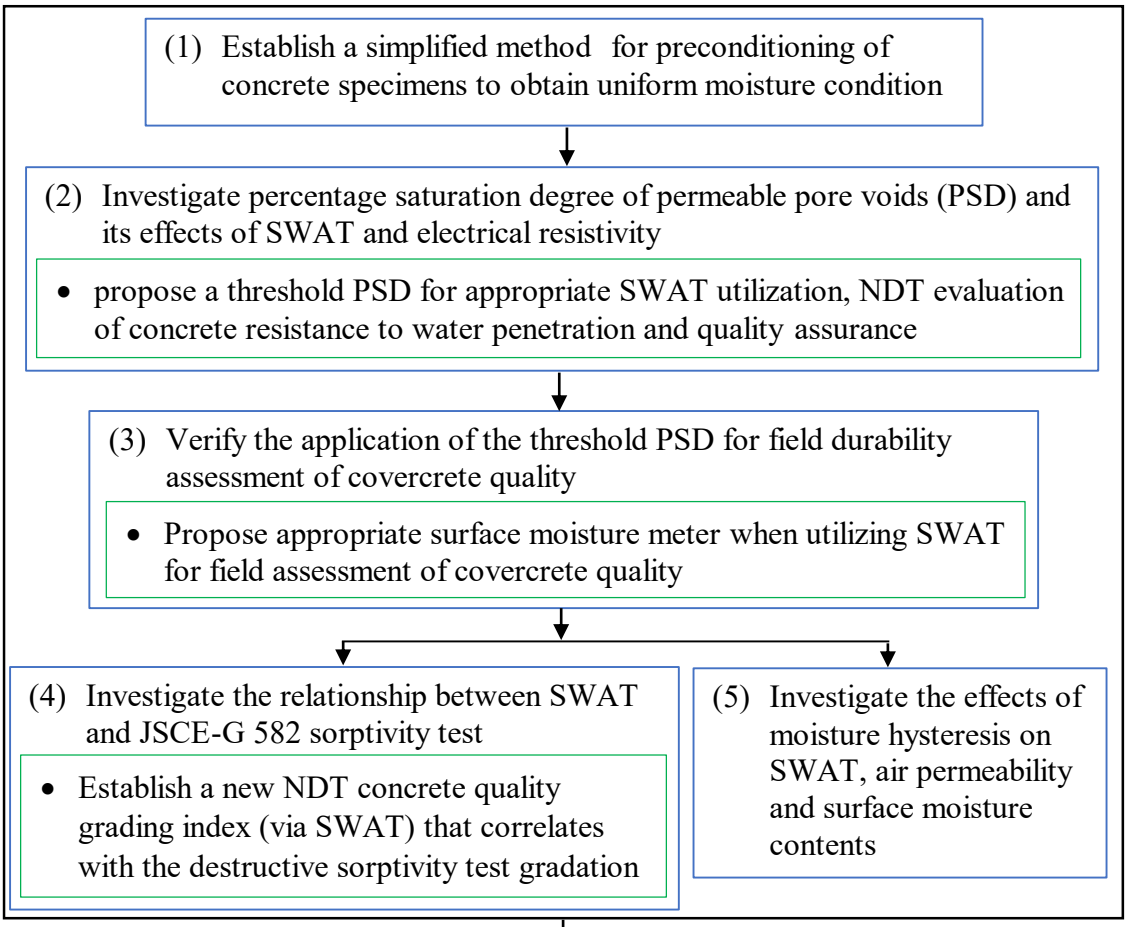

Figure 1-1 Flow of research aim and objectives

1.3 Significance of the Research

In literature, three common ways are used to measure and express moisture content of concrete viz: relative humidity (RH), saturation degree (SD) and moisture content (M). Neither of these expressions is related to the volume of permeable pore

voids and its connectivity, which is the major factor that controls mass transfer in concrete. In this context, this study eliminates the ambiguity in understanding the moisture content of concrete by utilizing percentage saturation degree of permeable pore voids. Besides, the combined influence of pore void volume, pore size distribution and the saturation degree of pore voids on surface water absorption, air permeability and electrical resistivity of concrete is explained, and appropriate thresholds are proposed for saturation degree of permeable pore void for nondestructive assessment of covercrete quality.

Furthermore, this study introduces a new Surface Water Absorption Test (SWAT) index- *coefficient of surface water absorption (CSWA).* CSWA could effectively be applied in a nondestructive way to evaluate sorptivity of concrete without going through the destructive and rigorous process of calculating the moisture penetration rate coefficient from laboratory-based sorptivity tests.

This dissertation will contribute to designing and constructing more durable concrete structures by establishing a systematic evaluation method for surface water absorption tests fully considering the effect of moisture content.

1.4 Research Methodology

Two methodologies (experimental and numerical analysis) are adopted to reach the aim and objectives of this research in the following two stages:

Stage 1: Preconditioned specimens

For a better understanding of the influence of different initial moisture contents of concrete on durability evaluation, quality grading and an in-depth investigation of the meaning and mechanism of the 'threshold value', experimental studies are conducted on different kinds of concrete by varying the initial moisture contents (expressed as a percentage saturation degree of permeable pore voids-PSD) through preconditioning and investigating the effects on surface water absorption by SWAT. In this step, specimens are first preconditioned to moisture equilibrium throughout the entire volume to

eliminate the influence of moisture gradient before conducting SWAT at different PSDs. Two surface moisture meters (HI-100 and HI-520-2) are calibrated at this stage for an NDT evaluation of PSD. Thereafter, the results of the effects of PSD on surface water absorption are further verified by numerical simulation. Furthermore, the effects of PSD on electrical resistivity are investigated by the Wenner probe method.

Stage 2: Unconditioned specimens

The verification of the results from stage 1 and the test for the applicability of the effects of PSD on surface water absorption (obtained from the laboratory preconditioned specimens) in structures under natural environmental conditions (with moisture gradient) are conducted. Different kinds of concretes are exposed to several environmental conditions, and the changing surface PSDs resulting from the exposures are investigated (utilizing the calibrated surface moisture meters) in addition to the surface water absorption rates at different PSDs.

1.5 Structure of the Dissertation

Seven chapters are presented in this dissertation. Chapter 1 introduces the research background, objectives, significance and methodology. Chapter 2 presents a literature review relevant to the scope of this dissertation. Chapter 3 establishes a simplified method for preconditioning of concrete specimens to obtain uniform moisture conditions, while the main findings of this dissertation are presented in the proceeding four chapters (Chapter 4 to 6).

Chapter 4 presents the percentage saturation of permeable pore voids (PSD) and the effects on Surface Water Absorption Test (SWAT). Experimental verification of the proposed PSD calculation formula- which derived its course from the ASTM C642 was conducted. The results showed that the existing ways of measuring and expressing moisture content of concrete such as saturation degree overestimated the moisture content of concrete. Furthermore, the results from the relationship between PSD and water absorption by SWAT revealed a plateau at some range, where PSD has no effects on surface water absorption of concrete. Numerical simulation with DuCOM software

also revealed a similar plateau within the same range of PSD when PSD was plotted against the increase in free water resulting from 10 minutes absorption and the combined influence of pore size distribution and the degree of saturation of pore void on water absorption is discussed. Moreover, the calibration of commercial surface moisture meters (HI-100 and HI-520-2) for nondestructive measurement of PSD is also presented in this chapter. Meanwhile, the effects of PSD on electrical resistivity was investigated.

Chapter 5 provides the influence of hysteresis on SWAT, air permeability and surface moisture meters (HI-100, HI-520-2 and CMEX II). Experimental specimens were conditioned in two processes: wet-to-dry (desorption process) and dry-to-wet (absorption processes) and the effects on the rate of water absorption, coefficient of air permeability and surface moisture contents were investigated.

In Chapter 6, an experimental investigation on the correlative assessment between the results from the JSCE sorptivity test standard and SWAT was presented. A new SWAT index, coefficient of surface water absorption-*CSWA* was introduced in this chapter and found to be correlated with the 48 hours-based moisture penetration rate coefficient-*A* from the JSCE test result.

Finally, the conclusions obtained in this research are summarized in Chapter 7. The implications of these findings are discussed, in particular clarifying the effects of the initial pore void saturation degree on nondestructive test assessment and grading of concrete quality utilizing surface water absorption, air permeability and electrical resistivity. Also, recommendations for further studies are given.

References

[1] Z. Wu, 'Influence of Microcracks on the Transport Properties of Concrete', *Ph.D. Thesis*'. Imperial College London: 2014.

[2] T. Ishida and I. Iwaki, 'Multi-scale and Multi-chemo-physical Modeling of Cementitious Composite and Its Application to Early Age Crack Assessment Of Reinforced Concrete Slab Decks', *2nd International RILEM/COST Conference on Early Age Cracking and Serviceability in Cement-based Materials and Structures - EAC2,* 12–14 September 2017, ULB-VUB, Brussels, Belgium.

[3] P. Azarsa and R. Gupta, 'Electrical Resistivity of Concrete for Durability Evaluation: A Review', *Advances in Materials Science and Engineering*, vol. 2017, pp. 1–30, 2017, doi: 10.1155/2017/8453095.

[4] E. William and J. S. Erik, 'Electrical Resistivity of Concrete'. Directorate of Public Roads, Norwegian Road Research Laboratory, Jun. 1995.

[5] R. J. Torrent, 'A Two-chamber Vacuum Cell for Measuring the Coefficient of Permeability to Air of the Concrete Cover on Site', *Materials and Structures*, vol. 25, no. 6, pp. 358–365, Jul. 1992, doi: 10.1007/BF02472595.

[6] K. Hayashi and A. Hosoda, 'Development of Surface Water Absorption Test Applicable to Actual Structures'. *Proceedings of JCI*, Vol. 33, No. 1 pp. 1769-1774, 2011. (in Japanese)

[7] K. Hayashi and A. Hosoda, 'Fundamental Study on Evaluation Method of Covercrete Quality of Concrete Structures by Surface Water Absorption Test'. *Journal of JSCE, Ser. E2 (Materials and Concrete Structures)* Vol. 69, No.1, pp.82-97, 2013. (in Japanese)

[8] Hayashi K., Akmal U., and Hosoda A., 'Analysis of Moisture Transfer is Surface Water Absorption Test of Concrete Using Embedded Sensors', *Proceedings of JCI*, vol. 35, p. 6, 2013. (in Japanese)

[9] A. Hosoda and K. Hayashi, 'Evaluation of Covercrete Quality of Concrete Structures by Surface Water Absorption Test', *International Symposium on Concrete and Structures for Next Generation, Ikeda & Otsuki Symposium (IOS2016)*, Tokyo, Japan, pp.223-230, 16-18 May 2016.

[10] M. H. Nguyen, K. Nakarai, Y. Kubori, and S. Nishio, 'Validation of Simple Nondestructive Method for Evaluation of Cover Concrete Quality', *Construction and Building Materials*, vol. 201, pp. 430–438, Mar. 2019, doi: 10.1016/j.conbuildmat.2018.12.109.

[11] T. V. Ngo, 'Proposal for Threshold of Moisture Content of Concrete for Appropriate Measurement of Surface Water Absorption Test' *Ph.D. Thesis*'. Yokohama National University, Japan: 2019.

[12] Shirakawa T., Shimazoe Y., Aso M., Nagamatsu S., and Sato Y., 'Relationship between Degree of Drying and Gas Diffusion Coefficient in Hardened Cement Paste', *Transactions of AIJ*, vol. 64, no. 524, pp. 7–12, 1999, doi: 10.3130/aijs.64.7_4. (in Japanese)

[13] M. Sosoro, 'Transport of Organic Fluids through Concrete', *Mat. Struct.*, vol. 31, no. 3, pp. 162–169, Apr. 1998, doi: 10.1007/BF02480390.

[14] M. Saleem, M. Shameem, S. E. Hussain, and M. Maslehuddin, 'Effect of Moisture, Chloride and Sulphate Contamination on the Electrical Resistivity of Portland Cement Concrete', *Construction and Building Materials*, vol. 10, no. 3, pp. 209–214, Apr. 1996, doi: 10.1016/0950-0618(95)00078-X.

Chapter 2

Literature Review

2.1 Introduction

Chapter 2 presents a literature review on the topics relevant to this dissertation. Since this dissertation centers on concrete durability, mass transfer and moisture content, the mechanisms for transport processes in concrete are first reviewed focusing on fluid transport mechanisms, followed by the factors influencing the three durability indices that are under consideration and a brief review of the major ways of measuring and expressing moisture contents of concrete. Subsequently, in the chapter, durability evaluations by water absorption and air permeability comprising test standards and test methods for measurement of water penetration resistance of concrete were reviewed. Lastly, durability evaluation by electrical resistivity was reviewed.

2.2 Transport processes and mechanisms in concrete

Deterioration of concrete such as sulphate attack, frost damage and reinforcement corrosion is caused by many different processes with common characteristics that all the processes require both a transport material and a medium of transport into the matrix of concrete [1], [2]. Even some deteriorations that are inherent in the component materials of concrete such as alkali-silica reaction require movement of water for the activation of the reaction. Eight transport processes and mechanisms in concrete are discussed: permeability (pressure-induced flow), diffusion, electromigration, thermal migration, absorption, adsorption, sorptivity/capillary suction and osmosis. [1],[3].

Permeability (pressure-induced flow) is defined as a characteristic of a porous medium to allow the passage of fluids through it under the action of pressure differentials.[3],[4]. 'Permeability is strictly related to the flow that occurs under an applied pressure differential' but often used loosely to cover different properties of concrete and

interchangeably confused with the porosity of concrete. On the other hand, porosity represents the volume content of pores which might not necessarily be inter-connected [3]. The significance of high permeability to a concrete structure might be more than just the water uptake but on the damage that may come from the dissolved deleterious substances (such as sulphates and chlorides) in the transported water.

Diffusion is the process by which liquid or gaseous ions (such as chloride) pass through concrete under the action of a concentration gradient. It is defined by a diffusivity value or a diffusion coefficient and generally controlled by Fick's law in a one-dimensional situation considered as:

$$J = -D\frac{dC}{dx} \qquad [2.1]$$

Where J is the flux of chloride ions, D is the effective diffusion coefficient, C is the concentration of chloride ions and x is a positive variable. Equation [2.1] can be used when concentration is constant and there is a steady-state condition. On the contrary, when the condition is non-steady-state and concentrations are changing during the time, Fick's second law: Eq [2.2] is applied as given [5]:

$$\frac{\partial C}{\partial t} = D\frac{\partial^2 c}{\partial x^2} \qquad [2.2]$$

Electromigration (often called migration) occurs in the presence of voltage difference (electric field). The driving force might be external such as leakage from a direct current power supply. Also, it is often caused by the electrical potential of the pitting corrosion of reinforcement steel. Electromigration can be measured from the electrical resistance of concrete and the flux due to electromigration and is given by the equation [1], [6]:

$$F = \frac{DzECF_a}{RT} \text{ (kg/m}^2\text{/s)} \quad [2.3]$$

where:

z is the valence of the ion (i.e. the charge on it divided by the charge of an electron), F_a is the Faraday constant = 9.65 x 10^4C/mol, E is the electric field (V/m), R = 8.31 J/mol/K and T is the temperature (K).

The flux can be expressed as an electric current:

$$I = zFF_aA \text{ (A)} \quad [2.4]$$

Ohm's law states that :

$$R = \frac{\phi}{I} \ (\Omega) \quad [2.5]$$

where ϕ is the voltage. The electric field, which is the voltage gradient is thus:

$$E = \frac{\phi}{x} = \frac{IR}{x} = \frac{zFF_aAR}{x} \text{ (V/m)} \quad [2.6]$$

where x is the distance (m). the resistivity ρ is defined from the equation:

$$R = \frac{\rho x}{A} = \frac{x}{A\sigma} \ (\Omega) \quad [2.7]$$

where σ is the electrical conductivity in $(\Omega m)^{-1}$, the inverse of resistivity

The rearrangement and combination of equations [2.5], [2.6] and [2.7] gives the Nernst Einstein equation:

$$D = \frac{RT\sigma}{z^2F_a^2aC} \quad [2.8]$$

Thermal migration: Just as the name implies, the transport process is driven by the presence of temperature difference. Water moves from hot region to cold region in solids and the rate at which it moves depends on the permeability of the solid.

Absorption is the mechanism by which concrete takes in fluid to fill up spaces within the material. Capillary absorption takes place in fine pores (10 nm to 10 μm) where the range of gravity forces in the liquid is at the same range as the surface tension and it is the major mechanism when the material is only in partially wetting stage [7]. It is usually defined by the *Lucas Washburn* equation:

$$h = k\sqrt{t} \qquad [2.9]$$

where h is the height of the liquid front (m), t is the wetting time (s) and k is the capillary coefficient (m $s^{-1/2}$)

Adsorption is a process in which molecules adhere to the surface of the concrete. It can either be physical adsorption (molecules are held to the surface by Van der Waals forces) or chemical adsorption (molecules are held as a result of the formation of chemical bonds). Adsorbed molecules or ions are fixed into the matrix of the concrete, unable to move and unlikely to cause any deterioration.

Sorptivity/Capillary suction is the major mechanism in systems where there is high liquid concentration and usually takes place in large pores. This occurs where forces resulting from pressure gradient is higher than surface tension.

2.3 Factors influencing electrical resistivity, water absorption and air permeability tests

The controlling factor for the passage of electrical current in concrete is predominately the ionic movement of the pore water. Similarly, the porosity, pore water and pore void system control water absorption and air permeability of concrete. This explains that any factor that affects the porosity, pore void system, pore water movement and the degree of pore connectivity and continuity will fundamentally affect the electrical resistivity, water absorption and the air permeability properties of concrete.

2.3.1 Cement type and paste volume

Generally, cement type and paste volume are among the intrinsic factors influencing electrical resistivity, water absorption and air permeability of concrete. These two factors have a great impact on both the characteristics of the pore structure and the chemistry of pore water. For constant water to cement ratio, [8] showed that increasing paste volume decreases resistivity with an approximately 1% to 1% rate. By increasing cement paste, the channel for the electrolytic liquid is also increased. Figure 2-1 is a finding by W. Piasta and B. Zarzycki [9], which shows a near 1:1 linear relationship between water absorption and past volume of high-performance concrete (HPC).

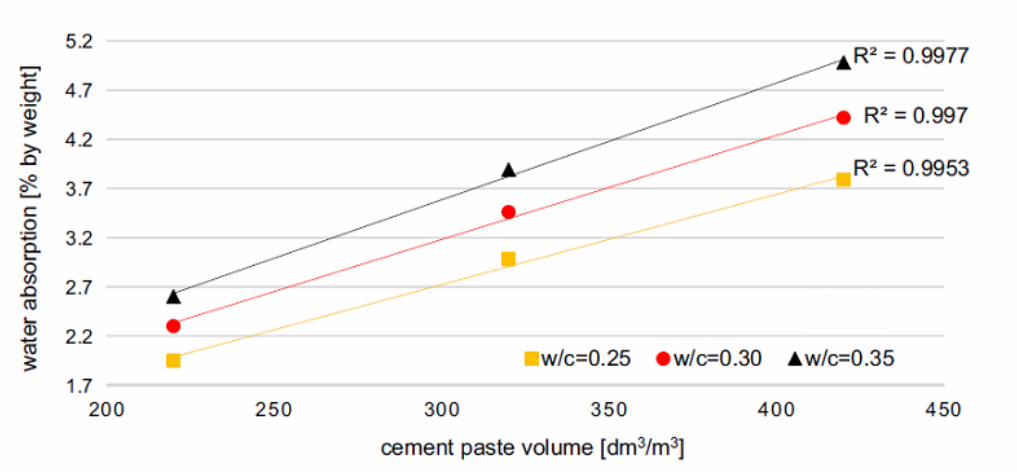

Figure 2-1 Effects of cement paste volume on water absorption (*culled from [9]*)

2.3.2 Water-to-content

Just like cement type and paste volume, water to cement (w/c) content is among the main factors contributing to the permeability of concrete. Higher w/c ratio leads to higher porosity, increases the channel for electrolytic liquid thereby decreasing the electrical resistivity [8], [10]. However, it has been revealed that concrete containing supplementary materials such as slag and rice husk ash showed irregular behaviour for various water to cement ratios [10]. An increase in water to cement ratio has been shown to increase the porosity of concrete increasing the air permeability and water absorption [11]–[14].

2.3.3 Volume of aggregate

In general, aggregates have lesser porosity, exhibit more resistance to the flow of electric current than the hardened cement paste, thus have higher electrical resistivity. Increasing the volume of aggregate means reducing the volume of paste as well as decreasing the flow of electric current. Nonetheless, the size, type and location of the aggregate affect its resistance to electric flow.

2.3.4 Curing condition

Curing condition affects electrical resistivity, water absorption and air permeability of concrete. The major resultant aspects of curing conditions that influence the variations of the durability indicators are the degree of hydration of the cementitious material and the saturation degree [10]. In an experimental study performed by Ngo T. V. [11], [12] investigated the water absorption and air permeability of ordinary Portland cement concrete with water to cement ratios of 0.40, 0.50 and 0.60 with three curing conditions: (a) sealed for one day after placement, (b) sealed for 7 days after placement and (c) sealed for 1 day plus immersed in water for 6 days after placement, it was concluded that the specimens that were sealed for 1 day plus immersed in water for 6 days had lower surface water absorption rates whereas the samples that were sealed for 1 day after placement had higher surface water absorption rates. Similar results were obtained for the coefficients of air permeability [11], [12].

Nam and Hosoda's [15] water and chloride penetration investigations of slag concrete comprising high alite cement (HAC) (Figure 2-2) show the effects of curing conditions on the water absorption rate of OPC and HAC concrete. Figure 2-2 shows that as the number of curing days increases, the rate of water absorption decreases. The difference was not significant for HAC slag concrete. In general, the effects of curing condition on water absorption of concrete and the higher resistance to water penetration by longer cured concrete can be explained by the higher hydration degree and denser matrix formation [15].

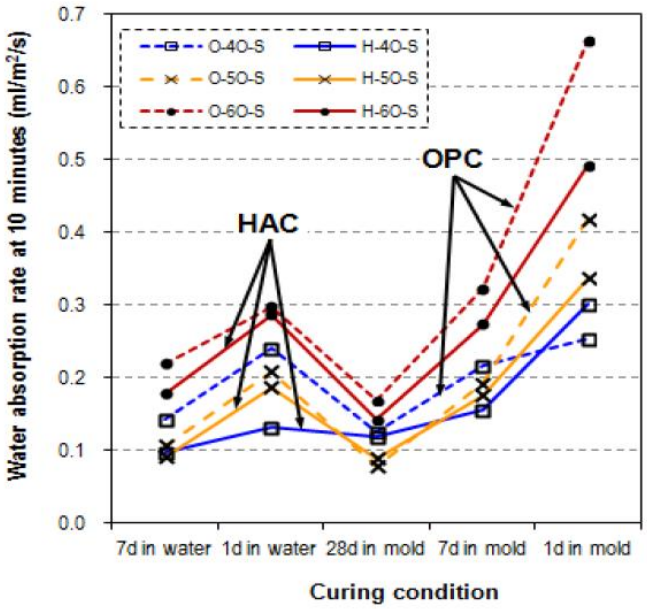

Figure 2-2 Effects of curing condition on the water absorption rate of OPC and HAC concrete (*culled from [15])*

2.3.5 Temperature

An increase of 1ºC results in a 3% decrease of resistivity was the conclusion from [8]'s investigation on the electrical resistivity of concrete (Figure 2-3). For temperature effect on moisture transfer in concrete, [16] conducted an investigation and found that elevating concrete temperature without a temperature gradient (in an isothermal condition) does not significantly affect the moisture transfer. "On the other hand, the effect of temperature gradient under a non-isothermal condition is significant and becomes more significant as the temperature gradient increases" [16]. In a practical situation, an isothermal condition of concrete may never be obtained, which implies that the influence of temperature on water absorption will always be significant.

Temperature affects absorption by the impact on the viscosity of liquids, surface tension, thermal expansion and change in pore structures. Similarly, the effects of temperature on electrical resistivity result from the expansion of the pore water molecules which creates more connectivity of the pore voids thereby reducing resistivity.

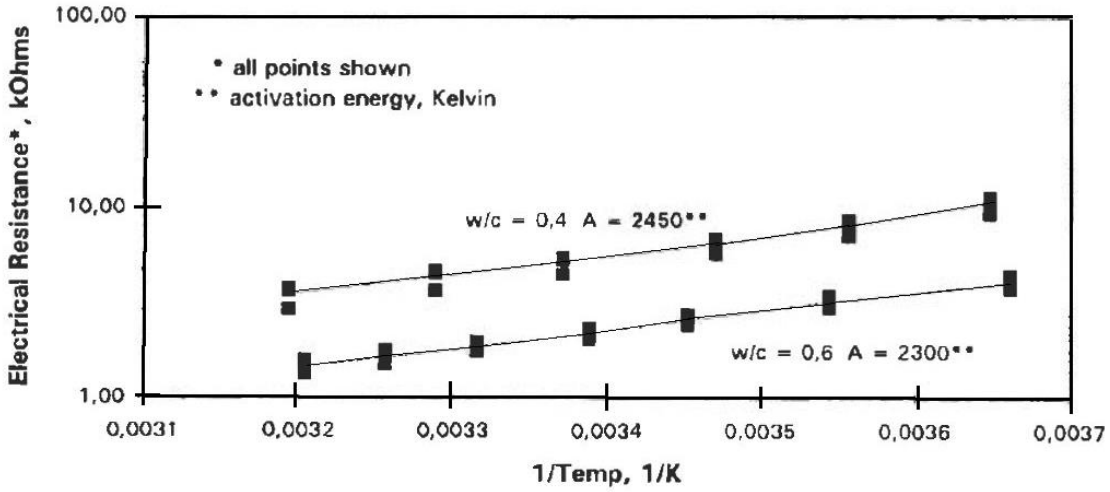

Figure 2-3 Effects of temperature on electrical resistivity of concrete(*culled from [8])*

2.3.6 Moisture content

Figure 2-4 shows an experimental result of the relationship between moisture content and electrical resistivity of concrete in the air-dry state, oven-dry state and saturated surface-dry state [17]. Sengul [17] revealed that concrete in the air-dry state had approximately 50% higher resistivity than that in the saturated surface-dry state. This showed that moisture content has a substantial influence on the electrical resistivity of concrete. William and Erik [8] had the same finding in which a normal OPC saturated concrete was shown to have resistivity between 1000-10,000 Ωcm while for normal OPC dry concrete, the resistivity reaches 10^8 -10^9 Ωcm and concluded that 1% increase in saturation degree of concrete decreases electrical resistivity by 3%.

Moreover, Ngo et al [12] recently revealed the same influence of moisture content of concrete on surface water absorption and air permeability with the conclusion that the effect of moisture concrete on the rate of water absorption is ambiguous and could mislead in evaluation and grading of the quality of concrete.

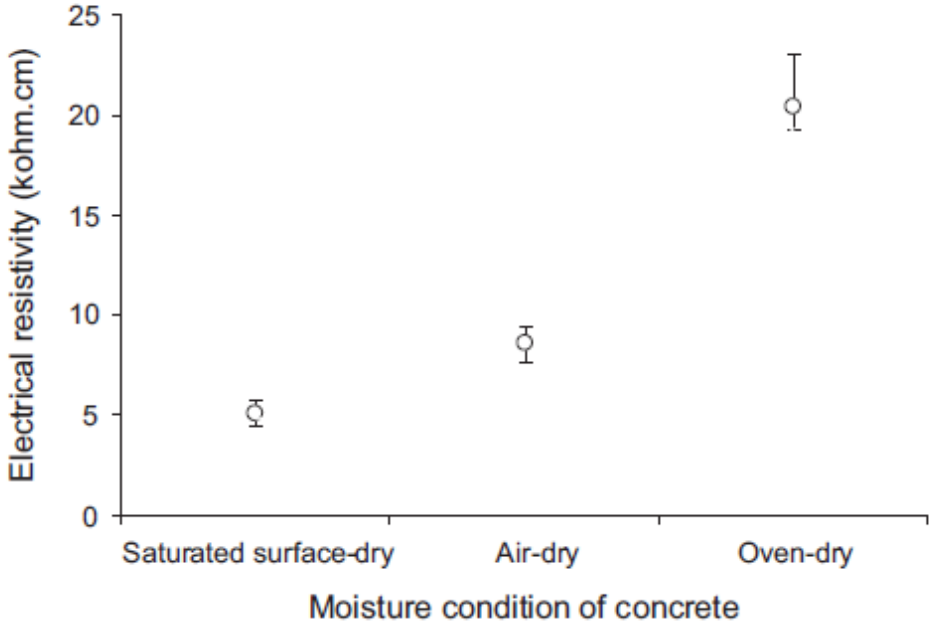

Figure 2-4 Effect of moisture content on electrical resistivity (*culled from [17])*

2.3.7 Chlorides

Chloride is known to be the main cause of steel corrosion in RC structures, thus several studies have investigated the effects of chloride on durability indicators like electrical resistivity. William and Erik [8] found a large but non-linear influence of chloride on electrical resistivity when they investigated with 3% and 6% NaCl solution. They concluded that "a 3% or 6% NaCl solution in the pore cuts the resistance by a factor of 2".

In the investigation of water adsorption isotherm of OPC concretes with w/c 0.7 (OPCC30), 0.48 (OPCC60) and OPC/Blast furnace slag concrete with w/b 0.48 (BFSC60) for different external chloride concentrations (Figure 2-5a-c) by [18], equilibrium water content was shown to increase with the chloride concentration. It was attributed to the presence of salt and other ions such as Na^+ and K^+ which created a modification of water activity coefficient [18].

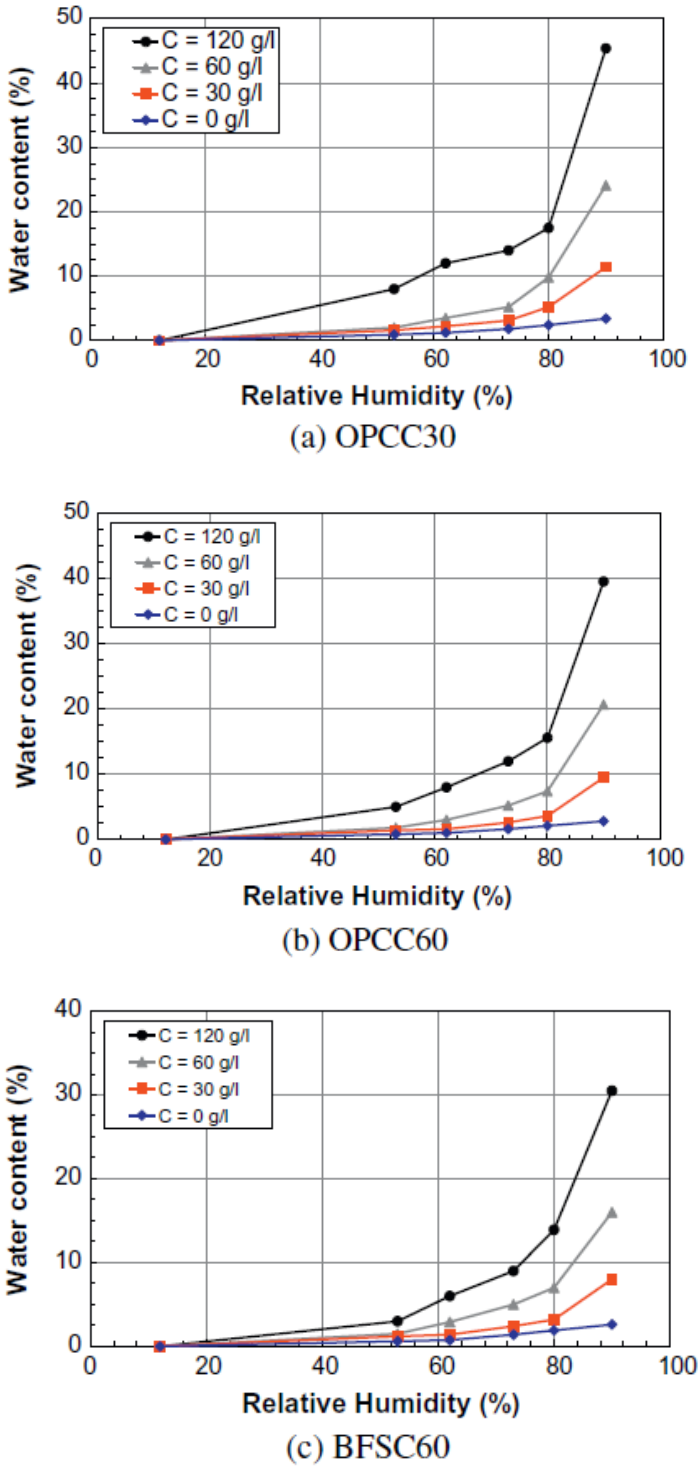

Figure 2-5 Effect of external chloride concentration on water absorption of concrete (*culled from [18]*)

2.4 Measurements and expressions of moisture content of concrete

The penetration of water into concrete, as well as other harmful solutes and ions (such as chlorides, sulphates), is considered of great importance as it is virtually the beginning of all deterioration processes. This explains why the moisture content of concrete is a very important property in the field assessment of the covercrete quality and durability in general. Over the years, the moisture content of concrete has been measured and expressed in the following three major forms:

i. ***Relative Humidity***

Relative humidity (RH) is among the common forms used in the expression of moisture content of concrete [16], [18]–[23]. However, some researchers have argued that RH is not an appropriate form to express moisture content of concrete as it is largely affected by hysteresis-whether the RH-value is obtained by adsorption or desorption. The RH alone is said to be a defining factor for the thermodynamic state of the pore water rather than the direct amount of pore water or the degree of saturation[8]. William and Erik stated that "the RH-value exerted by pore water is influenced by the concentration and the types of dissolved ions. Consequently, even reliable RH-records would give incomplete information about the moisture state in a concrete structure". The RH is measured directly by embedding an RH probe into the concrete.

ii. Saturation Degree

Saturation degree has been widely used to measure and express the moisture content of concrete.[8], [21], [24], [25]. According to Antón et al., 2013, the saturation degree, SD, of concrete is defined as;

$$\mathrm{SD} = \frac{m_h - m_d}{m_s - m_d} \qquad [2.10]$$

where; m_h = mass of partially saturated concrete, m_d = mass of the dried concrete, m_s = mass of the water-saturated concrete.

iii. Moisture Content

Also in the literature, the moisture content of concrete has been measured and expressed simply as 'moisture content' [19], [26]. For instance,[26] expressed moisture content in percentage determined by the following relationship:

$$M = \frac{W - W_d}{W_d} * 100 \qquad [2.11]$$

where; M is the moisture content, W= the mass of moist specimen in grams and W_d= the mass of the dry specimen in grams.

2.5 Test standards for measurement of water penetration resistance of concrete

Several testing techniques have been adopted by different countries as codes and for standardization. The standards include but not limited to the following:

- *Japanese Standards*

JSCE 2017 (Standard specifications for concrete structures- 2017)

JSCE- 582-2018 (Test method for water penetration rate coefficient of concrete subjected to water in short term)

- *British Standards*

BS 1881 Part 208-1996 (Recommendations for the determination of the initial surface absorption of concrete**)**

- *European Standards*

Euro codes BS EN 1002-2002

- *American Standards*

ASTM C1585-04 (Standard test method for measurement of the rate of absorption of water by hydraulic-cement concretes**)**

ASTM C642- 97 (Standard test method for density, absorption, and voids in hardened concrete)

ASTM C1757-13 (Standard test method for determination of one-point, bulk water sorption of dried concrete)

Three test standards one from each: the American Society for Testing and Materials (ASTM International), the British Standards (BS) and the Japan Society for Civil Engineering (JSCE) are briefly reviewed.

2.5.1 ASTM C1585: Standard test method for measurement of rate of absorption of water hydraulic cement concretes

The ASTM C1585 is used to determine the rate of water absorption for hydraulic cement concrete by exposing one surface of a test specimen to water and measuring the increase in the mass resulting from water absorption over time [27]. The test method, which was based on Hall's [28] water sorptivity phenomenon, is intended to access the resistance of unsaturated concrete to water penetration. Step by step sample preparations and test procedures (shown in Figure 2-6) is detailed in [27] where absorption, I (change in mass divided by the cross-sectional area of the test specimen), is calculated as follows:

$$\mathrm{I} = \frac{m_t}{a/d} \qquad [2.12]$$

where I = the absorption, m_t = the change in specimen mass in grams, at the time t, a = the exposed area of the specimen, in mm^2, and d = the density of the water in g/mm^3.

The initial rate of water absorption (in $mm/s^{1/2}$) is defined as "the slope of the line that best fit to I plotted against the square root of time ($s^{1/2}$)" [27] and obtained by using the least-squares linear regression of the plot I versus $time^{1/2}$.

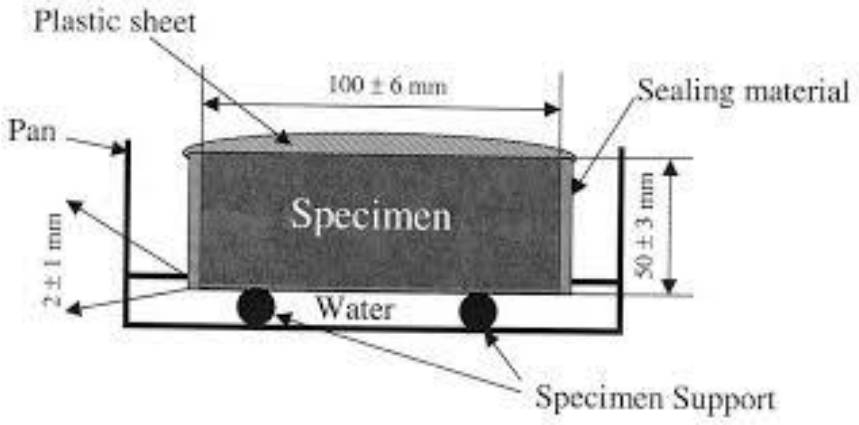

Figure 2-6 Schematic of ASTM C1585 test procedure (*culled from*[27]*)*

2.5.2 BS 1881, Part 5: Test for determining the initial surface absorption

The British Standards adopted and incorporated the ISAT method in 1970 as BS 1881, part 5: Test for determining the initial surface absorption [29]. In the method, a cap with a surface area not less than 5000 mm^2 is sealed to the surface of concrete, filled with water and measure the concrete's rate of water absorption through the movement along a capillary tube under a constant water head of 200 mm [3], [29]. The ISAT setup, testing and measurement procedures are detailed in 2.6.1.

2.5.3 JSCE-G 582, 2018: Test method for water penetration rate coefficient of concrete subjected to water in short term

The Japan Society of Civil Engineers (JSCE) sorptivity test standard for determining water penetration rate coefficients of concrete subjected to water in short time was established in 2018 as JSCE-G 582 and published in Japanese [30]. The outline of the steps for the sample preparations are as follows:

a) Prepare cylindrical concrete specimen of ϕ100 mm × 200 mm height.

b) After curing (curing condition should be the same with the actual structure under investigation), cut off 25 mm thickness from the face of the form-finished-surface with dry type concrete cutter.

c) Dry specimens in a controlled chamber at a temperature of 40 ± 2°C and relative humidity of 30 ± 5% for 28 days. Or dry in a controlled chamber at a temperature of 20 ± 2°C and relative humidity of 60 ± 5% for 91 days. If drying is done at 40 ± 2°C and 30 ± 5% R.H., drying can be stopped when a 24-hour mass change is less than 0.1%.

d) Allow specimens to return to room temperature by natural heat loss for a minimum of 1 hour and store in a closed container for 24 hours.

e) Seal the lateral sides of the specimen and the surface that was not exposed by cutting with water penetration resistant material such as aluminum tape or foil and epoxy resin. Allow the epoxy resin to dry before starting the test.

The standard also outlined the test procedures as follows:

f) Tap water of 20 ± 2°C temperature shall be used. To stabilize the temperature of the water and to expel the dissolved air in water after collecting it from the tap, store water in a controlled environment of 20 ± 2°C temperature for 24 hours or more.

g) Make a 10 mm mark from the bottom of the container that shall be used for the test and carefully place 5 mm height spacers (to raise the specimen from the bottom of the container) on the container. Ensure that the total contact area between the spacers and the specimen does not exceed 10% of the surface area of the specimen.

h) Pour the stabilized water into the container up to the marked 10 mm height and carefully immerse the specimen. The immersion period is 48 hours and the measurements shall be taken at 5 hours, 24 hours and 48 hours respectively. For each measurement time, a minimum of 3 samples shall be withdrawn and utilized.

i) Split specimen into two halves and measure the depth of penetration immediately after withdrawal from water. Measurement shall be in 0.5 mm units with a vernier caliper or a straight metal rule from one half of the split specimen. A minimum of 5 measurements L1 – L5 shall be recorded for each specimen and the distance from the sealed edge of the specimen shall not be less than 20 mm. Moisture penetration depth shall be determined by spraying a colour-differentiating water detector that conforms with NDIS 3423 specification.

The moisture penetration rate coefficient, A, which is the depth of water penetration obtained during the immersion of 5 to 48 hours is calculated thus:

$$A = \frac{\sum_{n=1}^{n} \left(\sqrt{t_i} - \overline{\sqrt{t}}\right) * \left(L_i - \overline{L}\right)}{\sum_{n=1}^{n} \left(\sqrt{t_i} - \overline{\sqrt{t}}\right)^2} \qquad [2.13]$$

where A: moisture penetration rate coefficient (mm/$\sqrt{hr}$), n: number of data, $\sqrt{t_i}$: square root of immersion time of "i"th data, $\overline{\sqrt{t}}$: average value of the square root of immersion time, L_i: penetration depth of the "i"th data, $\overline{L}$: average value of the penetration depth

The intercept of the approximate straight line is given as the constant B by the equation:

$$B = \overline{L} - A * \overline{\sqrt{t}} \quad [2.14]$$

where B: constant, A: moisture penetration rate coefficient (mm/$\sqrt{hr}$), $\overline{\sqrt{t}}$: average value of the square root of immersion time, $\overline{L}$: average value of the penetration depth.

2.6 Nondestructive Test methods for measurement of water absorption and air permeability resistance of concrete

A wide range and methods of absorption and permeability tests for cement-based materials exist, both destructive and non-destructive. The choice of any depends on the purpose of the test, available testing instrument and place of testing (in-situ or laboratory). In this section, only the few that are directly related to the aim of this study are reviewed.

2.6.1 Initial Surface Absorption Test (ISAT)

The initial surface absorption is defined as the rate of flow of water at a constant temperature and constant applied water head into the surface of concrete per unit area at a specified interval from the start of the test [31], [32]. The first version of ISAT was on the test for roof tiles [3] developed in 1931 by Glanville and the subsequent modified generations were in the 1970s by Levitt [3] [31]–[33]. It was further commercialized and incorporated into the British Standards [31] as a test standard for evaluating the resistance of concrete to surface water absorption.

ISAT is a quick, simple and non-destructive device which can be utilized to measure the water penetration rate in a normal cast in-situ concrete surface. The major limitation of ISAT is the difficulty in ensuring a water-tight seal during measurement [3], [31]. Another challenge in applying the ISAT method is the great influence of moisture content which [31] noted its effects on almost all the surface absorption and air permeability tests and therefore stated that the main application of "ISAT is as a quality control test for precast concrete units which can be tested whenever they are 'dry'" [31].

The general arrangement and measurement procedure of ISAT (Figure 2-7) monitors the movement of water in the capillary tube and the initial surface absorption value is be calculated and expressed in ml/m^2/s. The classification of covercrete (Table 2-1) by Levitt [33] is based on water absorption by ISAT values from a theoretical derivation for initial surface absorption (ISA) as:

$$ISA = at^{-n} \quad [2.15]$$

where t is time, a is constant, n is a second constant showing the decay rate of water absorption having a value of 0.5

Table 2-1 ISAT classification of water absorption of covercrete based on ISA value

Concrete absorption	ISAT results in ml/m^2/s			
	Time after starting test (minutes)			
	10	30	60	120
High	> 0.50	> 0.35	> 0.20	> 0.15
Medium	0.25 – 0.50	0.17 – 0.35	0.10 – 0.20	0.07 – 0.15
Low	< 0.25	< 0.17	< 0.10	< 0.07

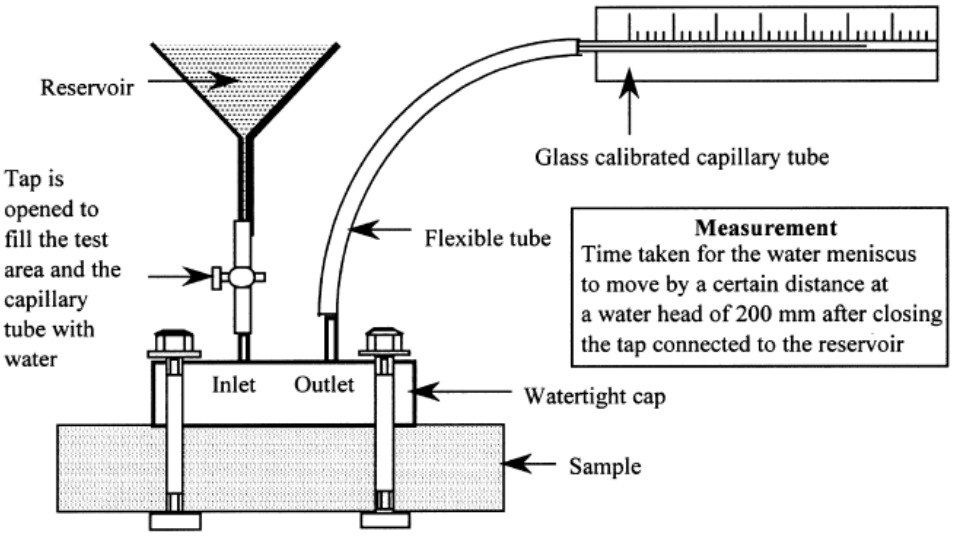

Figure 2-7 Setup for Initial Surface Absorption Test (ISAT) (*culled from*[31]*)*

ISAT is composed of a water reservoir unit with a control inlet tap, a calibrated glass capillary tube, which is connected to the third component- watertight cap, by a

flexible tube. The watertight cap is generally made of a transparent material such as clear acrylic, polyester or epoxy resin. The watertight cap (minimum water contact area of 5000 mm^2) is attached to the surface of the test concrete by a clamp and water tightness ensured. The measurement procedure can generally be summarized in the following steps [29]:

i. After attaching the components as shown in Figure 2-7, close the tap from the reservoir and fill the reservoir with water (NB: care should be taken to avoid undue fluctuations of the temperature of the water).
ii. Start the test by opening the tap to allow the water to run into the cap and record the starting time (flush air from the cap through the capillary tube by sharply pinching the flexible tube and replenish the reservoir to maintain the constant water head of 180 – 220 mm and raise one end of the capillary tube above the water level to prevent further outflow. Ensure that the reservoir does not run empty).
iii. Take readings at intervals after 10 minutes, 30 minutes, 60 minutes and 120 minutes.

2.6.2 Surface Water Absorption Test (SWAT)

Surface Water Absorption Test (SWAT) was developed by Hosoda and Hayashi [34], [35]. SWAT is a non-destructive device that evaluates the quality of concrete at the cover zone at 10 minutes.

SWAT has proven to be effective in detecting the influence of curing conditions and effects of microcracks in covercrete quality within 10-20 mm, which is the most affected by concreting works [12], [34]–[36]. Furthermore, good correlations have been demonstrated between SWAT results and:

- long term water penetration tests (Figure 2-8) [15],
- the carbonation rate coefficient of concrete (Figure 2-9) [37]
- the JSCE sorptivity test (Figure 2-10) [38]

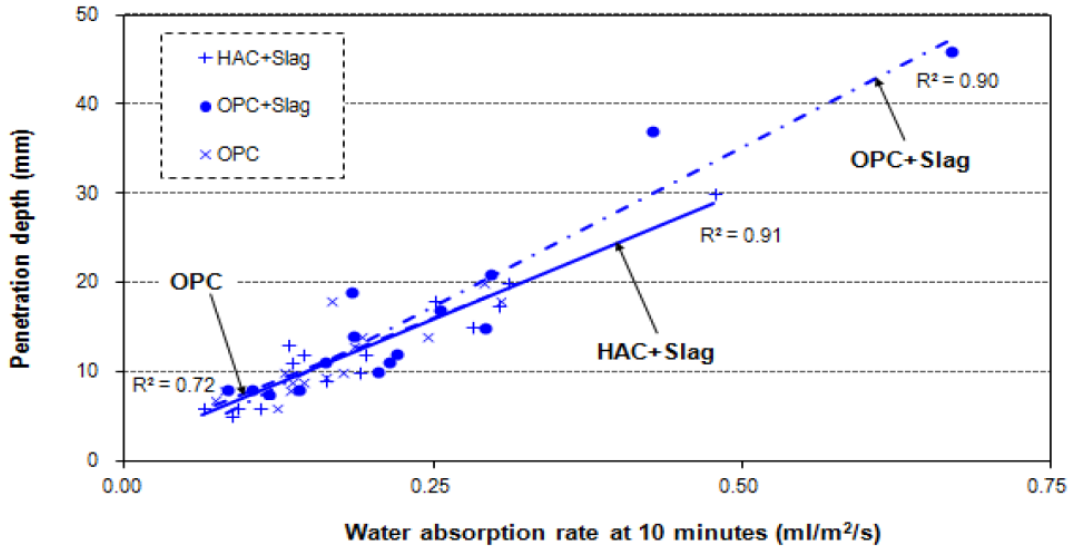

Figure 2-8 Relationship between SWAT and long-term water penetration test

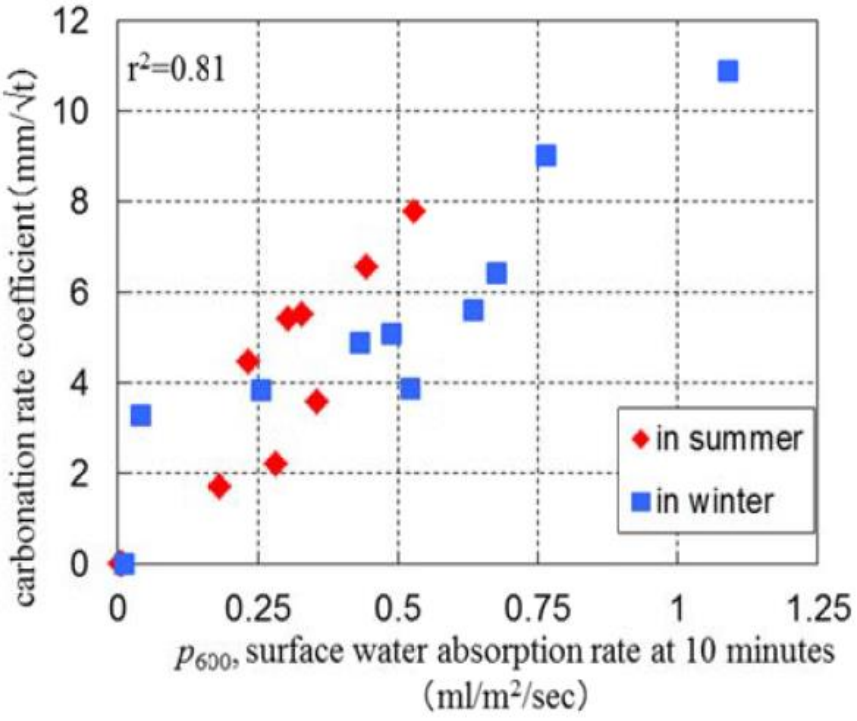

Figure 2-9 Relationship between SWAT and carbonation rate coefficient

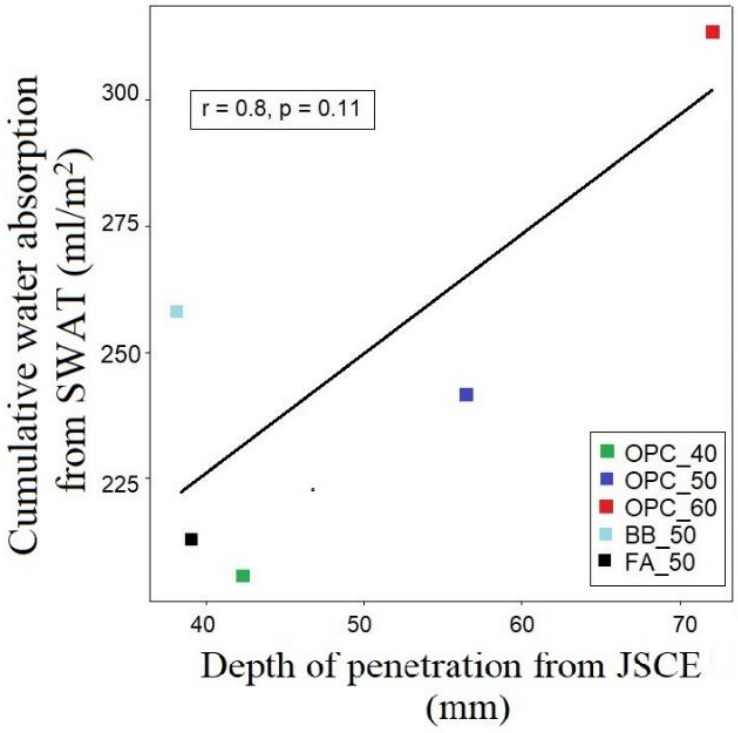

Figure 2-10 Relationship between SWAT and JSCE sorptivity test

The detailed SWAT apparatus (Figure 2-11) measures the resistance of concrete to water absorption under natural dominant water suction. SWAT is composed of a fully automatic machine unit, an absorption cup (80 mm inner diameter and 100 mm outer diameter) with a calibrated cylindrical tube, water inlet and tap, a sensor, a framed vacuum pump for fixing and a water container. The conventional SWAT result, which measures the rate of surface water absorption at 10 minutes, is termed p_{600} (in ml/m^2/s) and the criteria for quality grading proposed by the developers is shown in Table 2-2.

Table 2-2 Grading of covercrete quality by SWAT

Water absorption rate at 10 minutes (600 seconds)	Quality		
	Good	Ordinary	Poor
p_{600} (ml/m^2/s)	<0.25	0.25 - 0.50	> 0.50

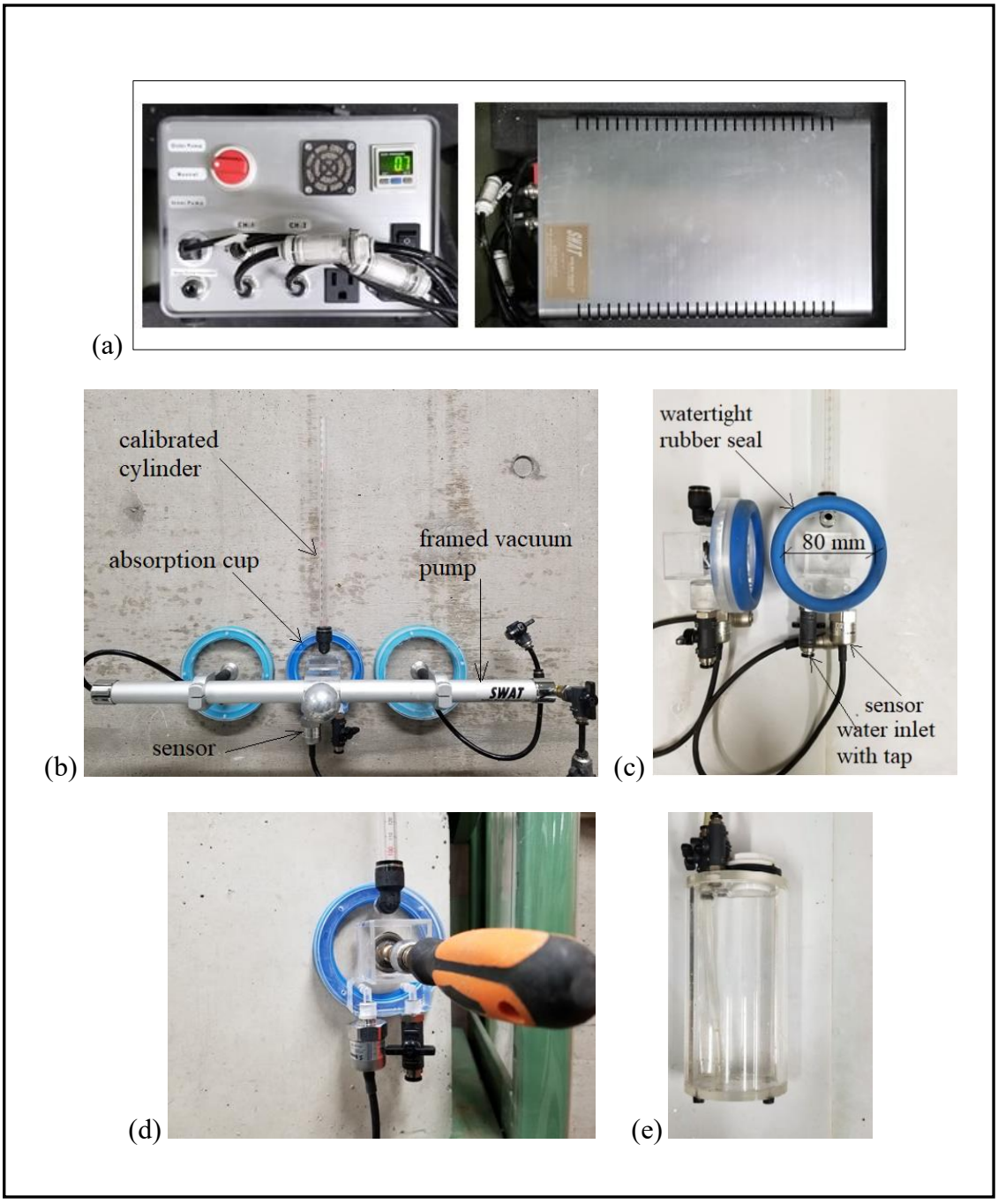

Figure 2-11 Surface Water Absorption Test (SWAT) device (a) machine unit (b) frame for attachment onto big structures; (b) absorption cup detail; (d) clamp for attachment onto small specimens; (e) water container

2.6.3 Autoclam water and air permeability tests

The ‘autoclam’ (Figure 2-12) is a non-destructive test device and was first developed as a water-only permeability test device in the early 1980s by Montgomery [31], [39]. It was further standardized and modified into a fully automatic universal clam for concrete’s water and air permeability test in the early 1990s by Basheer [40] [31].

Autoclam is composed of a control panel box (electronic controller), a base ring and a base unit (autoclam). Three types of tests are possible with the latest autoclam, which uses a microprocessor and allows complete data acquisition to enable easy result analysis by a computer: water absorption, water/air permeability. To measure water absorption (relating to the sorptivity test and corresponding to 200 mm water head by ISAT), a 0.02 bar (2 kPa) pressure is applied [31]. The same test principle is applied for the three available tests except for the different amounts of test pressures for each of the tests. For the water permeability test, the water pressure is maintained at 1.5 bar (150 kPa) while 0.5 bar (50 kPa) is applied for air permeability. The two basic steps for setting up autoclam device are (i) clamping or gluing the steel base ring onto the surface of the test concrete and ensuring air and water tightness (the internal diameter of the base ring is 50 mm) and (ii) clamping the ‘autoclam’ test device onto the base ring.

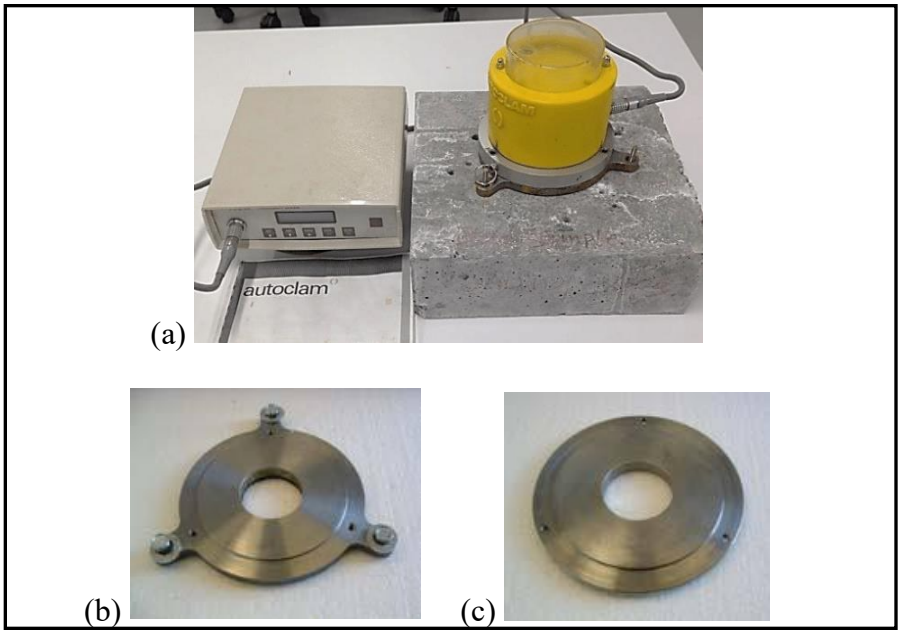

Figure 2-12 Autoclam water and permeability test (a) controller unit with clam (b) base unit (bonding ring type); (b) base unit (bolt-on ring type)

2.6.4 Double chamber air permeability test

The two-chamber air permeability tester (Figure 2-13) was invented in the early 1990s by R. J Torrent of 'Holderbank' Management & Consulting Ltd, Switzerland. It is fully non-destructive and fundamentally based on the principle in which a vacuum of a known airflow geometry is created inside a cell placed on the concrete surface by pumping over a certain period [41]. When the two-chamber vacuum cell is applied on the surface of the concrete, a unidirectional gas flow is generated into the inner chamber and pressure growth is measured. Based on a measured pressure growth and an assumption on the relevant porosity of the concrete tested, its gas permeability *kT* is calculated [14]:

$$kT = \left(\frac{V_C}{A}\right)^2 * \frac{\mu}{2\varepsilon P_a}\left[\frac{In\left(\frac{P_a+\Delta P}{P_a-\Delta P}\right)}{\sqrt{t}-\sqrt{t_o}}\right]^2 \ (\mathrm{m}^2) \qquad [2.16]$$

where V_c: volume of measuring (inner) cell ($2.2*10^{-6}$ m^3), A: cross-section of measuring cell ($19.6*10^{-4}$ m^2), μ: viscosity of air at 20°C ($2.0*10^{-5}$ Ns/m^2), ε : porosity of concrete (0.15), P_a: atmospheric pressure ($\approx$1000 N/m 2), ΔP: pressure increase, measuring cell (< 20 N/m 2), t_o: setting of stopcock, start of measurement (60 s), t: duration of measurement (< 720 s).

It is a fully automatic device with a microprocessor that can allow the transfer of results to a computer and the criterion for quality grading is shown in Table 2-3.

Two-chamber air permeability device is composed of a two-chamber cell (inner and outer chamber) with a diaphragm pressure regulator that keeps the pressure in both chambers balanced and the air pump. The basic operation is: with stopcock 3 open, attach the two-chamber cell on the surface of the test concrete by creating a vacuum in the two cells with the help of a vacuum pump. Stopcock 3 closes when the desired level of vacuum has been attained, and the pump then acts on the outer chamber as a regulator. Then all the excess air flowing into the outer chamber is evacuated allowing for unidirectional airflow in the inner chamber [41].

Table 2-3 Grading of covercrete quality by coefficient of air permeability

Quality	Excellent	Very good	Fair	Poor	Very poor
Coefficient of air permeability kT ($10^{-16}m^2$)	<0.01	0.01-0.1	0.1-1	1-10	>10

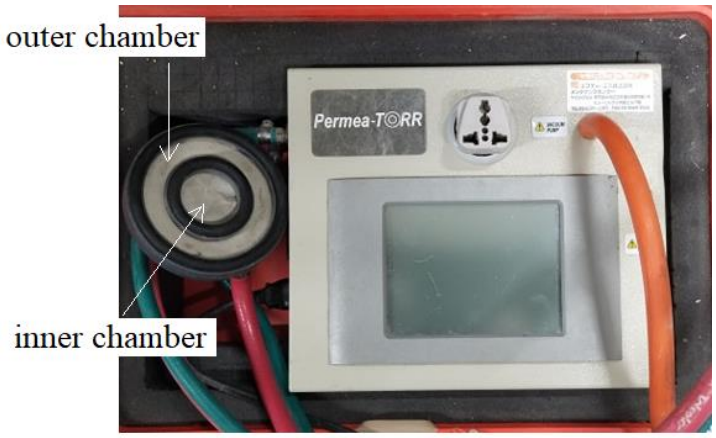

Figure 2-13 Double chamber air permeability test

2.7 Comparison between SWAT and ISAT

A simple comparison of the similarities and differences between SWAT and ISAT is highlighted as follows:

i. In the case of SWAT, concrete quality is evaluated by measuring the resistance against water absorption in 10 minutes while ISAT allows for measurement up to 2 hours.
ii. SWAT device can easily be attached with the aid of the vacuum pump. The easy and non-destructive attachment of the device to the surface of the test concrete is not available in ISAT due to the application of adhesives and resins for enabling water tightness.
iii. While SWAT is easily applied on the site and requires a very short set up time, ISAT due to its complexity in ensuring water tightness requires a longer setup and application time.
iv. The water head for SWAT during testing can vary with an initial water head of about 300 mm and above while a constant water head of 200 mm is required in ISAT for its entire testing duration.

2.8 Evaluation of covercrete quality by electrical resistivity

The electric resistivity of concrete, which is defined as the capability of concrete to prevent the transfer of ions subjected to an electric field [10], depends on the microstructural properties of the concrete such as pore size, pore connections, pore water composition and the degree of saturation of the concrete [8], [10]. Apart from being an important durability indicator of reinforced concrete structures for designing the electrochemical anti-corrosion [8], [26], [42], electrical resistivity is a potential way to access and monitor the moisture condition of in-situ concrete [8].

Electrical resistivity is widely used both as a destructive and nondestructive test and in two respective major ways: quality control test or quality evaluation/ service life prediction test. Several test methods are available for the former such as four-electrode and surface disc methods while the latter is majorly by Wenner (four-probe) resistivity method. Some electrical resistivity test standards include:

- ASTM Standard C1202-10: Standard test method for electrical indication of concrete's ability to resist chloride ion penetration
- AASHTO TP 95 (2011): Standard test method for surface resistivity of concrete's ability to resist chloride ion penetration. American Association of State Highway and Transportation Officials, Washington, D.C., U.S.A
- AASHTO Designation T 358-151: Surface resistivity indication of concrete's ability to resist chloride ion penetration
- JSCE Standards JSCE-K 562-2008: Test method for measuring resistivity of patching repair materials with four electrodes.

2.8.1 Four-probe (Wenner method) electrical resistivity method

The Wenner four-probe method was first introduced at the National Bureau of Standards by F. Wenner in 1915 as a method of measuring earth resistivity [43] and its application evolved to accommodate the measurement of concrete resistivity. The four-probe method (Wenner method) has two major methods for probe array and it is one of

the most applied non-destructive methods of assessing the electrical resistivity of concrete. The array pattern could be a four-point line array (Figure 2-14) or four-probe square array. The advantage of the Wenner method is that the electrical resistivity is simply calculated from the measurement results (by applying voltage and electrical current) using the below equation:

$$\rho = 2\pi a * \frac{V}{I} \qquad [2.17]$$

where ρ: electrical resistivity (Ωm), a : probe spacing (m), V: potential difference between probes (V), I: electrical current flowing through the specimen (A)

The Wenner four-probe method measures the apparent resistivity of the surface of the concrete by Wenner protocol on the assumption that concrete is a semi-finite homogenous material. It is fully a non-destructive method that is used for laboratory quality control tests as well as in-field service life prediction and quality evaluation.

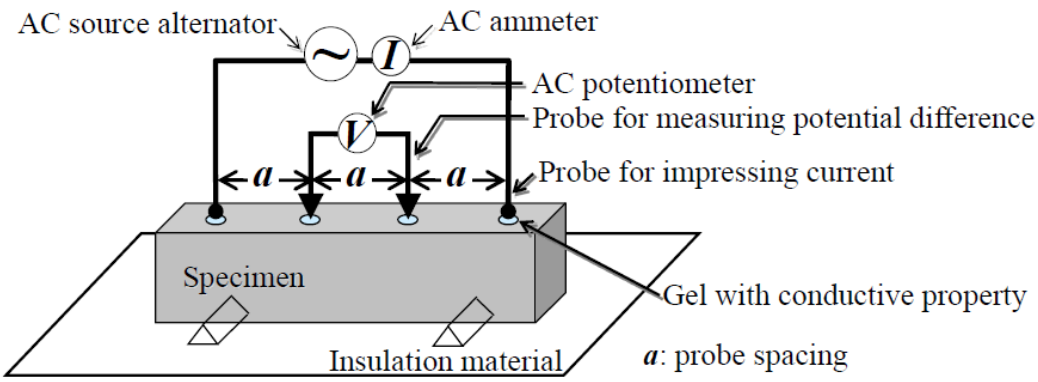

Figure 2-14 Schematic of Wenner (four-point line array) probe method (*culled from[42]*)

2.8.2 Four-electrode (volume resistivity method) electrical resistivity method

The four-electrode electrical resistivity method measures the volume resistivity of the concrete. It uses an alternating current method [44], [45] and sometimes referred to as volume resistivity, bulk resistivity or uniaxial resistivity [10]. The alternating

current method eliminates to some degree, the polarization that exists in the direct current method due to the constant and random movement of the charge carriers as the voltage polarity changes.

The method uses two electrodes and two metal plates. The two electrodes are placed on the surface of the concrete parallel to two metal plates placed on the opposite sides with a moist sponge or conductive material in between (Figure 2-15). It uses standard cylinders/prismatic specimens or concrete cores extracted from existing structures [10] and the geometrical factor is obtained by the equation:

$$k = \frac{A}{L} \qquad [2.18]$$

where A: cross-sectional area perpendicular to the current, L: length of the specimen

Four-electrode resistivity is a laboratory-based quality control test and its application is limited for field investigation due to the requirement of placing the two metal plates on opposite sides of the concrete member.

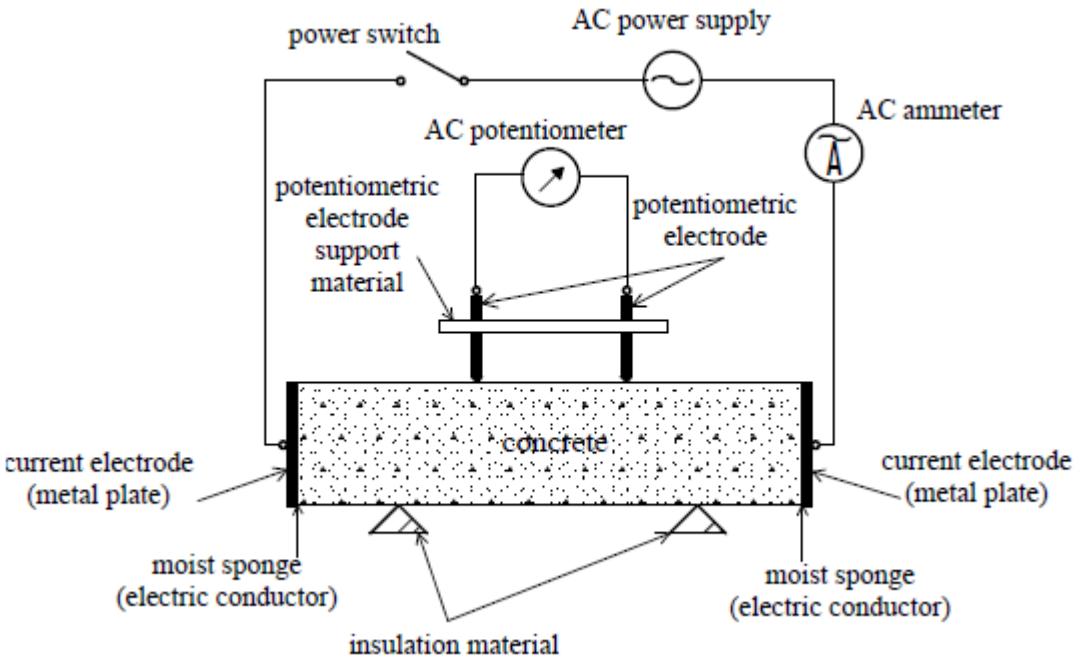

Figure 2-15 Schematic of four-electrode (volume) resistivity method

References

[1] P. Claisse, 'Transport Properties of Concrete' *Woodhead Publishing;* UK, 2014.

[2] M. Sosoro, 'Transport of Organic Fluids through Concrete', *Mat. Struct.*, vol. 31, no. 3, pp. 162–169, Apr. 1998, doi: 10.1007/BF02480390.

[3] Concrete Society, 'Permeability Testing of Site Concrete: A review of methods and experience'. US Department of Commerce, National Technical Information Service, Springfield VA. 22161, 2008.

[4] A. M. Neville, 'Properties of Concrete (4th Edition)' *Pearson Education Limited*, England. 2002.

[5] M. S. Hassani, G. Asadollahfardi, S. F. Saghravani, S. Jafari, and F. S. Peighambarzadeh, 'The Difference in Chloride Ion Diffusion Coefficient of Concrete made with Drinking Water and Wastewater', *Construction and Building Materials*, vol. 231, p. 117182, Jan. 2020, doi: 10.1016/j.conbuildmat.2019.117182.

[6] A. P. Claisse, 'Transport Properties of Concrete: Measurements and Applications' Measurement and Application' *Woodhead Publishing;* UK, 2014.

[7] L. Hanžič, L. Kosec, and I. Anžel, 'Capillary Absorption in Concrete and the Lucas–Washburn Equation', *Cement and Concrete Composites*, vol. 32, no. 1, pp. 84–91, Jan. 2010, doi: 10.1016/j.cemconcomp.2009.10.005.

[8] E. William and J. S. Erik, 'Electrical Resistivity of Concrete'. Directorate of Public Roads, Norwegian Road Research Laboratory, June. 1995.

[9] W. Piasta and B. Zarzycki, 'The Effect of Cement Paste Volume and W/C Ratio on Shrinkage Strain, Water Absorption and Compressive Strength of High-Performance Concrete', *Construction and Building Materials*, vol. 140, pp. 395–402, Jun. 2017, doi: 10.1016/j.conbuildmat.2017.02.033.

[10] P. Azarsa and R. Gupta, 'Electrical Resistivity of Concrete for Durability Evaluation: A Review', *Advances in Materials Science and Engineering*, vol. 2017, pp. 1–30, 2017, doi: 10.1155/2017/8453095.

[11] T. V. Ngo, 'Proposal for Threshold of Moisture Content of Concrete for Appropriate Measurement of Surface Water absorption Test'. *Ph.D. Thesis*'. Yokohama National University, Japan: 2019.

[12] V. T. Ngo, A. Hosoda, S. Komatsu, and N. Ikawa, 'Effect of Moisture Content on Surface Water Absorption Test and Air Permeability Test' *Proceedings of JCI*, vol. 40, p. 6, Jun. 2018.

[13] M. H. Nguyen, K. Nakarai, Y. Kubori, and S. Nishio, 'Validation of Simple Nondestructive Method for Evaluation of Cover Concrete Quality', *Construction and Building Materials*, vol. 201, pp. 430–438, Mar. 2019, doi: 10.1016/j.conbuildmat.2018.12.109.

[14] M. Romer, 'Effect of Moisture and Concrete Composition on the Torrent Permeability Measurement', *Mater. Struct.*, vol. 38, no. 279, pp. 541–547, Apr. 2005, doi: 10.1617/14321.

[15] H. P. Nam and A. Hosoda, 'Improvement of Water and Chloride Penetration Resistance of Slag Concrete by Using High Alite Cement', *Proceedings of JCI*, vol. 36, p. 6, Jun. 2014.

[16] Y. Wang and Y. Xi, 'The Effect of Temperature on Moisture Transport in Concrete', *Materials*, vol. 10, no. 8, p. 926, Aug. 2017, doi: 10.3390/ma10080926.

[17] O. Sengul, 'Use of Electrical Resistivity as an Indicator for Durability', *Construction and Building Materials*, vol. 73, pp. 434–441, Dec. 2014, doi: 10.1016/j.conbuildmat.2014.09.077.

[18] A. Ben Fraj, S. Bonnet, and A. Khelidj, 'New Approach for Coupled Chloride/Moisture Transport in Non-saturated Concrete with and without Slag',

Construction and Building Materials, vol. 35, pp. 761–771, Oct. 2012, doi: 10.1016/j.conbuildmat.2012.04.106.

[19] J. Castro, D. Bentz, and J. Weiss, 'Effect of Sample Conditioning on the Water Absorption of Concrete', *Cement and Concrete Composites*, vol. 33, no. 8, pp. 805–813, Sep. 2011, doi: 10.1016/j.cemconcomp.2011.05.007.

[20] L. J. Parrott, 'Moisture Conditioning and Transport Properties of Concrete Test Specimens', *Materials and Structures*, vol. 27, no. 8, pp. 460–468, Oct. 1994, doi: 10.1007/BF02473450.

[21] P. A. M. Basheer and é. Nolan, 'Near-surface Moisture Gradients and In-situ Permeation Tests', *Construction and Building Materials*, vol. 15, no. 2–3, pp. 105–114, Mar. 2001, doi: 10.1016/S0950-0618(00)00059-3.

[22] K. Yang, P. A. M. Basheer, B. Magee, and B. Y, 'Investigation of Moisture condition and Autoclam Sensitivity on Air Permeability Measurements for both Normal Concrete and High-Performance Concrete', *Construction and Building Materials*, vol. 48, pp. 306–314, Nov. 2013, doi: 10.1016/j.conbuildmat.2013.06.087.

[23] J. J. Ekaputri, A. Bongochgetsakul, T. Ishida, and K. Maekawa, 'Internal Relative Humidity Measurement on Moisture Distribution of Mortar Considering Self-desiccation at Early Ages', vol. 31, no. 1, p. 8, 2009.

[24] C. Antón, M. A. Climent, G. de Vera, I. Sánchez, and C. Andrade, 'An Improved Procedure for Obtaining and Maintaining Well-characterized Partial Water Saturation States on Concrete Samples to be used for Mass Transport Tests', *Mater Struct*, vol. 46, no. 8, pp. 1389–1400, Aug. 2013, doi: 10.1617/s11527-012-9981-4.

[25] M. Khanzadeh Moradllo, C. Qiao, H. Hall, M. T. Ley, S. R. Reese, and W. J. Weiss, 'Quantifying Fluid Filling of the Air Voids in Air Entrained Concrete using Neutron Radiography', *Cement and Concrete Composites*, vol. 104, p. 103407, Nov. 2019, doi: 10.1016/j.cemconcomp.2019.103407.

[26] M. Saleem, M. Shameem, S. E. Hussain, and M. Maslehuddin, 'Effect of Moisture, Chloride and Sulphate Contamination on the Electrical Resistivity of Portland Cement Concrete', *Construction and Building Materials*, vol. 10, no. 3, pp. 209–214, Apr. 1996, doi: 10.1016/0950-0618(95)00078-X.

[27] 'ASTM International Standard Test Method for Measurement of Rate of Absorption of Water by Hydraulic-Cement Concretes C1585-04, December 2007'.

[28] C. Hall, 'Water Sorptivity of Mortars and Concretes: A Review', *Magazine of Concrete Research*, vol. 41, no. 147, pp. 51–61, Jun. 1989, doi: 10.1680/macr.1989.41.147.51.

[29] British Standards Institution., 'Testing Concrete - Recommendations for the Assessment of Concrete Strength by Near-surface Tests, BS 1881, Part 207.' London: BSI, 1992.

[30] 'JSCE-G 582-2018 Standard: Test Method for Water Penetration Rate Coefficient of Concrete Subjected to Water in Short Term'.

[31] A. E. Long, G. D. Henderson, and F. R. Montgomery, 'Why Assess the Properties of Near-surface Concrete?', *Construction and Building Materials*, vol. 15, no. 2–3, pp. 65–79, Mar. 2001, doi: 10.1016/S0950-0618(00)00056-8.

[32] J. H. Bungey, S. G. Millard, and M. Grantham, Testing of Concrete in Structures, 4th ed. London ; New York: Taylor & Francis, 2006.

[33] M. Levitt, 'Non-destructive Testing of Concrete by the Initial Surface Absorption Method'. *Proceedings of Symposium on Non-destructive Testing of Concrete and Timber*, London, 11-12 June 1969. Institution of Civil Engineers, 1970, pp. 23-28, 1969.

[34] K. Hayashi and A. Hosoda, 'Development of Surface Water Absorption Test Applicable to Actual Structures'. *Proceedings of JCI,* vol. 33, No. 1 pp. 1769-1774, 2011. (in Japanese)

[35] K. Hayashi and A. Hosoda, 'Fundamental Study on Evaluation Method of Covercrete Quality of Concrete Structures by Surface Water Absorption Test'. *Journal*

of JSCE, Ser. E2 (Materials and Concrete Structures) Vol. 69, No.1, pp.82-97, 2013. (in Japanese)

[36] S. Komatsu, R. Tajima, and A. Hosoda, 'Proposal of Quality Evaluation Method for Upper Surface of Concrete Slab with Surface Water Absorption Test', *Concrete Research and Technology*, vol. 29, no. 0, pp. 33–40, 2018, doi: 10.3151/crt.29.33.

[37] A. Hosoda and K. Hayashi, 'Evaluation of Covercrete Quality of Concrete Structures by Surface Water Absorption Test', *International Symposium on Concrete and Structures for Next Generation, Ikeda & Otsuki Symposium* (IOS2016), Tokyo, Japan, pp.223-230, 16-18 May 2016.

[38] R. N. Uwazuruonye and A. Hosoda, 'Investigation on Correlation between Surface Water Absorption Test and JSCE Sorptivity Test' *Proceedings of JCI*, vol. 42, p. 7, Jun. 2020.

[39] F. R. Montgomery and A. Adams, 'Early Experience with A New Concrete Permeability Apparatus'. *Proceedings Structural Faults-85*, ICE London, 1985.

[40] P. A. M. Basheer, '"Clam" Permeability Test for Assessing the Durability of Concrete, *Ph.D. Thesis*'. The Queen's University of Belfast, 1991: 438pp, 1991.

[41] R. J. Torrent, 'A Two-chamber Vacuum Cell for Measuring the Coefficient of Permeability to Air of the Concrete Cover on Site', *Materials and Structures*, vol. 25, no. 6, pp. 358–365, Jul. 1992, doi: 10.1007/BF02472595.

[42] H. Minagawa, S. Miyamoto, and M. Hisada, 'Relationship of Apparent Electrical Resistivity Measured by Four-Probe Method with Water Content Distribution in Concrete', *Journal of Advanced Concrete Technology*, vol. 15, no. 6, pp. 278–289, 2017, doi: 10.3151/jact.15.278.

[43] F. Wenner, 'A Method of Measuring Earth Resistivity', *Bulletin of the Bureau of Standards*, p. 10: 1916

[44] , Committee on Concrete S.-C. on T. M. and S., 'JSCE Standards "Test Method for Measuring Resistivity of Patching Repair Materials with Four Electrodes"', *JSCE*

Journal of Materials, Concrete Structures and Pavements, vol. 64, no. 3, pp. 427–434, 2008, doi: 10.2208/jsceje.64.427.

[45] S. W. Tang *et al.*, 'The Review of Pore Structure Evaluation in Cementitious Materials by Electrical Methods', *Construction and Building Materials*, vol. 117, pp. 273–284, Aug. 2016, doi: 10.1016/j.conbuildmat.2016.05.037.

Chapter 3

Establishing a Simple Method for Preconditioning of Concrete Specimens to Obtain Uniform Moisture Condition

3.1 Introduction

The resistance of concrete to mass transfer is a very important property regarding the quality assurance and service life prediction of concrete structures. Several mechanisms such as migration, diffusion, capillary suction and permeation are either independently or simultaneously responsible for the ingress of deleterious substances into the matrix of concrete [1]. The interaction zone between the concrete and the environment, which is the surface (10 -50 mm thick layer - 'covercrete' [2]), contributes a great deal and is known to be the most vulnerable resulting from the impact of concreting works and the heterogeneous nature of concrete.

Moisture content and moisture distribution, especially at the covercrete, is one of the most influential conditions affecting the transport properties of concrete [1] and has remained the limitation for almost every near-surface absorption and permeability tests[3].

This chapter presents the investigations conducted to establish a simplified method for obtaining an equilibrium moisture distribution throughout the volume of experimental concrete samples by varying sealing materials, sealing conditions and temperature.

3.2 Past researches

Several experimental investigations that adopted 50°C temperature for drying and conditioning of concrete samples to moisture equilibrium have been reported [1], [4]–[6]. Parrot [4] reported the conditioning to equilibrium moisture distribution of 100 mm concrete cubes by drying and sealing in a lidded plastic container at 50°C. The relative

humidity was monitored at two locations: the surface of the concrete and 35 mm depth from the surface through a 20 mm diameter cylindrical cavity. William and Erik [6] conditioned 100 mm (length) x 20 mm (width) x 50 mm (height) OPC prismatic specimens (0.6 w/c ratio) in two separate series, the desorption and absorption, at 50°C and defined the outer edge of the hysteresis curve. For desorption, [6] dried saturated specimens from 90% and down to 80% by open-air while below 80% drying was accomplished at 50°C oven drying and equilibrium moisture distribution for both desorption and absorption processes were obtained by sealing with plastic. The RILEM TC 116-PCD [5] recommended drying and redistribution steps to obtain moisture equilibrium in normal grade concrete for the measurement of gas permeability and capillary absorption of water. Both pre-drying and redistribution phases are performed at 50°C temperature (and the lateral sides of the specimens sealed with impermeable and tight materials) which leads to a homogeneous distribution of the equilibrium evaporable water content at 75 ± 2% relative humidity in ϕ150 mm x 50 mm thick specimens. A proposal for 'an improved procedure for obtaining and maintaining well-characterized partial water saturation states on concrete samples to be used for mass transport tests' [1] propounded a drying and redistribution curves obtained at 50°C drying and conditioning to equilibrium moisture distribution for medium-strength OPC concrete (ϕ100 mm x 30 mm), using water/cement ratios between 0.38 and 0.60.

It has been noted that conditioning at the temperature of 50°C could adversely affect the microstructure of concrete depending on the degree of hydration. To counter the effects of conditioning at 50°C temperature on the microstructure of concrete samples, Antón et al [1] cured the concrete specimens by total immersion into a saturated $Ca(OH)_2$ solution for one year. Before drying, [1] sealed the lateral sides of the samples with vinyl electric insulation tape to ensure unilateral moisture movement and utilized polypropylene lidded container in sealing the samples to attain moisture equilibrium. The utilized samples were obtained by slicing ϕ100 mm x 110-130 mm cylindrical specimens, which resulted in the exposure of coarse aggregate, making the samples unrepresentative of the covercrete.

3.3 Experimental programme

3.3.1 Materials used

For a wider range of concrete types, specimens were prepared with ordinary Portland cement (OPC) and ground granulated blast furnace slag cement (JIS type B slag cement). Table 3-1 shows the concrete mix proportion. For each of the concrete mix designs, prismatic specimens measuring 150 mm × 150 mm × 75 mm were prepared. Threaded M4 moisture sensors were embedded at 10 mm, 25 mm, 30 mm, 45 mm, 50 mm and 60 mm depths from the surface (Figure 3-1) to monitor the internal moisture distribution during preconditioning.

The concrete specimens were named as OPC40 for OPC concrete 40% W/C, as OPC50 for OPC concrete 50% W/C, as OPC60 for OPC concrete 60% W/C, and BB50 for BB cement concrete 50% W/C. The specimens were de-moulded after 1 day of placement and cured in water for 6 days. Thereafter sealed and kept in a controlled environment at a temperature of 20°C and relative humidity of 60% until 90 days after casting before test preparations and actual tests were conducted.

Table 3-1 Concrete mix proportion 1

Specimen name	s/a ratio (%)	W/C ratio (%)	Mix composition (kg/m^3)				Admixtures type[1] and dosage[2] (%)	
			Water	Cement	Sand	Coarse aggregate (20 mm max)	Ad	AE
OPC40	45	40	160	400	777	950	1.0	0.0025
OPC50	47	50	160	320	841	948	1.0	0.0025
OPC60	48.5	59.9	160	267	890	945	1.0	0.0025
BB50	47	50	160	320	841	950	1.0	0.0025

[1] *Admixture types, Ad: water-reducing admixture, AE: Air entraining agent*
[2] *Admixture dosage: percentage of admixtures to binder, weight-to-weight ratio*

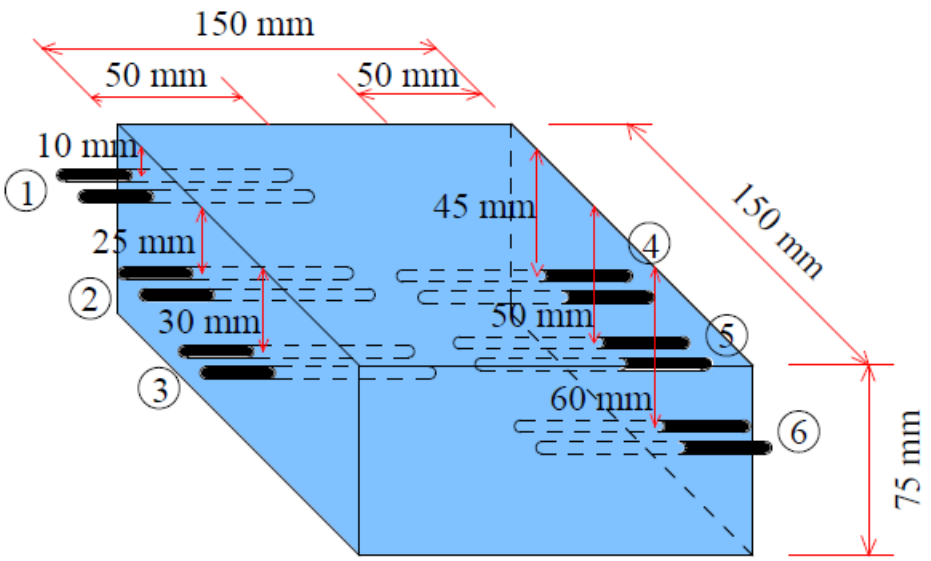

Figure 3-1 Description of the prismatic specimen (no 1) showing M4 sensor locations

3.3.2 Experimental Variables

Two different temperatures were selected for drying and moisture redistribution. Since extensive research has adopted 50°C temperature for conditioning [1], [4]–[6], this temperature was first selected. Given the effects of the temperature of sample conditioning on the absorption properties of concrete [7], [8] and the possible effect of 50°C on the microstructural change of the concrete [1], 40°C temperature was also selected for drying and moisture redistribution.

3.3.3 Specimen preparations and sealing materials

Based on the literature review, careful selection of sealing material for moisture redistribution, to obtain moisture equilibrium throughout the volume of the specimen was done. To ensure unilateral moisture movement during drying, preconditioning and for easy and less redistribution time, vinyl electric insulation tape was used to seal the lateral sides of the specimens [1] in the four sealing conditions before adding other different sealing material. The sealing materials were combined and designated as sealing type A, sealing type B, sealing type C and sealing type D as illustrated below:

Type A: Vinyl Electric Insulation Tape only

Type B: Vinyl Electric Insulation Tape with Polypropylene Lidded Container

Type C: Vinyl Electric Insulation Tape with Aluminum Polythene Sheet

Type D: Polythene Sheet with Tape

3.3.4 Preconditioning and measuring

The prismatic specimens were saturated by complete immersion in water and stepwise drying and moisture redistribution was carried out as follows:

- After saturation of pores by total immersion into water, the four sides of the prismatic specimens were sealed with vinyl electric insulation tape to ensure unilateral moisture transfer during drying and conditioning
- Stepwise drying for about 4 to 5 hours was done in an oven at the temperature of 40^{o}C and moisture redistribution (to attain moisture equilibrium throughout the volume of the specimens) was conducted by sealing the two remaining faces with

the different materials (type a to d) explained in section 3.3.3. The same procedure was conducted with the sealing materials using 50ºC temperature for drying and moisture redistribution.

Moisture movement during redistribution was constantly monitored for the specimens with the respective sealing materials until moisture equilibrium is obtained in any one of the sealed conditions. Then, the specimens were withdrawn from the oven and allowed to cool to a temperature of 20 – 25ºC by natural heat loss inside closed containers before measurements were taken for all the sealing conditions. Drying and moisture redistribution was repeated in this manner.

3.3.4.1 Kett HI-800 Moisture Meter

Kett HI-800 is an electrical resistance-type moisture meter (Figure 3-2), made by Kett Electric Laboratories, Tokyo, Japan, which is composed of an integrated unit and sensor connecting section. The output is expressed in percentage or count values and the investigated relationship between the two outputs is shown in Figure 3-3. It was previously confirmed by [9] (Figure 3-4) that HI-800 count values have an inverse linear relationship with electric resistance.

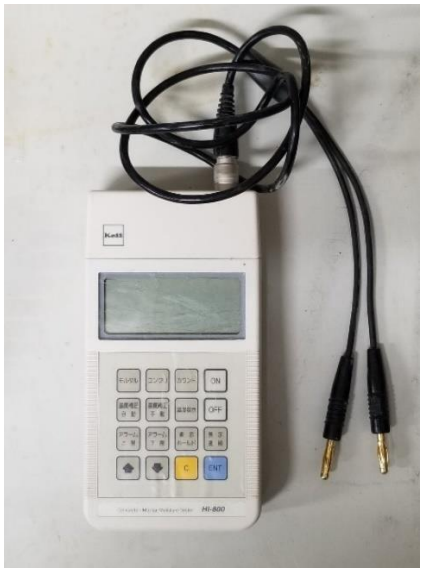

Figure 3-2 Kett HI-800 moisture meter

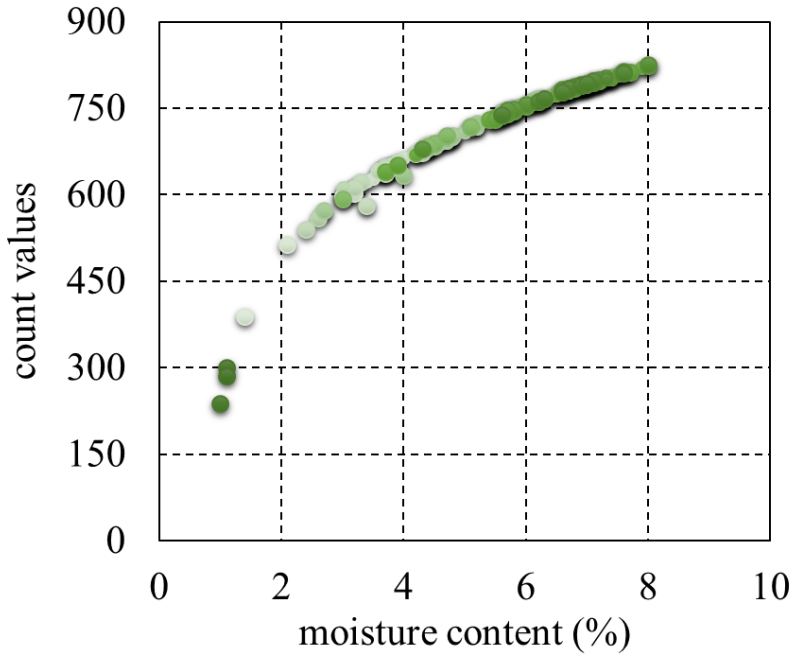

Figure 3-3 Count values versus percentage values of Kett HI-800 moisture meter

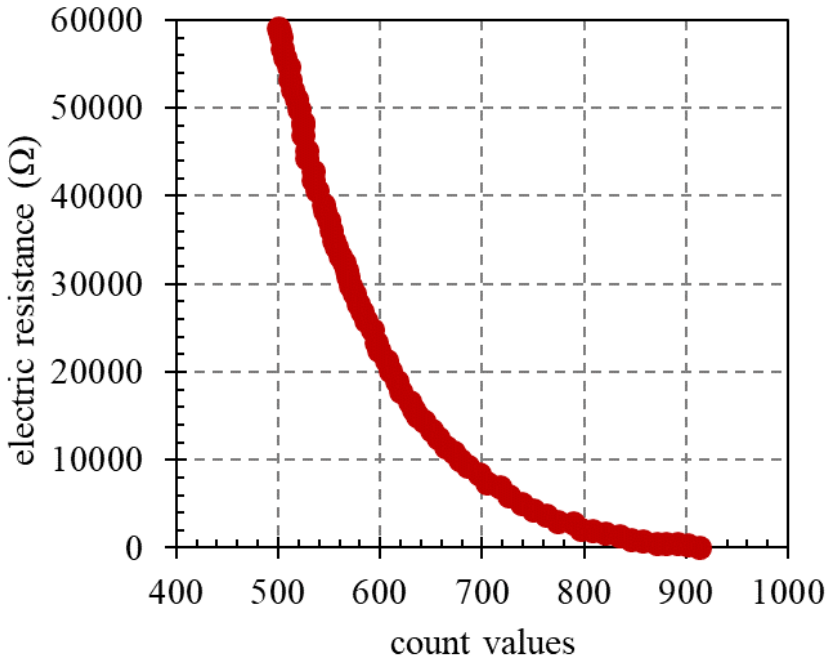

Figure 3-4 Relationship between electrical resistance and kett HI-800 count values (*culled from [9]*)

3.3.4.2 M4 Threaded Electrode Moisture Sensor

Stainless φ 4 mm threaded rods- M4 were embedded in pairs (10 mm apart) into the concrete as the connecting electrodes to the HI-800 moisture meter and the output was expressed in count values. The threaded M4 moisture sensors were embedded at 10 mm, 25 mm, 30 mm, 45 mm, 50 mm and 60 mm depths from the surface and designated as point 1, point 2, point 3, point 4, point 5 and point 6 respectively. Moisture movement during the redistribution was constantly monitored until equilibrium moisture distribution was achieved.

3.4 Results and discussions

Some typical plots of the kett HI-800 values against the moisture content distributions obtained at experimental temperatures of 50ºC and 40ºC for the four different sealing materials are shown in Figures 3-5 and 3-6 respectively.

For the experimental temperature of 50ºC, moisture equilibrium throughout the specimens for several pore water saturation degrees was achieved through only two sealing materials: sealing type B *(vinyl electric insulation tape with polypropylene lidded container)* and sealing type C *(vinyl electric insulation tape with a polythene sheet).* It was observed that higher moisture loss and weight change after drying until the time of attaining equilibrium moisture distribution during redistribution was seen in specimens by sealing type B than in specimens by sealing type C. The higher moisture loss may be because of a large room for moisture movement between the two surfaces of the specimen and the polypropylene lidded container. While moisture profile of specimen from sealing type D was almost constant from the beginning to the end of redistribution (as moisture movement within the specimen was observed to have been inhibited by the combination of polythene sheet and aluminum tape), that of sealing type A could not support moisture redistribution into obtaining equilibrium moisture content.

As shown in Figure 3-6, equilibrium moisture distribution at 40ºC preconditioning temperature was achieved by only sealing type C *(vinyl electric*

insulation tape with a polythene sheet). The reduction of 10°C resulted in non-achievement of equilibrium moisture distribution of specimens by sealing type B. Similar to the preconditioning at 50°C, sealing types A and D could not support the redistribution of pore water to achieve equilibrium moisture distribution.

When the effect of preconditioning temperature on the microstructure of concrete is put into consideration, which necessitated curing of the concrete samples in a saturated $Ca(OH)_2$ solution for one year by [1], it becomes beneficial to adopt sealing type C at 40°C preconditioning temperature in achieving equilibrium moisture distribution for experimental specimens.

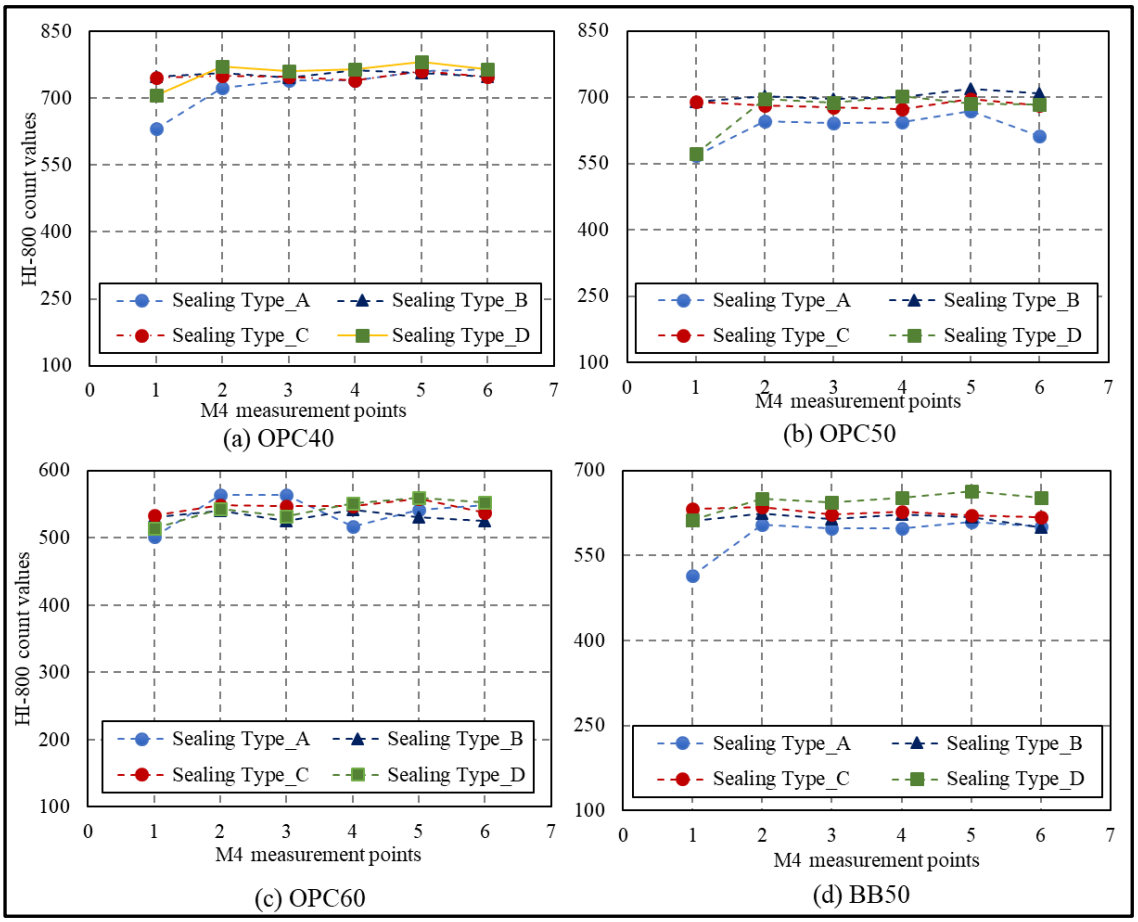

Figures 3-5 Preconditioned concrete at 50°C for four sealing conditions to obtain equilibrium moisture distribution

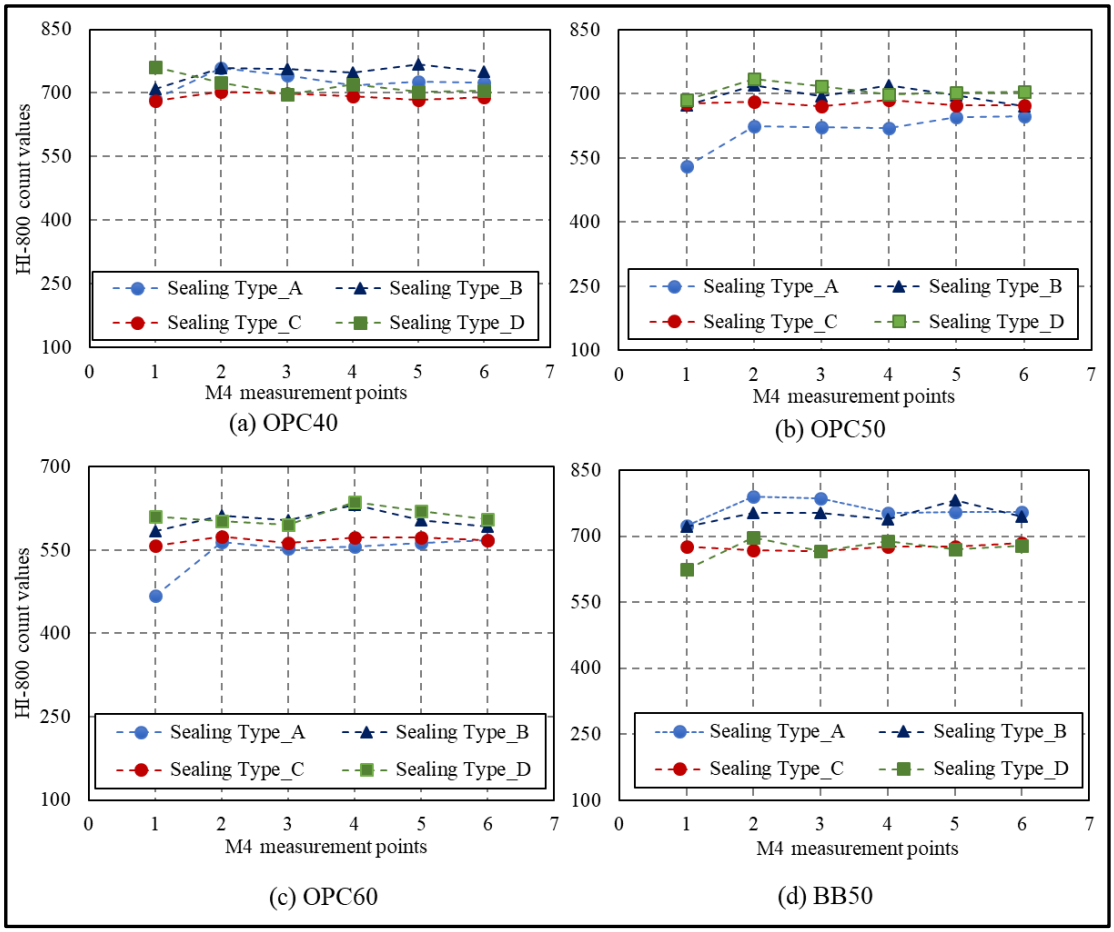

Figures 3-6 Preconditioned concrete at 40ºC for four sealing conditions to obtain equilibrium moisture distribution

3.5 Summary of Findings

Based on the results of the present experimental work which utilized 150 mm x 150 mm x 75 mm ninety-day old prismatic concrete specimens (ordinary Portland cement with 0.4%, 0.50% and 0.60 % water-to-cement ratio and ground granulated blast furnace slag cement-JIS type B slag cement with 0.50% water-to-cement ratio), it may be stated that the proposed steps could be used to obtain equilibrium moisture distribution throughout the volume of concrete specimens at many water saturation degrees of pore voids. At preconditioning temperature of 40ºC, the combination of vinyl electric insulation tape and polythene sheet as sealing materials could be used to obtain equilibrium moisture distribution in concrete specimens. The steps involve a desorption

process as follows: saturate the permeable pore voids by total immersion into water, seal the lateral sides with vinyl electric insulation tape, dry at 40ºC to the desired weight, seal the two remaining surfaces with a layer of polythene sheet and return to 40ºC temperature until equilibrium moisture distribution is attained.

References

[1] C. Antón, M. A. Climent, G. de Vera, I. Sánchez, and C. Andrade, 'An Improved Procedure for Obtaining and Maintaining Well Characterized Partial Water Saturation States on Concrete Samples to be Used for Mass Transport Tests', *Mater Struct*, vol. 46, no. 8, pp. 1389–1400, Aug. 2013, doi: 10.1617/s11527-012-9981-4.

[2] M. Romer, 'Effect of Moisture and Concrete Composition on the Torrent Permeability Measurement', *Mater. Struct.*, vol. 38, no. 279, pp. 541–547, Apr. 2005, doi: 10.1617/14321.

[3] A. E. Long, G. D. Henderson, and F. R. Montgomery, 'Why Assess the Properties of Near-Surface Concrete?', *Construction and Building Materials*, vol. 15, no. 2–3, pp. 65–79, Mar. 2001, doi: 10.1016/S0950-0618(00)00056-8.

[4] L. J. Parrott, 'Moisture Conditioning and Transport Properties of Concrete Test Specimens', *Materials and Structures*, vol. 27, no. 8, pp. 460–468, Oct. 1994, doi: 10.1007/BF02473450.

[5] 'RILEM TC 116-PCD (1999) Recommendations: Preconditioning of Concrete Test Specimens for the Measurement of Gas Permeability and Capillary Absorption of Water'. *Materials and Structures* 32: 174-176.

[6] E. William and J. S. Erik, 'Electrical Resistivity of Concrete'. Directorate of Public Roads, Norwegian Road Research Laboratory, Jun. 1995.

[7] J. Castro, D. Bentz, and J. Weiss, 'Effect of Sample Conditioning on the Water Absorption of Concrete', *Cement and Concrete Composites*, vol. 33, no. 8, pp. 805–813, Sep. 2011, doi: 10.1016/j.cemconcomp.2011.05.007.

[8] S. Zhutovsky and R. Douglas Hooton, 'Role of Sample Conditioning in Water Absorption Tests', *Construction and Building Materials*, vol. 215, pp. 918–924, Aug. 2019, doi: 10.1016/j.conbuildmat.2019.04.249.

[9] Hayashi K., Akmal U., and Hosoda A., 'Analysis of Moisture Transfer is Surface Water Absorption Test of Concrete using Embedded Senors', *Proceedings of JCI*, vol. 35, p. 6, Jun. 2013. (in Japanese)

Chapter 4

Percentage Saturation Degree of Permeable Pore Voids (PSD) and Its Effects on SWAT and Electrical Resistivity

4.1 Introduction

The penetration of water into concrete, as well as other harmful solutes and ions (such as chlorides, sulphates), is considered of great importance as it is virtually the beginning of all deterioration processes. This explains why the moisture content of concrete is a very important factor in-field assessment of the covercrete quality and durability in general. Over the years, the moisture content of concrete has been measured and expressed in three major forms as explained in chapter 2 (section 2.8). In all the forms of measurement and expression of moisture content of concrete, the pore structure (pore voids, pore connectivity, and pore radius) is not directly considered, irrespective of the fact that the pore structure governs mass transfer in concrete[1]. Also, it has been observed from the forms of expressing moisture content of concrete that a total saturation by immersion into water is shown. However, the total saturation of permeable pore voids of concrete cannot be achieved by complete immersion into water. Evidence of this is that at the so-called saturated state, surface water absorption still occurs when the presumed saturated concrete is subjected to test. Furthermore, this has been made clear by the ASTM standards test C 642-97 by specifying a 5-hour boiling in of water-saturated concrete.

Within the context, the objectives of this chapter are to;

(1) Propose a mathematical formula for the calculation of the percentage saturation degree of permeable pore voids (PSD) of concrete and establish the same as an enhanced way to measure and express the absolute moisture content of concrete relating to the permeable pore voids.

(2) Calibrate kett HI-100 and HI-520-2 surface moisture meters for on-site NDT measure of moisture content of concrete as a percentage of the permeable pore voids.
(3) Investigate the relationship between PSD and SD of concrete.
(4) Investigate the effects of PSD on SWAT and establish the threshold and edge saturation degrees of permeable pore voids (PSD) before starting SWAT for an accurate evaluation of the quality of covercrete.
(5) Verify the application of the proposed threshold moisture contents for field durability assessment of covercrete quality and propose the most appropriate surface moisture meter to be used in combination with SWAT during field assessment of covercrete quality.
(6) Investigate the effects of PSD on electrical resistivity

4.2 Theoretical background for PSD

In this section, the basic principle of the derivation of the equation for the calculation of PSD is introduced. The formula derived its course from the ASTM International designation C 642-97; Standard test method for density, absorption, and voids in hardened concrete[2]. For clarity purposes, a recap of the said ASTM standard test method is necessary.

4.2.1 ASTM C 642

The determination of permeable pore space (voids in %) in concrete involves four steps in the experimental standard test method of the ASTM C 642. The steps are;

(1) Determination of oven-dry mass of the specimen; The specimen is oven-dried at a temperature of 100 to 110ºC for not less than 24 hours. Thereafter, the specimen is allowed to cool in dry air (preferably in a desiccator) to a temperature between 20 to 25ºC and the mass is determined. The process is repeated until the two successive mass values have a difference of less than 0.5% of the lesser mass value. The value of the mass is then designated as A: *oven-dry mass*.

(2) Determination of saturated mass after immersion; After obtaining the oven-dry mass, the specimen is immersed in water at approximately 21°C for not less than 48 hours, surface water is removed with a towel and the mass is determined. The process is repeated until two successive mass values have a difference of less than 0.5% of the higher mass value. The obtained mass value is then designated as *B*.

(3) Determination of saturated mass after boiling; After step 2 above, the specimen is then placed in a suitable receptacle, covered with tap water and boiled for 5 hours. Thereafter, it is allowed to cool for no less than 14 hours to a temperature between 20 to 25°C by a natural loss of heat. The surface moisture is removed with a towel and the mass is determined and designated as *C*.

(4) Determination of immersed apparent mass; the specimen obtained from step 3 above is suspended by a wire and the apparent mass in water is obtained and designated as *D*.

The obtained designated values are applied for the following calculation shown in equations (3)-(5). :

$$volume\ of\ permeable\ pore\ space\ (void)\% = (g_2 - g_1)/g_2\ X\ 100 \quad [4\text{-}1]$$

$$g_1\ (bulk\ density,\ dry) = [A/(C-D)].\ \rho \quad [4\text{-}2]$$

$$g_2\ (apparent\ density) = [A/(A-D)].\ \rho \quad [4\text{-}3]$$

where: *A* is Oven-dry mass, *C* is Saturated mass after boiling, *D* is Immersed apparent mass, ρ is Density of water.

4.2.2 PSD calculation formula

As shown in the mathematical expressions above, the volume of permeable pore voids of concrete (in %) is calculated using values for mass determined by oven drying, saturated mass after immersion/boiling and immersed apparent mass. Since the total permeable pore void is calculated by the combination of absorption through immersion and desorption through drying, it is implied that at saturation, the total percentage of permeable pore space is filled by water, hence, 100% PSD. The PSD is calculated by the following equation:

Percentage saturation degree of permeable pore voids (PSD)

$$= 100 - [\ (100 \times PPS_h) / PPS_d\ ] \quad [4\text{-}4]$$

where: PPS_h is Permeable pore space at partially saturated state, PPS_d is Permeable pore space at completely dried state.

Permeable pore space at partially saturated state, PPS_h, is the permeable pore space obtained when the partially saturated state which is under consideration is assumed as the completely saturated state

4.3 Experimental programme

4.3.1 Materials used

Two sets of concrete were prepared for this study. Table 4-1 summarises the nine different types of concrete in the first set employed in the investigation of moisture content as a percentage and its effects on SWAT while Table 4-2 is a summary of the five different types in the second set employed to investigate the effects of PSD on electrical resistivity.

(1) Concrete specimens in set 1

Ordinary Portland cement was used to prepare prismatic specimens. The prismatic concrete specimens, 300 mm x 150 mm x 300 mm height were cast with wooden form following the mix design in Table 4-1. Three different mixtures were prepared in total with different water-to-cement ratios (0.40, 0.50, and 0.60). For each of the mix design, two prismatic specimens were prepared with an M4 embedded moisture sensor at 5 mm, 10 mm, 15 mm, 30 mm and 50 mm from the surface to monitor the internal moisture distribution. The specimens were prepared for validation and verification of PSD for structures under natural environmental exposure. Four additional specimens were prepared for the selected specimens indicated in Table 4-1 from which cores were taken for preconditioning and subsequent PSD testing its effects on SWAT.

The specimens with 0.40 water-to-cement ratios were designated OPC-40, 0.50 water-to-cement ratio were designated OPC-50 while 0.60 water-to-cement ratios were

OPC-60. To verify the effects of curing conditions on PSD, OPC-60 specimens were cured with three different conditions. They were 1 day in mould, 7 days in the mould and 1 day in mould plus 6 days in water. To distinguish the curing conditions, the designation of the specimens were further advanced to OPC-40-1D (for 1 day in the mould), OPC-40-7D (for 7 days in the mould), OPC-40-1D6W (for 1 day in mould plus 6 days in water), OPC-50-1D (for 1 day in the mould), OPC-50-7D (for 7 days in the mould), OPC-50-1D6W (for 1 day in mould plus 6 days in water), OPC-60-1D (for 1 day in the mould), OPC-60-7D (for 7 days in the mould), OPC-60-1D6W (for 1 day in mould plus 6 days in water). The 7 days in mould curing condition were selected to replicate the common curing condition in real concrete structures.

Table 4-1 Concrete mix proportion 2

Specimen name	s/a ratio (%)	W/C ratio (%)	Mix composition (kg/m^3)				Admixtures type[1] and dosage[2] (%)	
			Water	Cement	Sand	Coarse aggregate (20 mm max)	Ad	AE
[O] OPC-40-7D	45	40	160	400	777	950	1.1	0.2
OPC-40-1D6W	45	40	160	400	777	950	1.1	0.2
[O] OPC-50-7D	47	50	160	320	841	948	1.0	0.2
OPC-50-1D6W	47	50	160	320	841	948	1.0	0.2
[O] OPC-60-1D	48.5	60	160	267	890	945	1.0	0.1985
[O] OPC-60-7D	48.5	60	160	267	890	945	1.0	0.1985
OPC-60-1D6W	48.5	60	160	267	890	945	1.0	0.1985

[O] Selected specimens without embedded M4 moisture sensor from which cores were extracted: [1] Admixture types, Ad: water-reducing admixture, AE: Air entraining agent
[2] Admixture dosage: percentage of admixtures to binder, weight-to-weight ratio

After curing, the specimens were left in room condition until a period of seventeen months (1year and 5months) from the time of casting. The long period before testing was necessary to achieve a desirable maturity and to eliminate the possibilities of microstructural changes in pores and re-hydration during tests[3], [4].

(1) Concrete specimens in set 2

To evaluate the effects of PSD on electrical resistivity, prismatic specimens measuring 100 mm x 100 mm x 400 mm were prepared with five types of concrete shown in Table 4-2. The names of the specimens were coded to portray the cement type, water-binder ratio and type of curing. The type of curing adopted after placement was 28 days in mould. The specimens were left in room condition after curing until seven months from the time of casting before commencing the tests.

Table 4-2 Concrete mix proportion 3

Specimen name	s/a ratio (%)	w/b ratio (%)	Water (kg/m^3)	Binder type[1] (kg/m^3)			Admixtures (kg/m^3) type[2] and dosage[3] (%)		Coarse aggregate (20 mm max) (kg/m^3)
				N	BB	FA	Ad	AE	
N40-28D	45.0	40	160	400	-	-	1.0	0.0015	973
N50-28D	47.0	50	160	320	-	-	1.0	0.0015	975
N60-28D	48.5	60	160	267	-	-	0.8	0.0015	970
BB50-28D	46.7	50	160	-	320	-	0.8	0.0015	975
FA41-28D	47.7	41.6	154	308	-	62	1.0	0.0045	975

[1] Binder types N: ordinary Portland cement, BB: ground granulated blast furnace slag cement (JIS type B slag cement), FA: JIS type II fly ash (FA) as 20% by weight of OPC replacing fine aggregate
[2] Admixture types, Ad: water-reducing admixture, AE: Air entraining agent
[3] Admixture dosage: percentage of admixtures to binder, weight-to-weight ratio

4.3.2 Extraction of test samples and preparations

Concrete cores (φ100 mm) were taken from the selected prismatic specimens without embedded sensors shown in table 4-1 (OPC-40-7D, OPC-50-7D, OPC-60-1D and OPC-60-7D) across the 150 mm thickness (see Figure. 4-1(a)). The cores with two formwork-finished faces (Figure 4-1(b)) were then sliced at 45 mm (as shown in Figure 4-1(c)) from the surface with a dry-type concrete cutter to form samples φ100 mm x 45 mm. The choice of this specimen size was made to satisfy the volume of the test specimen adopted in ASTM C 642-97 for the determination of the permeable pore voids in hardened concrete. Secondly, the chosen specimen size will ensure easy moisture

redistribution for eliminating the moisture gradient. For each specimen type, 20 samples were prepared and preconditioned to have several saturation degrees. Two specimens were tested for each saturation degree.

(a)

(b)

(c)

Figure 4-1 Extraction of samples from prismatic specimens

4.3.2.1 Conditioning of samples

To achieve the desired percentage saturation degrees of permeable pore void in the specimens, the cylindrical specimens were pre-conditioned before conducting Surface Water Absorption Test and other measurements. Also as earlier stated, it was

necessary to redistribute the internal moisture in the specimens to eliminate the possible effects of the moisture gradient on surface water absorption.

First, the cylindrical specimens were saturated by total immersion in water. Thereafter, the lateral surfaces of the cylindrical specimens were sealed with vinyl electric insulation tape, to eliminate trilateral moisture transfer during pre-conditioning [4]. The specimens were then pre-conditioned in a controlled humidity chamber, where constant RH and temperature was maintained throughout the study. The inside RH and temperature of the chamber were 50% and 40^{o}C respectively. The efficient temperature and RH were carefully selected after a series of preliminary investigations to eliminate the possibility of microstructural change. The drying of the specimens was continued until the desired kett HI-100 surface moisture tester count values are achieved. Afterward, the two surfaces of the specimens were sealed with a layer of polythene sheet to enable redistribution of the internal moisture. The moisture redistribution time for each of the PSD was calculated by multiplying the drying time (used in attaining that particular PSD) by 2. The decisions on the sealing materials and the moisture redistribution time were made based on several preliminary investigations conducted on similar specimens with many sealing materials. Also, the previous research conducted with different sealing materials by Antón et al. revealed a similar moisture redistribution time.

4.3.2.2 Exposure of specimens to a natural environment

To verify the applicability of PSD and the moisture meter calibration curves obtained from the preconditioned samples, the specimens with embedded sensors were exposed to the natural environment. The specimens were kept in two different orientations (shown in Figure 4-2): wall orientation and slab orientation. The internal moisture distribution and moisture contents on the surface were monitored.

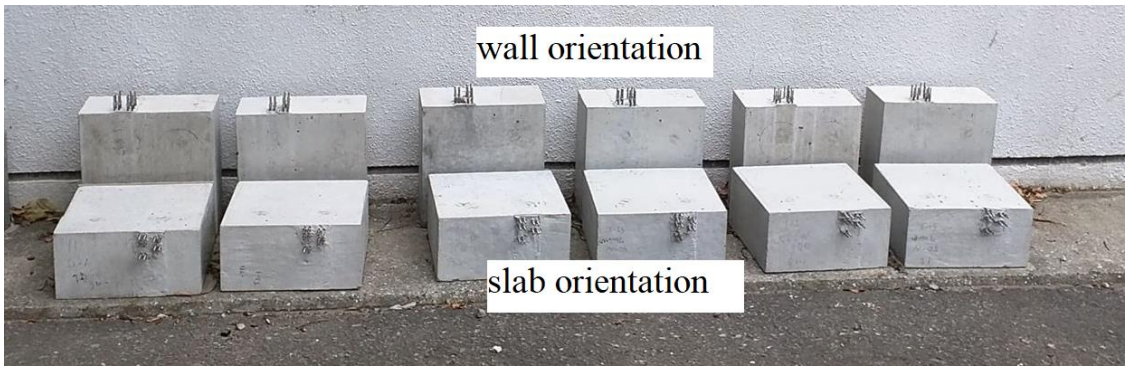

Figure 4-2 Exposure condition of specimens to a natural environment

4.3.3 Measurements and testing

Specimens were allowed to cool down to 20-25ºC in a different closed chamber before the sealing materials were removed and the measurements were conducted.

4.3.3. 1 Surface moisture contents

For the precondition specimens, surface moisture contents were measured with Kett HI-100 and Kett HI-520-2 surface moisture meter while for the outdoor exposed specimens, surface moisture contents were measured with Kett HI-100, Kett HI-520-2 and Tramax CMEXpert II. The internal moisture profile for the outdoor exposed specimens was measured with kett HI-800 (see Chapter 3 in 3.3.4.1 for details). The outline of the surface moisture meters is shown in Table 4-3.

Table 4-3 Outline of moisture meters

Name of moisture meter	HI-100	HI-520-2	CMEX II
Measuring principle	Electric resistance	Radio frequency capacity	Impedance
Measured objects	Concrete slab	Concrete, mortar, ALC, etc.	Concrete
Measuring range	0-6 (%), 40-990 (count)	Concrete 0-12 (%), mortar 0-15 (%), ALC 0-100 (%)	Concrete 0-6.9 (%)

The Kett HI-100 surface moisture meter (Figure 4-3(a)), (which is based on the measuring principles of electrical resistivity) results are displaced in percentage (0-6%)

or count values (40-990 counts). The count values have been shown to have an inverse linear relationship with electrical resistance . The advantages of this surface moisture meter over others are the ability to access both the pore water and the pore connectivity during measurements for moisture content and the ability to measure moisture content up to the depth of 5mm from the surface. This was confirmed by Komatsu et al, where a kett HI-100 revealed a higher correlation with the moisture content obtained at the depth of 5 mm from the surface[5].

The HI-100 surface moisture tester uses a rubber-type sensor- figure 4-3(b), that compresses with the exerting hand-measuring pressure. It is observed that the count values change with change in the pressure exerted during measurements resulting from the rubber sensor. To investigate whether this change is significant to the count values and surface moisture interpretations, a statistical test considering firm contact and non-firm contact was conducted with the null hypothesis, H_0: PSD is not significantly affected by the differences in count values resulting from rubber sensor and contact degree.

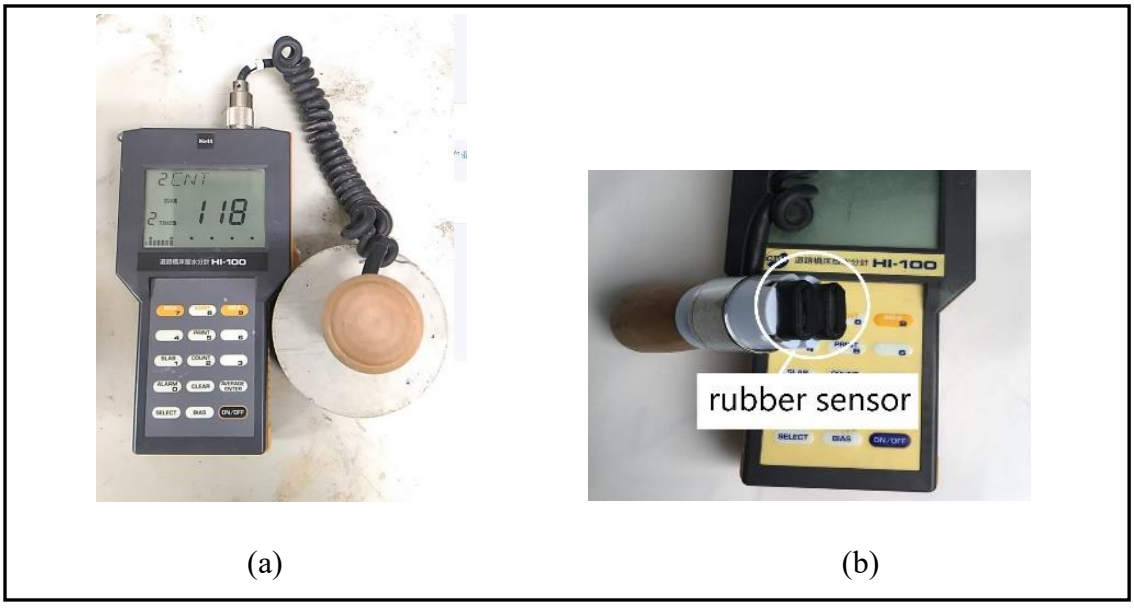

Figure 4-3 [(a)Kett HI-100 surface moisture meter (b)Kett HI-100 surface moisture meter rubber sensor]

The Kett HI-520-2 moisture meter (Figure 4-4) has the measuring range for concrete, 0-12 (%), mortar, 0-15 (%) and alcohol, 0-100 (%). It uses high frequency measuring principles [6]. While the measuring sensor for the HI-100 is rubber type, that of the HI-520-2 is not rubber, thus not affected by contact degree.

Figure 4-4 Kett HI-520-2 surface moisture meter

The Tramex CMEXpert II surface moisture meter (Figure 4-5) measures the moisture content of concrete by the transmission and conversion of low frequency into the concrete through parallel co-planar electrodes. It operates on the measurement principle of non-destructive impedance and displays moisture content of concrete in the range 0-6.9 (%).

Figure 4-5 Tramex CMEXpert II surface moisture meter

4.3.3.2 SWAT

SWAT described in chapter 2 (2.2.2) was applied to measure the surface water absorption at different PSDs for the preconditioned samples.

4.3.3.3 Electrical resistivity

Surface electrical resistivity was measured with direct type commercial 'resipod proceq' device Wenner probe (Figure 4-6). The prismatic specimens were saturated by total immersion into water and measurements were taken. Thereafter, moisture contents of the specimens were reduced by drying at a temperature of 40ºC and subsequent resistivity measurements for lower surface moisture conditions were taken. To reduce variability, the prismatic specimens were tested at 20°C ± 2.0 °C and probe spacing was set at 4 cm and 6 cm.

Figure 4-6 Surface electrical resistivty measurement

4.3.3.4 Percentage saturation degree of permeable pore voids of concrete (PSD)

After all the measurements were carried out on the specimens, the SD was determined as per [4]'s equation explained in chapter 2 (2.4.2). Along the same line, the test for the percentage void volume of each of the specimens was conducted following the procedure by the ASTM standard test method C 642-97. The volume of the permeable pore voids (%) was calculated as per the ASTM procedure and the PSD at each measured saturation level was calculated using the formula proposed in section 4.2.2 above.

4.4 Numerical simulation about the effects of PSD on water absorption of concrete

To investigate the pore size distribution and the effective pore radius at different percentage saturation degrees of permeable voids (PSD) for the concrete, a multi-scale and nonlinear structural analysis software-DuCOM, in which the thermodynamic moisture transfer model has been severally applied and validated [7], [8] was used. The constitutive model is capable of predicting the hydration of cement and its densification by continuous hydration of the un-hydrated cement particles.

The hydration of cement particles and moisture transport are inherently coupled during microstructure development and pore structure formation [8]. DuCOM applies the computational prediction of pore structure of concrete as a basis for moisture transport computation. Through the application of dynamic coupling of pore structure development to both the hydration and moisture models, the increase in the degree of hydration for any arbitrary initial and boundary conditions aids in the computation of strength development, moisture content and temperature [8]. The formation of new hydration products and their deposition in the large water-filled capillary pores is explained with the expanding cluster model illustrated in Figure 4-7 where ϕ_{in} is the porosity of the inner products while ϕ_{ou} is the porosity of the outermost boundary of the expanding cluster. The ϕ_{ou} equals unity when the expanding cluster has not reached the outermost representative cell particle [8].

Each capillary and gel porosity distributions, $\phi_{cp}(r)$ and $\phi_{gl}(r)$ is represented as

$$V = 1 - \exp(-Br),\ dV = \mathrm{Br}\ \exp(-Br) d\ \mathrm{In}\ r \qquad [4\text{-}5]$$

where V; fractional pore volume of the distribution up to pore radius r, B; the peak distribution in a logarithmic scale of the sole porosity distribution parameter. The overall microstructure is represented as a bimodal porosity distribution through the combination of the inner and outer product contribution to the total porosity function $\phi(r)$ as

$$\phi(r) = \phi_{lr} + \phi_{gl}\,(1 - \exp(-B_{gl}r)) + \phi_{c}\,(1 - \exp(-B_{cp}r)) \qquad [4\text{-}6]$$

where B_{gl} and B_{cp} correspond respectively to the gel and capillary porosity components

The illustration for Ducom multi-scale constitutive model that models concrete as a two-phase material (aggregate and cement paste) is given in Figure 4-8 while the schematic representation of porosity classification in concrete by Ducom is shown in Figure 4-9.

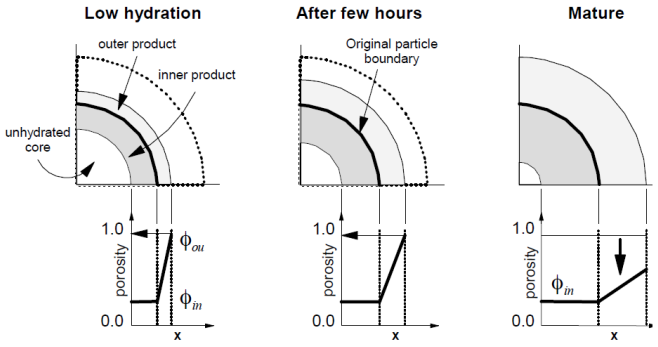

Figure 4-7 Bulk porosity function of outer product and cluster expansion model (*culled from* [8])

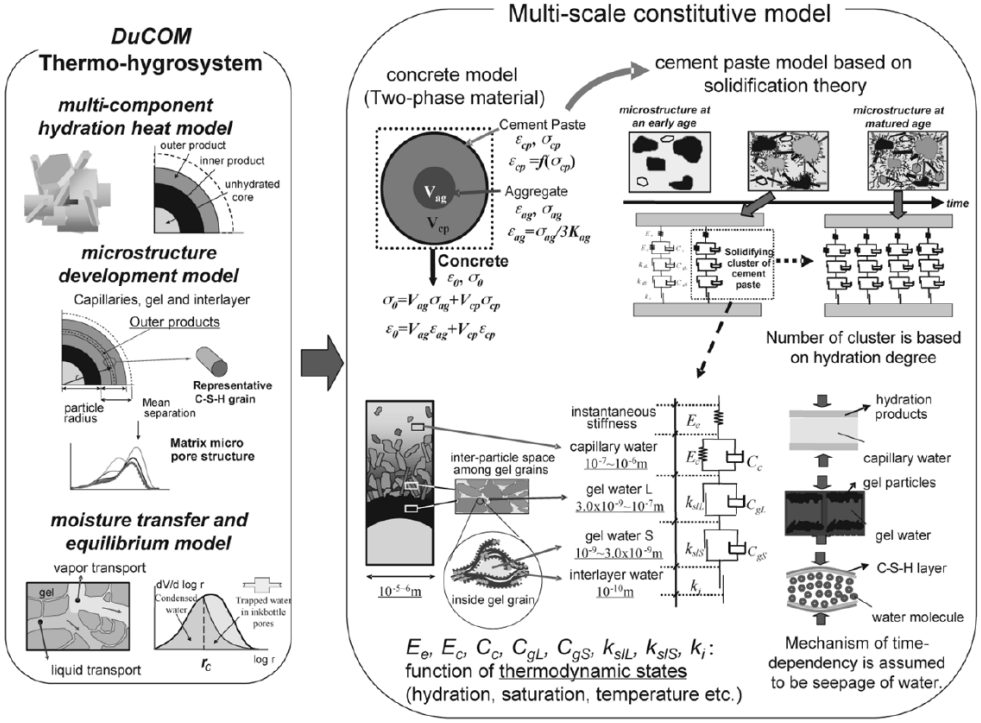

Figure 4-8 Modeling of solidifying cluster of cement hydrate (*culled from* [8])

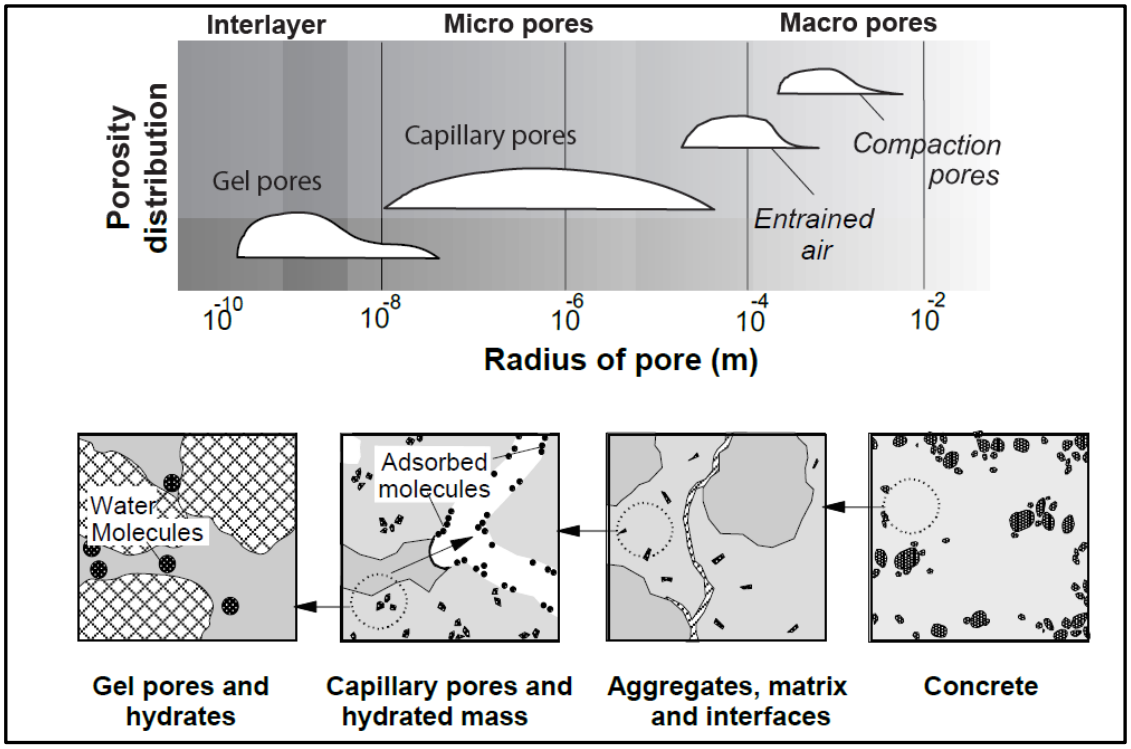

Figure 4-9 A schematic representation of porosity classification in concrete (*culled from* [8]*)*

4.5 Results and discussions

4.5.1 Relationship between saturation degree (SD) and PSD

It is a known fact that the most important aspects of determining the acceptability of a new method or proposal were its reproductivity, the consistency of results in identical specimens, and the accuracy when the results are compared with other accepted methods. The relationship between PSD and SD was investigated as shown in Figure 4-10. The result revealed that PSD has a good co-relation with SD in 112 tested specimens.

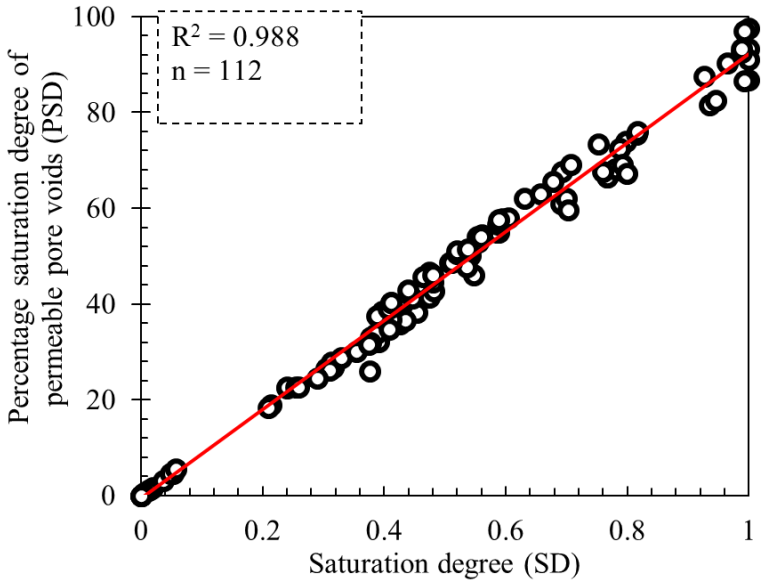

Figure 4-10 Relationship between PSD and SD

It is generally accepted that pore voids of concrete cannot attain complete saturation by immersion in water[2]. This, however, has not been reflected in the measure and expressions of moisture content of concrete in the literature. As such this aspect was investigated in this study using a destructive method and by proposing a mathematical formula in which comparison with the popular measure of moisture content-saturation degree, in the literature, was carried out. Also, a computational model of the best fitting curve for the conversion of kett HI-100 count values to the absolute moisture content of concrete as PSD has been proposed.

As saturation of pore voids of concrete reaches 42%, kett HI-100 count values related to the PSD started showing differences with different water-to-cement contents and curing conditions. The lower water-to-cement ratio concrete exhibited lower count values. It is evident that the better concretes were comprised of finer pore radii and lesser pore connectivity. Three salient points were identified in the relationship between SD and PSD as follows:

(1) Pore radius and connectivity are more significant influences in water absorption and desorption that the pore volume

(2) The influences of pore radius, pore volume, and pore connectivity are observed by PSD and the computational model.
(3) Complete saturation of permeable pore voids cannot be achieved by immersion into water.

4.5.2 Effects of water-to-cement ratio on pore volume

As expected, PSD could detect the effects of water-to-cement ratios and curing conditions on the moisture content of concrete. Figure 4-11 shows that OPC-40 retained more moisture at desorption than OPC-50, OPC-60-7D, and OPC-60-1D. Similarly, OPC-50 retained more than OPC-60-7D and OPC-60-1D. The same was the trend for OPC-60-7D and OPC-60-1D. Also in a reverse manner, water absorption was faster in OPC-60-7D than OPC-60-1D, OPC-50, and OPC-40. The OPC-60-1D absorbed water faster than OPC-50 and OPC-40, while OPC-50 absorbed faster than OPC-40. In the same vein, figure 4-12 revealed the influence of curing condition on moisture content, in which OPC-60-7D retained more moisture than OPC-60-1D.

These were clear indications that the pore radius and connectivities for the mix designs are different from each other due to the different water-to-cement ratios. Higher water-to-cement ratio concretes had a bigger pore radius and higher pore connectivity, thus faster moisture transfer both in absorption and desorption. These differences were not visible in the volume of permeable pore voids (%) for the studied specimens.

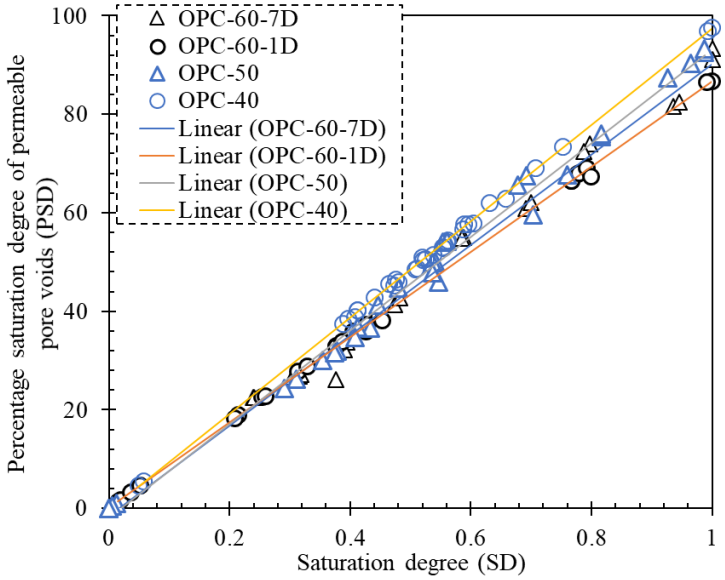

Figure 4-11 Effects of water-to-cement ratio on PSD

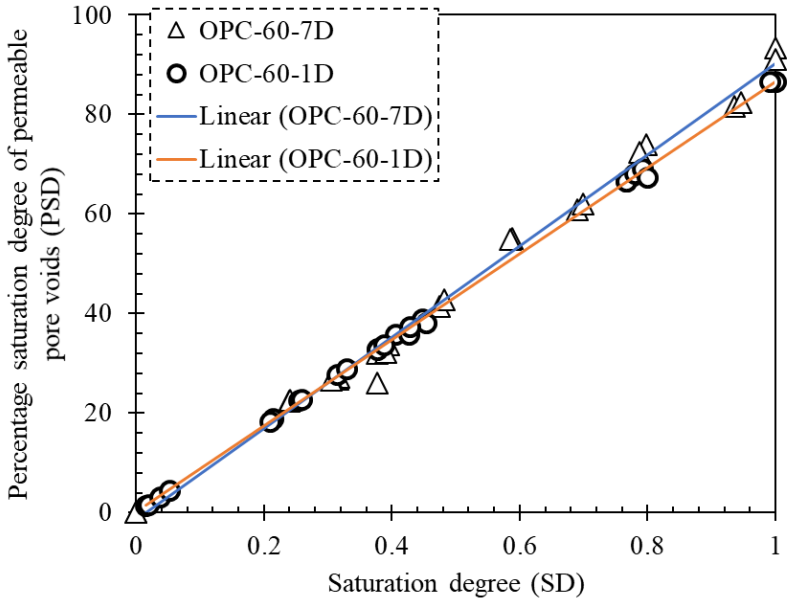

Figure 4-12 Effects of curing condition on PSD

4.5.3 Effects of kett HI-100 rubber sensor and contact degree on count values

Figures 4-13(a), and 4-13(b) show the effects of the rubber sensor of HI-100 on count values resulting from contact degree. For all the water/cement ratios studied, the influence of the rubber sensor and the resulting contact pressure increases with increasing PSD values. Figure 4-13 (a) revealed that the contact pressure did not show much effect when moisture contents were lower than 45%PSD. This could be as a result of the reduction in the degree of connectivity of the pore water at these PSD values.

From a simple t-Test: two-sample assuming unequal variances statistical tests conducted (Tables 4-4(a) and 4-4(b) the null hypothesis, H_0: PSD measurement is not significantly affected by the differences in count values resulting from rubber sensor and contact degree is rejected. This implies that the rubber sensor of HI-100 and the degree of contact significantly affects the moisture content measurement and the interpretations, especially when the surface moisture content is above 45%PSD.

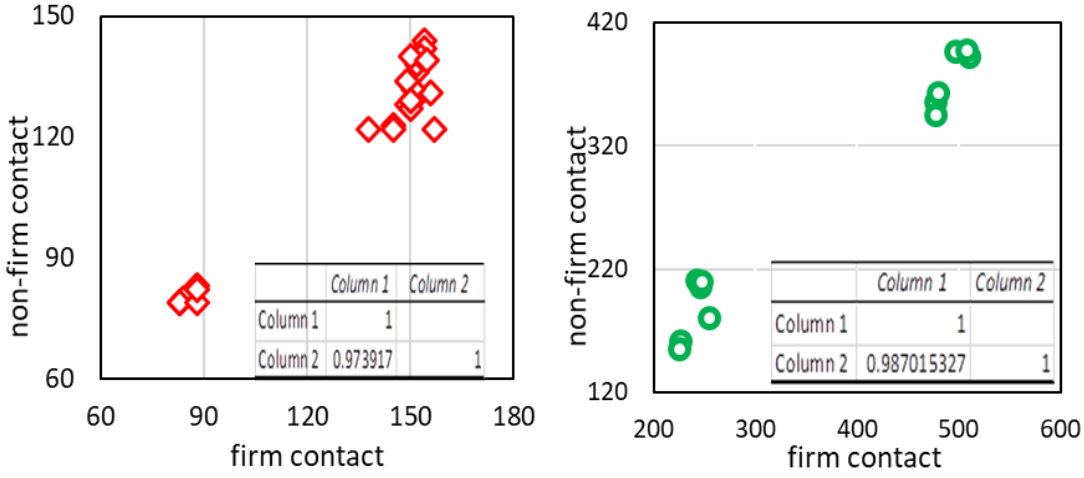

(a) (b)

Figure 4-13 (a) Kett HI-100 rubber sensor effects of measuring pressure on count values for 45%PSD and below
(b) Kett HI-100 rubber sensor effects of measuring pressure on count values for 46%PSD and above

Table 4-4 (a) t-Test: two-sample assuming unequal variances for 45% PSD and below

Observations	23	23
Hypothesized Mean Difference	0	
df	42	
t Stat	1.876113	
P(T<=t) one-tail	0.0338	
t Critical one-tail	1.681952	
P(T<=t) two-tail	0.067601	
t Critical two-tail	2.018082	

Table 4-4 (b) t-Test: two-sample assuming unequal variances for 46% PSD and above

Observations	11	11
Hypothesized Mean Difference	0	
df	19	
t Stat	1.61074	
P(T<=t) one-tail	0.061862	
t Critical one-tail	1.729133	
P(T<=t) two-tail	0.123725	
t Critical two-tail	2.093024	

4.5.4 Relationship between PSD and moisture content measured by moisture meters

Figures 4-14(a) and 4-14(b) show the relationship between kett HI-100 count values and PSD at covercrete for the general OPC concretes and the individual mix proportions respectively.

From figure 4-14(b), the specimens exhibited different count values at the same PSD except for OPC-60-1D and OPC-60-7D which revealed the same count values at the same PSDs. The differences in count values could be attributed to differences in pore diameters as it was observed that OPC-60-1D and OPC-60-7D revealed the same volume of permeable pore voids. The variation in count values among OPC-60s, OPC-50, and OPC-40 was widened as PSD increased. This is a clear indication of the variations in the pore connectivity of the specimens in terms of electric resistivity. Secondly, there is a possibility that the effects of the degree of contact resulting from rubber sensors may have contributed. Count values obtained from kett HI-100 surface moisture meter, which are directly related to the electric resistance of covercrete, showed good correlations with PSD of concrete.

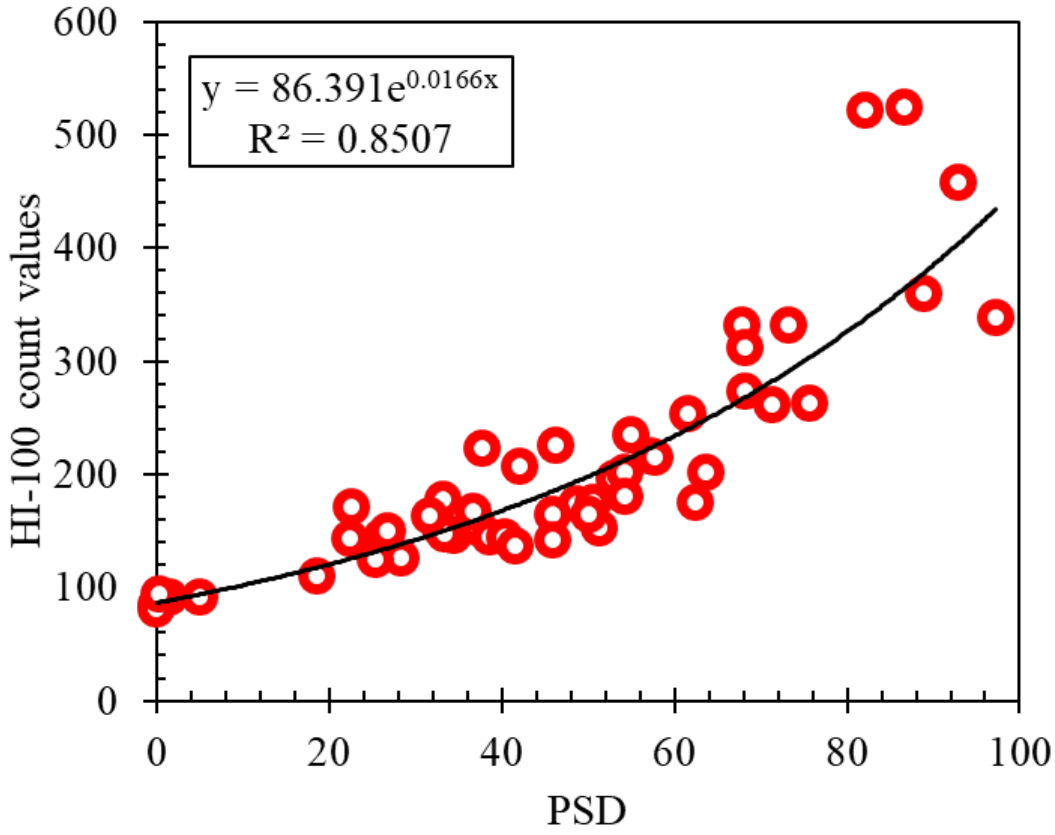

Figure 4-14(a) Kett HI-100 fitting curve for OPC concrete

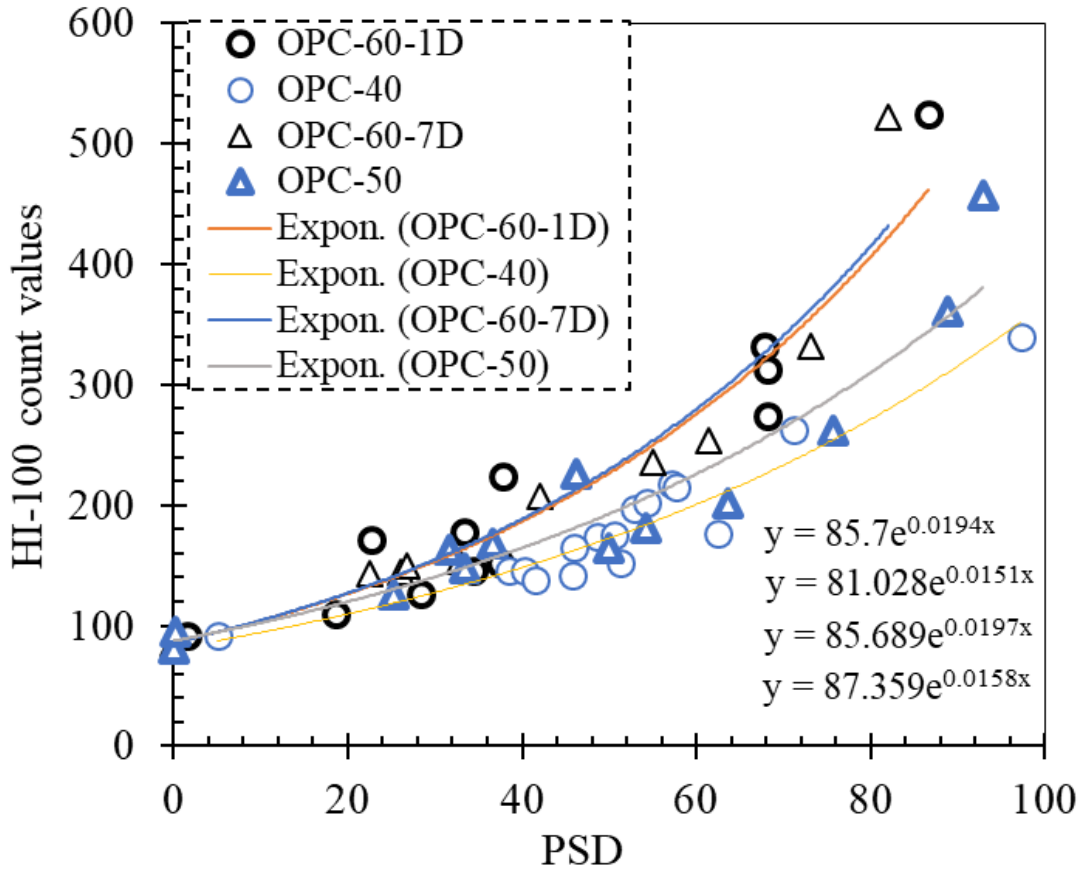

Figure 4-14(b) Kett HI-100 fitting curve for OPC concrete considering water/cement ratios

Figures 4-15(a) and 4-15(b) show the relationship between kett HI-520-2 count values and PSD at covercrete for the general OPC concretes and the individual mix proportions respectively. Similar to the results in Figure 4-15(a) and 4-15(b), the specimens exhibited different percentage values of kett HI-520-2 readings at the same PSD but in a lesser order than the kett HI-100 count values. These differences in percentage values could also be attributed to differences in pore voids. Unlike in kett HI-100 results, variations in the percentage values of kett HI-520-2 among OPC-60s, OPC-50, and OPC-40 became visible from 30%PSD and above. A higher correlation with PSD was obtained with HI-520-2.

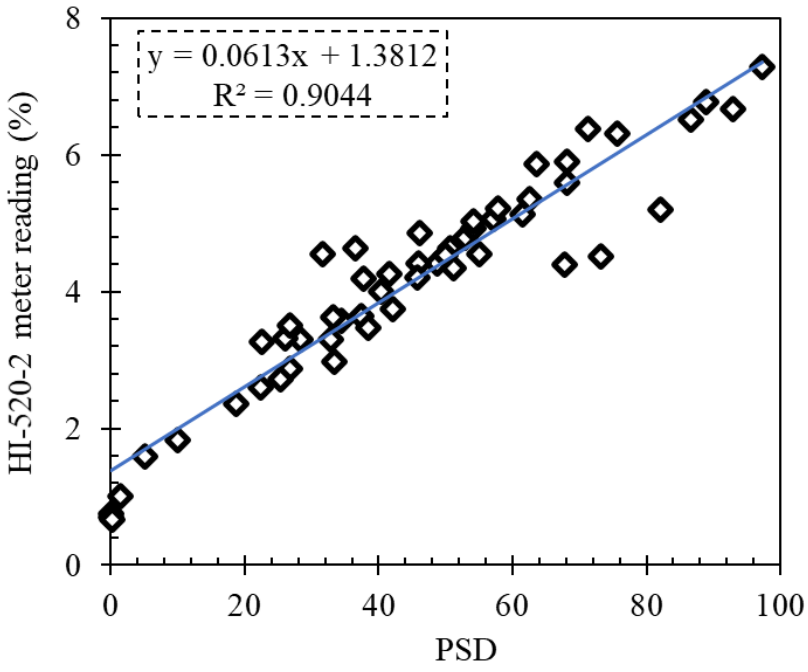

Figure 4-15(a) Kett HI-520-2 fitting curve for OPC concrete

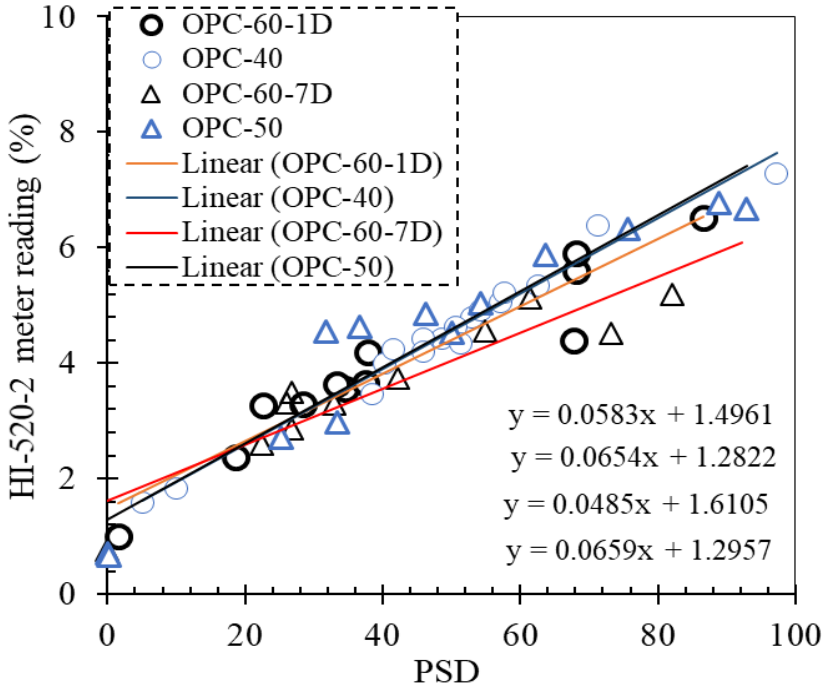

Figure 4-15(b) Kett HI-520-2 fitting curve for OPC concrete considering water/cement ratios

4.5.5 Relationship between PSD and SWAT

Figure 4-16(a) shows the effects of PSD on surface water absorption measured by SWAT, while Figure 4-16(b) shows the pattern diagram for the regions, A, B, and C observed for the different OPC concretes investigated. It was revealed that the surface water absorption rate at 10 minutes (p_{600}) exhibited a near-linear inverse relationship with PSD for all the specimens when the PSD was between 0% to 20%. According to the increase of PSD, p_{600} decreased in this region. A different trend was exhibited by all the specimens after 20% PSD. For OPC-60-1D, from 21%PSD to 40%PSD, PSD was seen to have little or no influence on the surface water absorption. For OPC-60-7D, the same tendency was seen from 21%PSD to 42%PSD. For OPC-50, from 21%PSD to 53%PSD little or no influence was seen on the surface water absorption while for OPC-40 the plateau range was between 21%PSD to 58%PSD. The plateau range that is common to all the specimens is best seen as 21%PSD to 45%PSD. The range of region B increased with a decrease in the water-to-cement ratio of the concrete. For the same water-to-cement ratio concrete (OPC-60s), the range increased with better curing conditions. These could be emanating from the fact that water absorbency and moisture content of concrete have different pore diameter thresholds. While water absorbency is affected by the volume of pore diameters of ca. 100 nm (10^{-7}m) and larger [9], the moisture content is further affected by the connectivity of pores regardless of the diameter sizes. Furthermore, it can be seen from Figure 4-16(c) that the SWAT results in region B showed the influences curing and mix design thereby revealing the accurate quality grading that conforms with the original SWAT gradation.

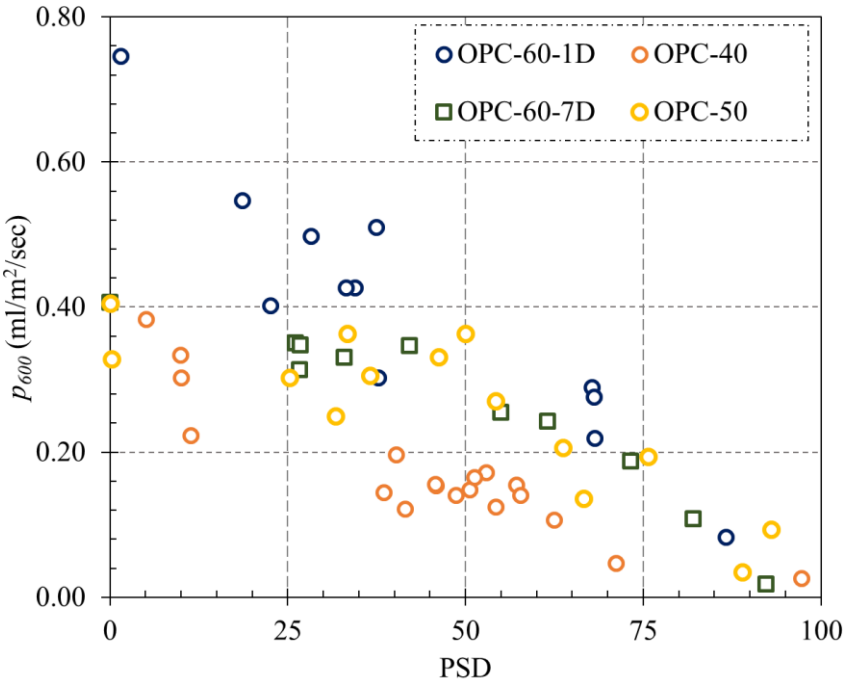

Figure 4-16(a) Relationship between PSD and surface water absorption

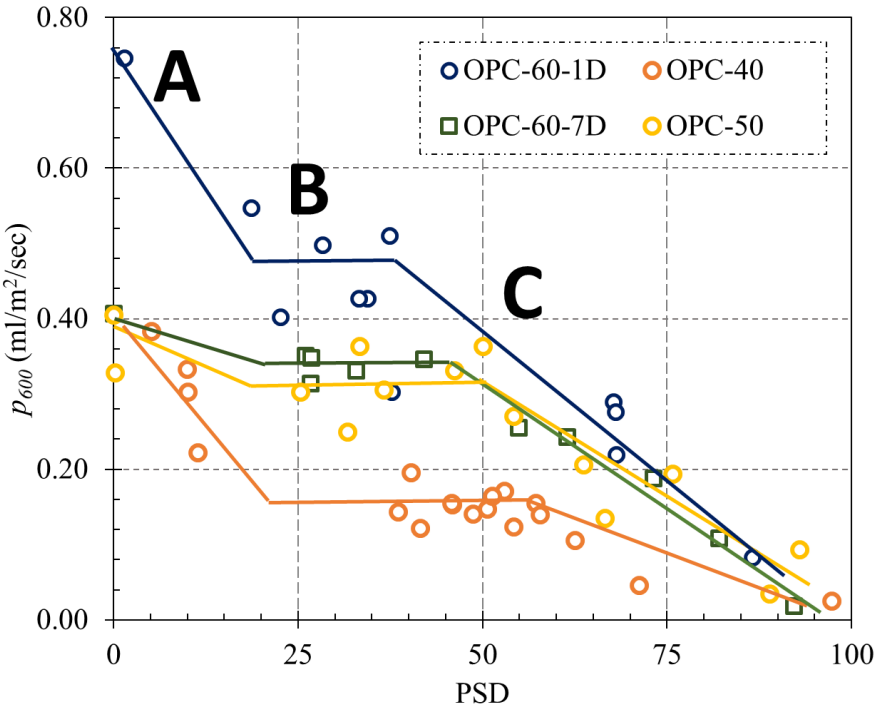

Figure 4-16(b) Pattern diagram showing the effects of PSD on surface water absorption

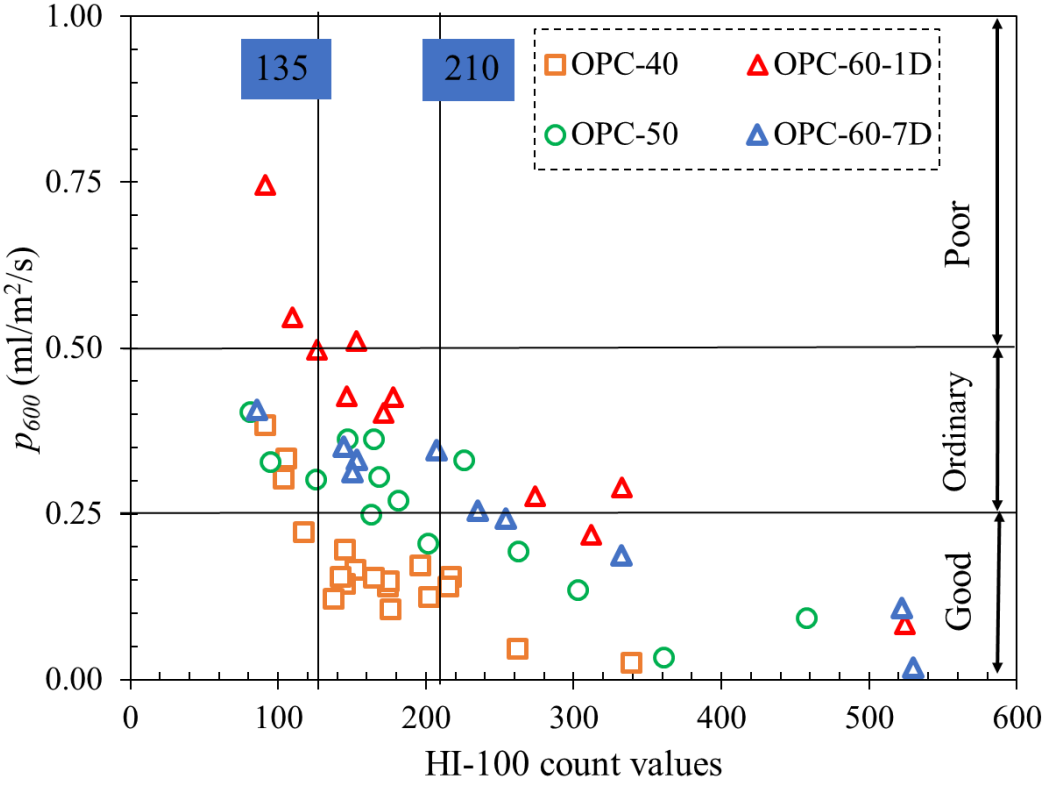

Figure 4-16(c) P_{600} versus HI-100 count values showing the threshold

The results shown in Figures 4-17 and 4-18 were measurements from specimens exposed to a natural environment in the wall and slab orientations respectively. The temperature and humidity of the environment during the exposure period are shown in Figure 4-19.

Figure 4-17 and Figure 4-18 verify the applicability of PSD in concrete structures under a natural environment. From Figures 4-17(a) and 4-18(a), it can be inferred that the threshold count value (210 count value) by HI-100 surface moisture meter is achievable for OPC40-7D, OPC40-1D6W, OPC50-7D, OPC50-1D6W, OPC60-1D and OPC60-1D6W. Contrary to the results from HI-100 moisture meter, Figures 4-17(b) and 4-18(b) revealed a difficulty in the practical application of the threshold moisture content (4.1%) for HI-520-2 surface moisture meter.

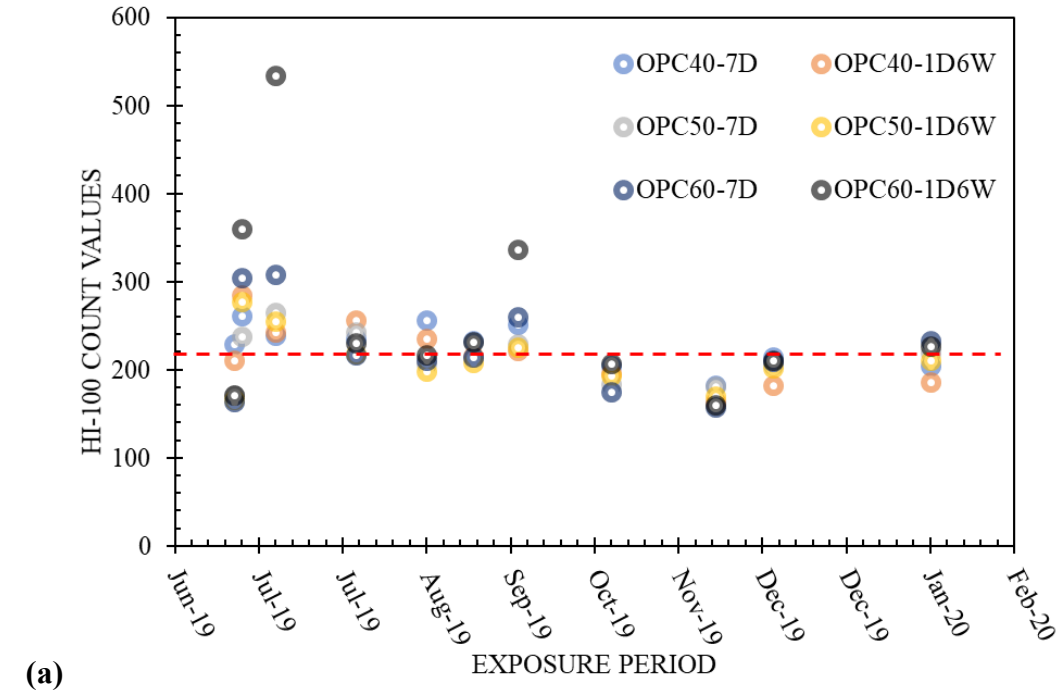

(a)

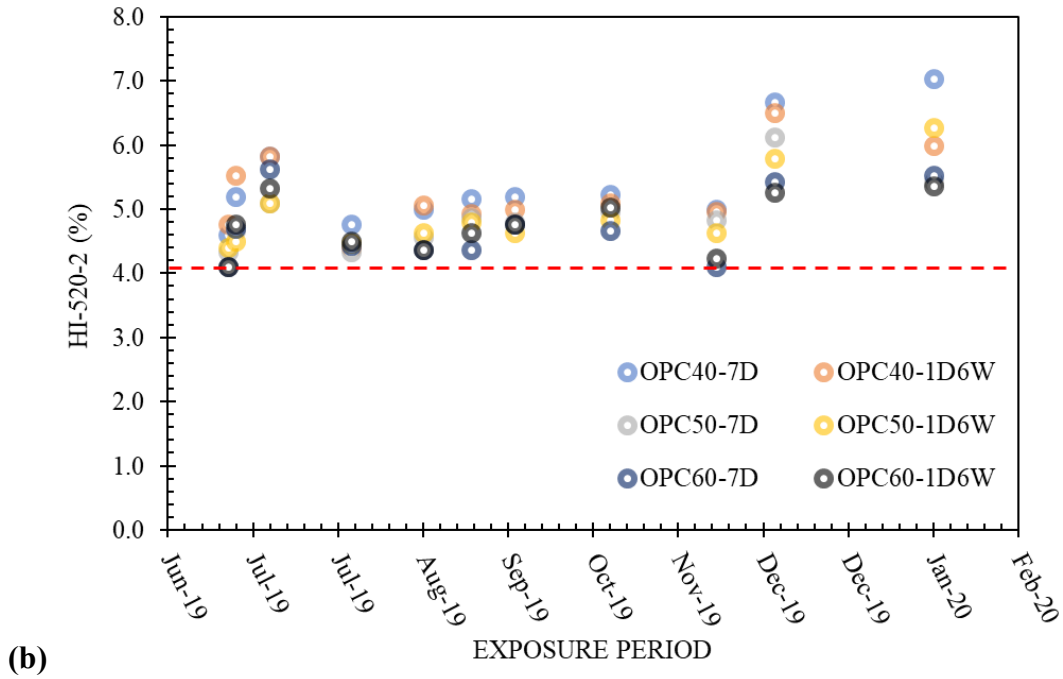

(b)

Figure 4-17(a) Moisture content by HI-100 surface moisture meter for OPC concretes exposed to the natural environment in a wall orientation
(b) Moisture content by HI-520-2 surface moisture meter for OPC concretes exposed to the natural environment in a wall orientation

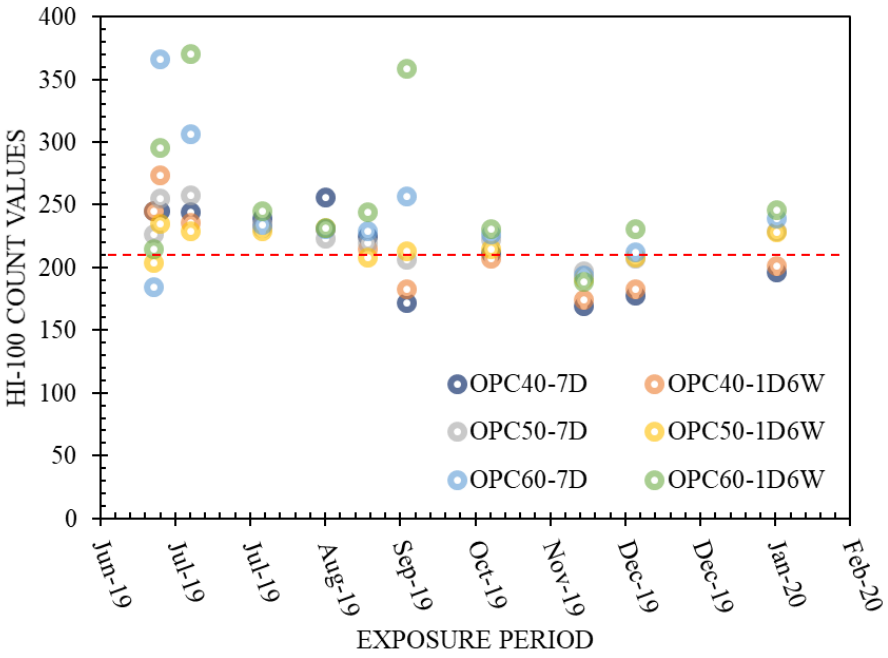

(a)

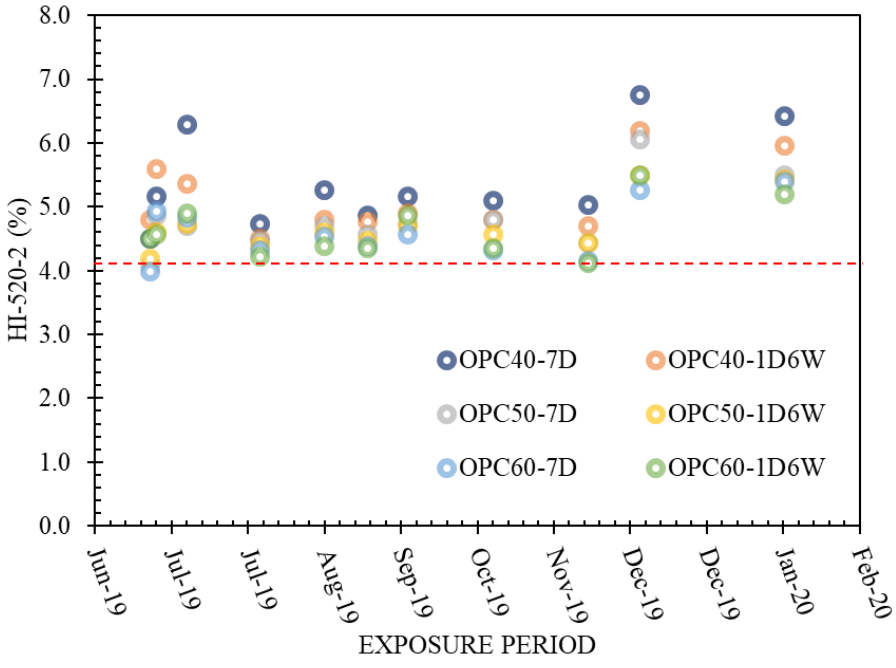

(b)

Figure 4-18(a) Moisture content by HI-100 surface moisture meter for OPC concretes exposed to the natural environment in a slab orientation
(b) Moisture content by HI-520-2 surface moisture meter for OPC concretes exposed to the natural environment in a slab orientation

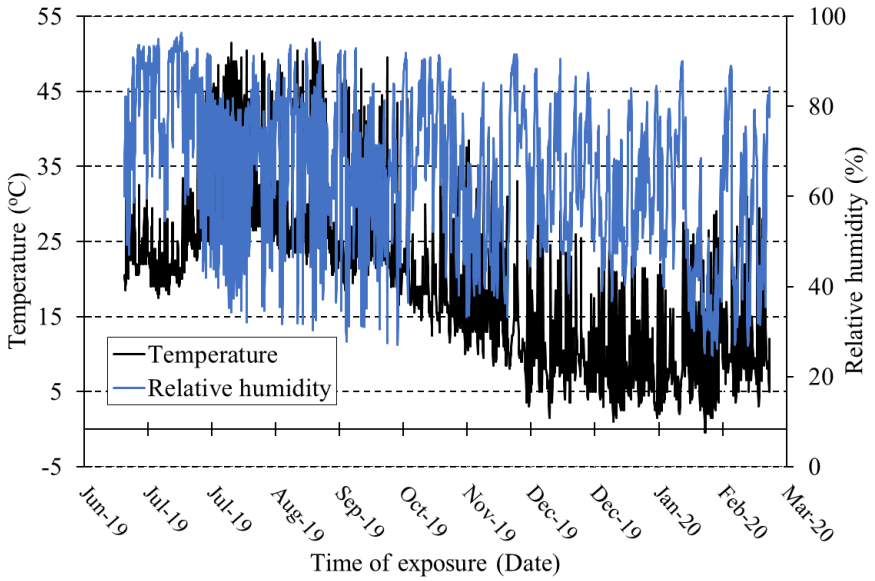

Figure 4-19 Variations in outdoor temperature and relative humidity at the exposure location of the concrete specimens

Verification of the application of PSD to field assessment of covercrete quality

Practical application of the threshold/edge moisture contents for field NDT assessment of covercrete quality is verified with 90-day old concrete specimens shown in Figures 4-20 to 4-23. The concrete specimens used in the figures were prepared with ordinary Portland cement (OPC) and ground granulated blast furnace slag cement (BB cement-JIS type B slag cement). For the OPC concretes, 40%, 50% and 60% W/Cs were prepared and represented as N40, N50 and N60 respectively while only 50% W/C was prepared for the BB concrete and represented as BB50. Three curing conditions were applied viz: 1 day in mould represented as "1D", 10 days in mould as "10D", 1 day in mould + 9 days in water as "10W". The specimens were exposed to 60%, 80% and 99% RH to obtain several PSDs within and above the threshold PSD.

For all mixtures, the surface water absorption rate (p_{600}) displays the expected plateau range within the threshold of 45% PSD that is equivalent to 210 count values of HI-100 moisture meter. This plateau range was only virtualized in HI-520-2 and CMEX II moisture meter measurements for the N60 and BB50 series. The N60 and BB50 series were seen to exhibit high surface water absorption rates. It is inferred from the Figures

that HI-520-2 and CMEX II moisture meters misjudge the pore void saturation degrees of good quality concretes. Both PSDs within and above the threshold values were virtually dictated as similar moisture contents for N40_10W and N50-10W concretes by HI-520-2 and CMEX II moisture meters.

The most likely explanations are shallow measurement depths by the two moisture meters and/or the inability in dictating existing pore water in discontinuous pore voids, which seemingly demonstrates that HI-520-2 and CMEX II are unable to appropriately measure the pore void connectivity. The HI-100 moisture meter seems to be the most appropriate to be used together with SWAT in dictating the PSD of covercrete before SWAT application.

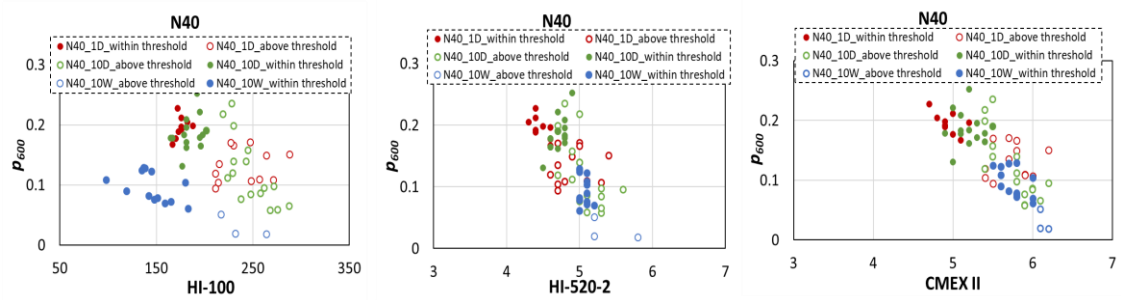

Figure 4-20 Surface water absorption rate against moisture contents by HI-100, HI-520-2 and CMEX II for OPC concrete with 40% water-to-cement content

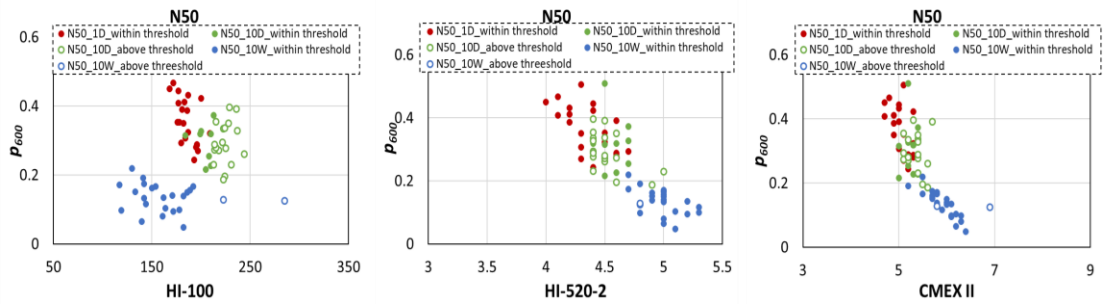

Figure 4-21 Surface water absorption rate against moisture contents by HI-100, HI-520-2 and CMEX II for OPC concrete with 50% water-to-cement content

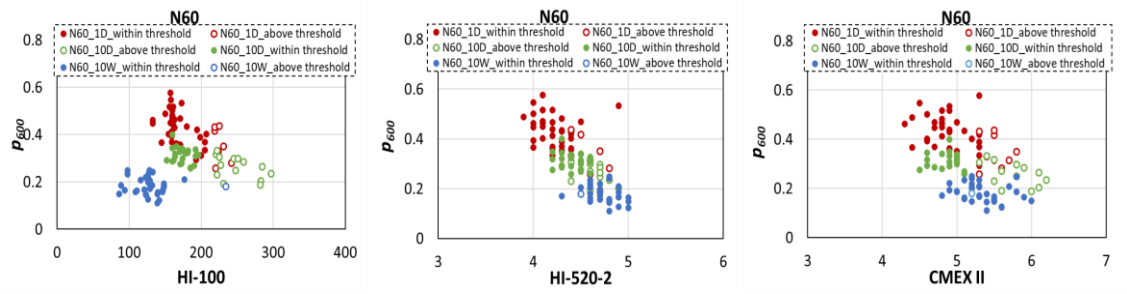

Figure 4-22 Surface water absorption rate against moisture contents by HI-100, HI-520-2 and CMEX II for OPC concrete with 60% water-to-cement content

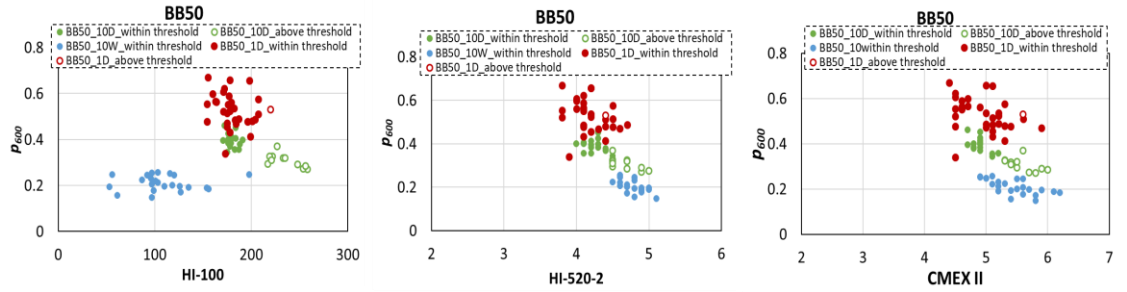

Figure 4-23 Surface water absorption rate against moisture contents by HI-100, HI-520-2 and CMEX II for BB concrete with 50% water-to-cement content

4.5.6 Relationship between PSD and electrical resistivity

Surface electrical resistivity for drying concrete with internal moisture profile is plotted in Figure 4-24. As expected, surface resistivity generally increased with decreasing PSD, with a more pronounced increase noted from around 75% PSD and below (300 count value). The rapid increase is attributed to the beginning of the loss of pore water connectivity that substantially decreases the available electrical channels [10]. The increase in resistivity is by no means linear to the decrease in PSD. It can be inferred that estimating PSD of concrete by HI-100 moisture meter is appropriate since it generally reflects the effects of moisture content on electrical resistivity, which has already been established by many pieces of research.

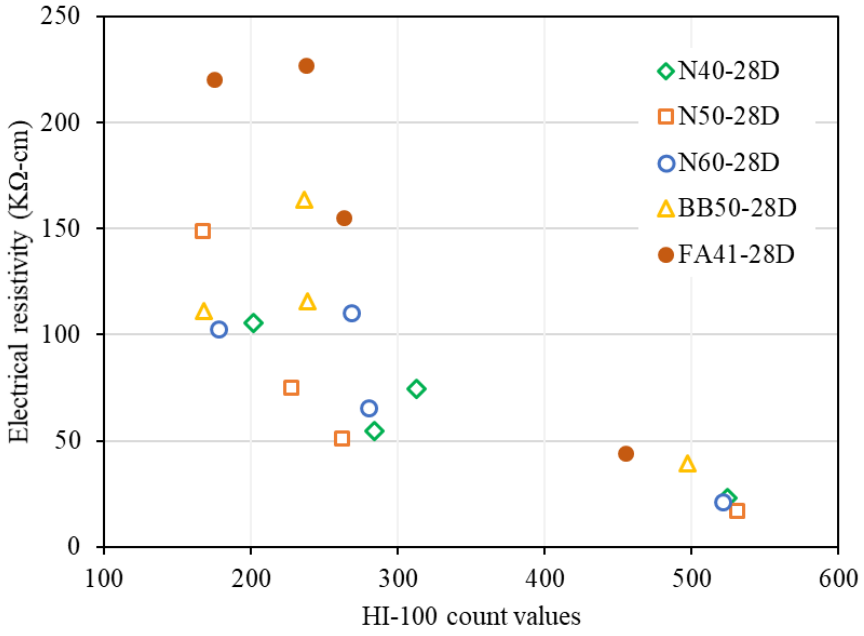

(a)

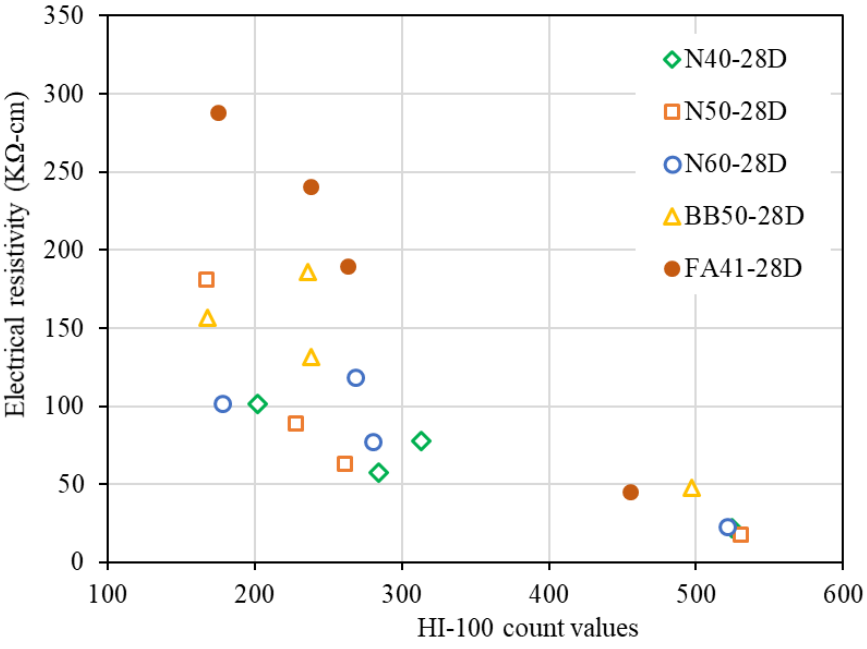

(b)

Figure 4-24 Electrical resistivity vs HI-100 count values
(a) 40 mm probe spacing (b) 60 mm probe spacing

4.5.7 Relationship between PSD and water absorption by simulation

The outline of the simulation model shown in Figure 4-25 replicates the conditioning of the experimental specimens. A comparison of the two results, which measured the relationship between surface water absorption at 10 minutes and the percentage saturation degree of pore voids for OPC-40-7D (see Table 4-1 for mix composition) is shown in Figure 4-26. It is apparent that the two results are in good agreement and showed a similar trend for the plot of cumulative water absorption against the percentage saturation degree of permeable pore voids.

At percentage saturation degrees of pore voids above 60%, the water absorption amount in 10 minutes rapidly decreases with an increase in pore void saturation. The trend was the same for percentage saturation degrees of pore voids below 30% while 30% to 60% demonstrates the expected plateau for the virtualized plots.

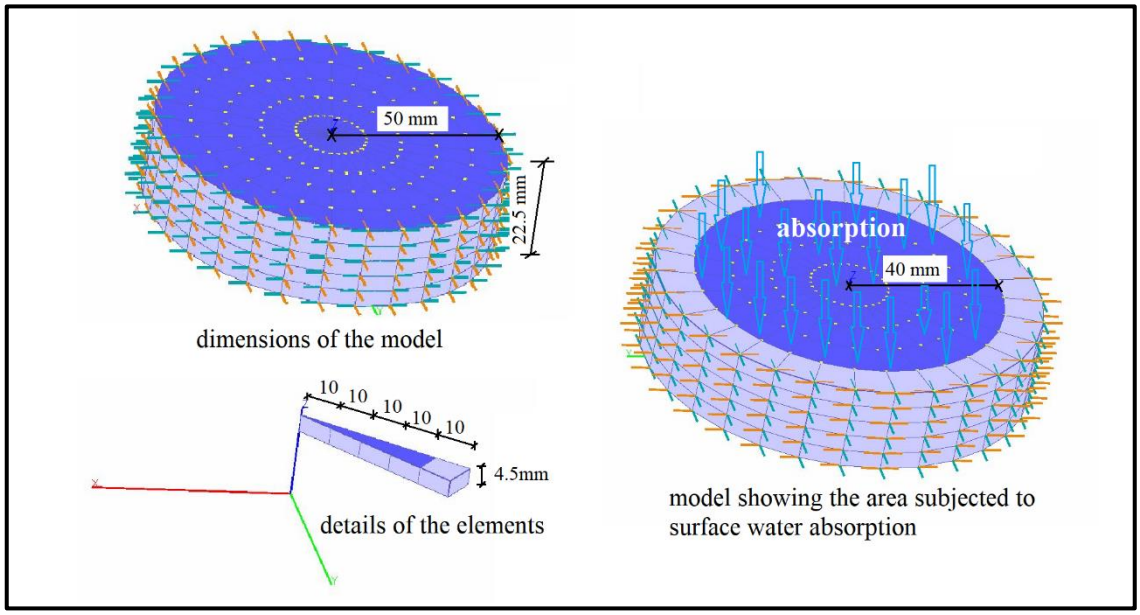

Figure 4-25 Outline of the numerical simulation model

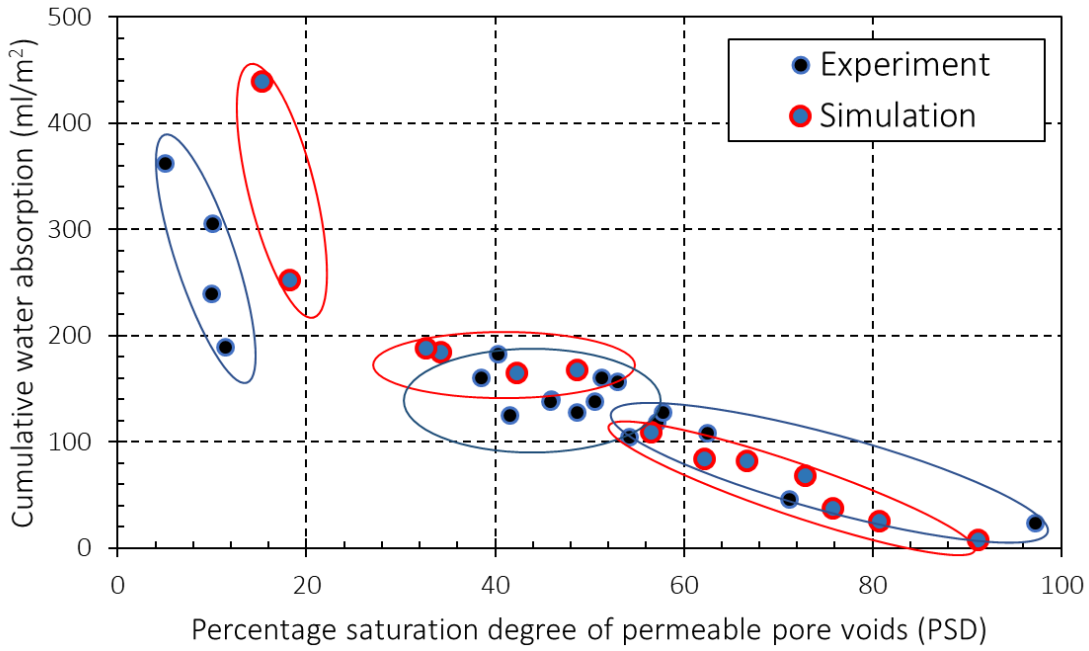

Figure 4-26 Cumulative water absorption per unit area at 10 mins vs percentage saturation degree of permeable pore voids (PSD) for OPC-40-7D

4.5.8 Combined effects of pore size distribution and pore size volume on water absorption by simulation

The surface water absorption is expected to be a function of the degree of dryness which has a strong dependence on the amount of empty permeable pores. Thus surface water absorption should decrease with an increase in the saturation degree of permeable pores. Given this, the non-dependency of surface water absorption on the degree of dryness (saturation degree of permeable pore voids) between 21% to 45% saturation degree of permeable pore voids shown in Figure 4-16(b) is surprising. It can be seen from the figure that within the said percentage saturation degree of permeable pore voids, a plateau was formed on the surface water absorption for all the concrete mix design shown in different indices.

Initial saturation degree of permeable pore voids within region A and C

In region A (predominately 0% to 20%PSD), which could be seen as a relatively dry region, the capillary pore system is empty thus rapid surface water absorption occurs when concrete is placed in contact with water. Since the bigger gel pores are not filled, as water enters the large capillary pores, rapid-partial redistribution into the smaller empty pores occurs; similar to [11] revelation of the influence of gel pore water in the transport of water in much larger capillaries, thereby allowing for an increase in internal swelling that reduces the pore connectivity and lowering the amount of absorption. For this reason, surface water absorption in this region has a near-linear inverse relationship with the saturation degree of permeable pore voids until the critical size radii that aid in moisture redistribution are filled up. The critical pore is seemingly within 20%PSD and below.

Region C which could be seen as a wet region similarly shows a water absorption relationship with PSD as a near-linear inverse relation. The entire region ranged from 21% to 58%PSD with variations therein. For the concrete mixes, the range increased with a decrease in water-to-cement ratio and increased with better curing for the OPC-60s. In this region, only bigger pores that have sole water absorbency [9] are empty. As absorption proceeds, smaller pores are filled reducing the available empty pore for absorption.

Initial saturation degree of permeable pore voids within region B

Nearly zero influence of PSD to water absorption was observed in this region, thus a plateau in the pattern diagram was observed. Here, the critical pore radii that contribute to the partial redistribution of moisture have already been filled resulting in reduced water absorption. In this region, capillary water absorption requires a longer time due to discontinuity in pore connections together with the tortuous property of concrete. As can be seen in Figure 4-27, increasing surface water absorption time to 6 hours eliminated the plateau region. The empty capillary pore diameter in this region is seemingly between 10^{-8} m (10 nm) and 10^{-7} m (100 nm) (Figure 4-28) relating to [9] assertion that water absorbency is affected by pores with capillary diameter 10^{-7} m (100

nm) and above. The pore radii in the region have strong relations with the threshold pore size by the mercury intrusion porosimetry (MIP) test. Water absorption measurements that are conducted in this PSD region will best assess the pore size distribution and threshold pore size characteristics of the concrete.

The threshold for the saturation degree of permeable pore voids for the evaluation of surface water absorption is in the region (the shaded portions of Figure 4-28(b)-(e)) since the obtained rate of absorption (p_{600}) reflects the covercrete quality grading shown in Chapter 2, Table 2-2. Furthermore, the PSD in region A could hardly be observed in concrete structures under natural atmospheric exposure, thus the upper threshold is the most important and could be regarded as 45%PSD. The schematic diagram of the water absorption mechanism for the plateau formation is shown in Figure 4-29.

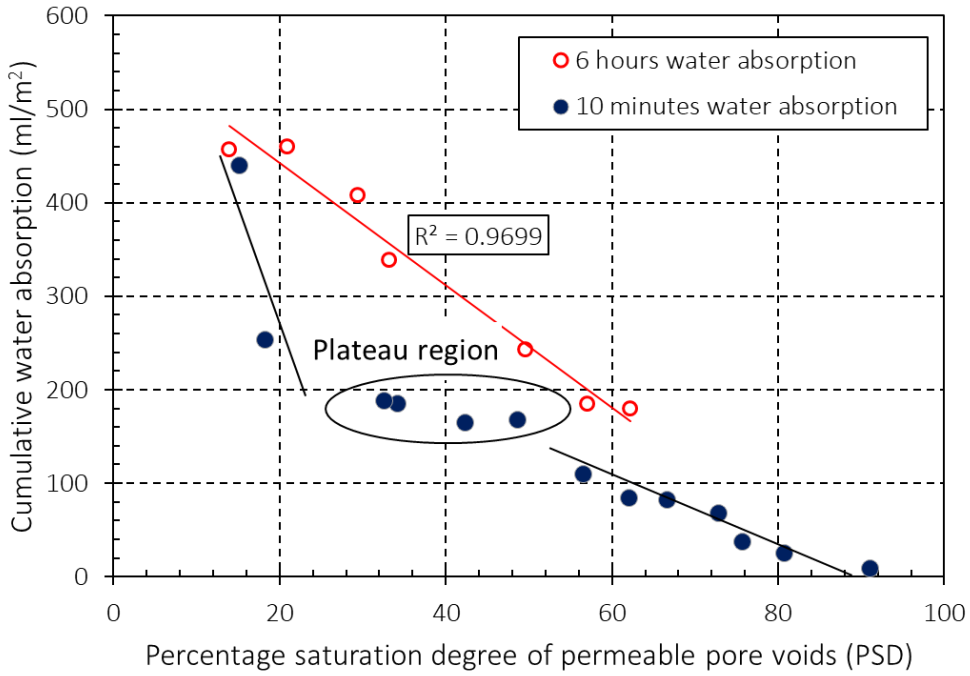

Figure 4-27 Numerical result showing long- and short-term surface water absorption for OPC-40 concrete

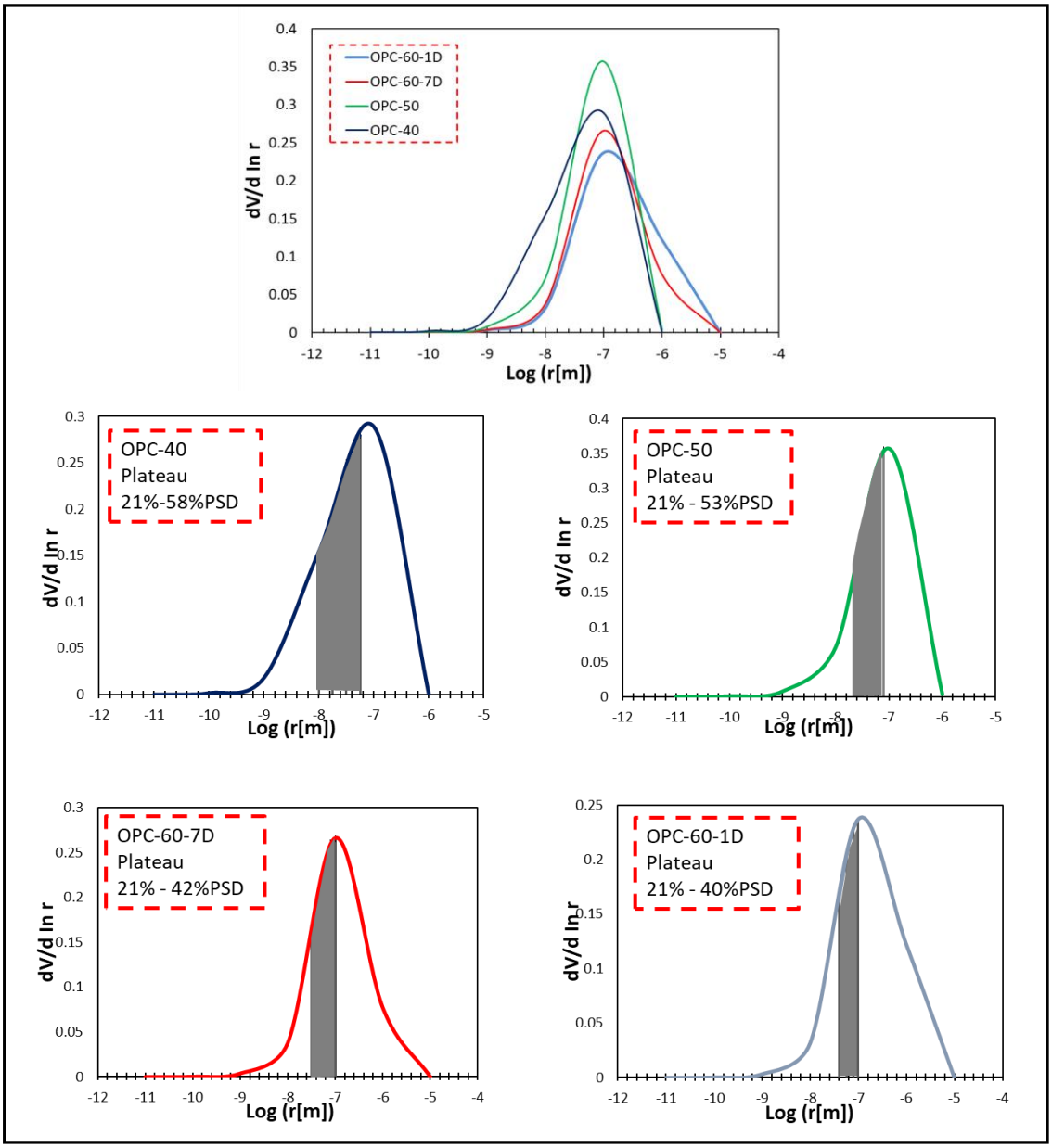

Figure 4-28 Combined effects of pore size distribution and pore size volume on water absorption showing the 'plateau' region obtained by simulation

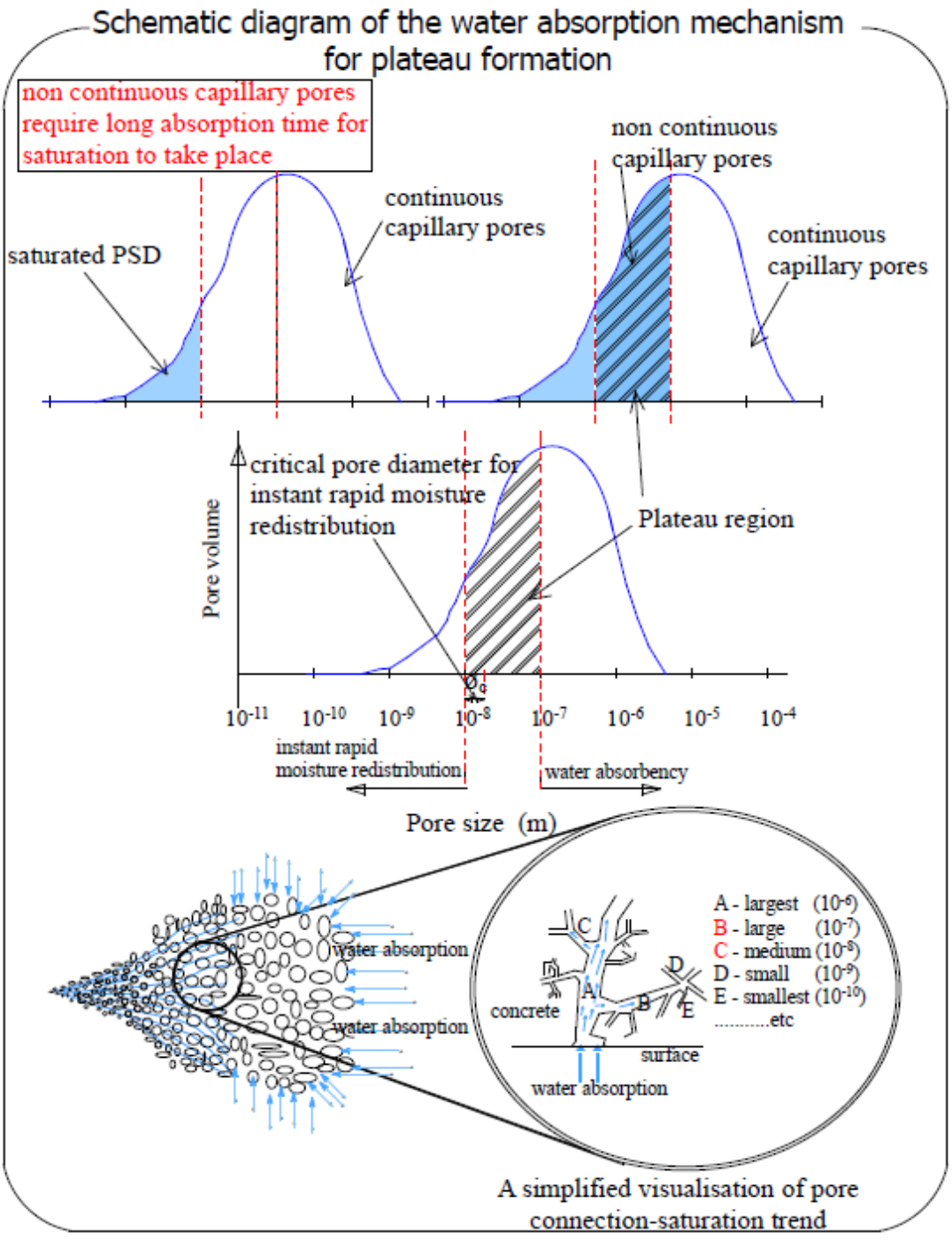

Figure 4-29 Schematic diagram of the water absorption mechanism for the plateau formation

4.6 Summary of findings

Based on the experimental investigation and the analysis of the results, the following conclusions are drawn:

1. There is an over-estimation of moisture content of concrete when the moisture contents were measured without referencing the permeable pore voids of the concrete.
2. For accurate and absolute measurement of moisture content of concrete, it is necessary to consider the percentage volume of permeable pore voids of the concrete. The boiling process is necessary for obtaining the accurate volume of permeable pore voids of concrete.
3. Count values obtained from Kett HI-100 surface moisture meter, which are directly related to the electric resistance of covercrete, showed good correlations with PSD of concrete. HI-100 may be utilized for detecting PSD of concrete to check whether concrete is sufficiently dried for appropriate measurement of SWAT.
4. Similar to Kett HI-100, surface moisture tester, Kett HI-520-2 results showed good correlations with PSD of concrete and may also be utilized to obtain the PSD at the covercrete.
5. For accurate covercrete quality evaluation when utilizing SWAT, the threshold and edge PSD should be within region B, i.e the common plateau range for all the specimens. The threshold PSD is 21% and the edge PSD is 45%PSD. For kett HI-100, the threshold and edge PSDs are 135 count values and 210 count values respectively. Similarly, the threshold and edge PSDs for kett HI-520-2 obtained from the linear function are 3.0% and 4.1% respectively. However, the HI-520-2 threshold may not be appropriate for field estimation of PSD as revealed by further investigations. The SWAT results obtained when the surface moisture content of concrete is within this PSD range conforms with the graduation of covercrete quality shown in Table 1. This plateau range depends on the volume of empty capillary pore diameter between ca. -10^{-8} and 10^{-7}.

References

[1] S. Ahmad, A. K. Azad, and K. F. Loughlin, 'A Study of Permeability and Tortuosity of Concrete', p. 9.

[2] A. C. ASTM International, 'Standard Test Method for Density, Absorption, and Voids in Hardened Concrete'. 2006.

[3] P. A. M. Basheer and é. Nolan, 'Near-surface Moisture Gradients and In-situ Permeation Tests', *Construction and Building Materials*, vol. 15, no. 2–3, pp. 105–114, Mar. 2001, doi: 10.1016/S0950-0618(00)00059-3.

[4] C. Antón, M. A. Climent, G. de Vera, I. Sánchez, and C. Andrade, 'An Improved Procedure for Obtaining and Maintaining Well Characterized Partial Water Saturation States on Concrete Samples to be used for Mass Transport Tests', *Mater Struct*, vol. 46, no. 8, pp. 1389–1400, Aug. 2013, doi: 10.1617/s11527-012-9981-4.

[5] S. Komatsu, R. Tajima, and A. Hosoda, 'Proposal of Quality Evaluation Method for Upper Surface of Concrete Slab with Surface Water Absorption Test', *Concrete Research and Technology*, vol. 29, no. 0, pp. 33–40, 2018, doi: 10.3151/crt.29.33.

[6] Tanikura I., Enokizono M., and Goto A., 'Study on the Application of the Moisture Tester Applied to Concrete Surface for Waterproofing Works', *Journal of Structural Engineering, Japan Society of Civil Engineering*, vol. Vol. 59A, p. 6, Mar. 2013.

[7] K. Maekawa, A. Pimanmas, and H. Okamura, *Nonlinear mechanics of reinforced concrete*. London; New York: Spon Press, 2003.

[8] K. Maekawa, T. Ishida, and T. Kishi, *Multi-scale modeling of structural concrete*. London ; New York: Taylor & Francis, 2009.

[9] Y. Yokoyama, T. Yokoi, and J. Ihara, 'The Effects of Pore Size Distribution and Working Techniques on the Absorption and Water Content of Concrete Floor Slab

Surfaces', *Construction and Building Materials*, vol. 50, pp. 560–566, Jan. 2014, doi: 10.1016/j.conbuildmat.2013.10.013.

[10] E. William and J. S. Erik, 'Electrical Resistivity of Concrete, Directorate of Public Roads, Norwegian Road Research Laboratory, Jun. 1995.

[11] P. Rucker-Gramm and R. E. Beddoe, 'Effect of Moisture Content of Concrete on Water Uptake', *Cement and Concrete Research*, vol. 40, no. 1, pp. 102–108, Jan. 2010, doi: 10.1016/j.cemconres.2009.09.001.

Chapter 5

Effects of Hysteresis on SWAT, Air Permeability and Surface Moisture Contents

5.1 Introduction

The transfer and penetration of deleterious substances into the matrix of concrete structures largely depends on the pore structure and the saturation degree of the permeable pore voids. Also, the path in which the permeable pore voids underwent to attain a particular saturation degree may subsequently affect its resistance to gaseous and liquid penetrants. In this context, the objective of this chapter is to evaluate the influence of wet-dry path (desorption) and dry-wet path (absorption) on surface water absorption, air permeability and surface moisture contents.

5.2 Experimental programme

5.2.1 Experimental variables

Concrete specimens were preconditioned to study the influence of moisture hysteresis on surface water absorption and air permeability at different saturation degrees of permeable pore voids. Eighteen prismatic specimens were preconditioned to moisture equilibrium for each concrete mix in two different ways. The moisture profile during redistribution was monitored with embedded M4 moisture sensors at 4 different depths in 6 specimens (Figure 5-1) for each mix design. The conditioning of the specimens was done in two ways- desorption and absorption processes, one for each of the series.

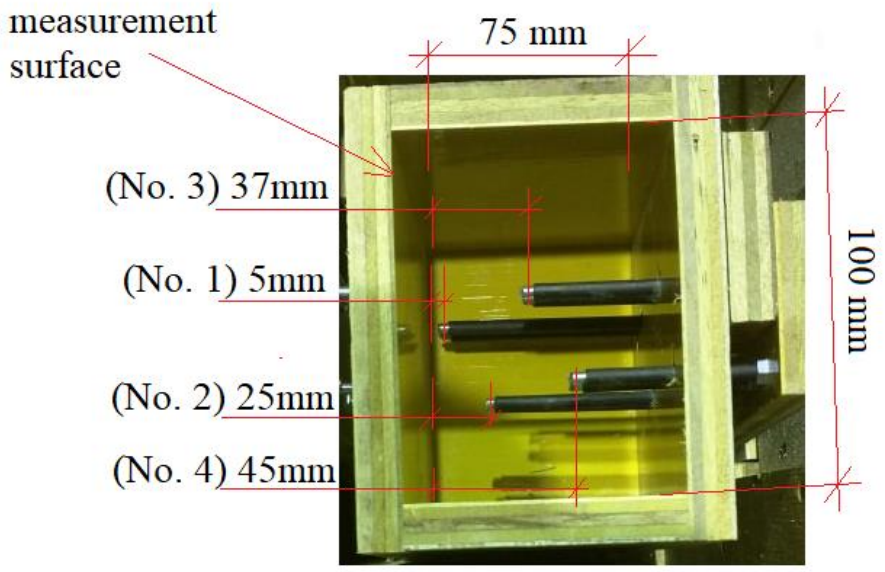

Figure 5-1 Description of prismatic specimen (no 2) showing M4 sensor locations

5.2.1.1 Moisture equilibrium at different PSDs through desorption process

For wet-to-dry path (desorption process) conditioning, one set of the prismatic specimen (3 with sensors and 6 without sensors) was saturated by complete immersion in water and step-wise drying and moisture re-distribution was carried out as follows:

- After saturation of pores by total immersion into water, the four sides of the prismatic specimens were sealed with vinyl electric insulation tape to eliminate multi-lateral moisture transfer during conditioning [1].
- The specimens were then dried for 6 hours in a controlled humidity chamber at 40ºC temperature and 50% relative humidity and moisture re-distribution (to attain moisture equilibrium throughout the volume of the specimens) was conducted by sealing the two remaining faces with a layer of polythene sheet and returning them in the controlled chamber, at the same temperature and relative humidity.

5.2.1.2 Moisture equilibrium at different PSDs through absorption process

To condition the specimens and obtain moisture equilibrium at different PSDs by dry-to-wet path (absorption process), the pore water in the permeable pore voids of a set of the prismatic specimens (3 with sensors and 6 without sensors) was emptied to its lowest possible degree by drying at a temperature of 40^{o}C and 50% relative humidity. This temperature was selected to ensure that only the water in the permeable pore voids was removed by the drying and further and to avoid inducing cracks to the specimens. After drying, the lateral sides of the specimens were sealed with vinyl electric insulation type to ensure unilateral absorption and limit speedy saturation during step-wise wetting. Thereafter, step-wise saturation by total immersion into water for 15 minutes and internal moisture re-distribution was carried out in a controlled humidity chamber at 40^{o}C temperature and 50% relative humidity. After every withdrawal from water, the surfaces were dried with a towel, the mass was recorded and the two remaining faces were sealed with a layer of polythene sheet before returning them into the controlled chamber for moisture redistribution.

On confirming moisture equilibrium at every redistribution, moisture re-distribution time was recorded, the specimens were transferred into a closed container until a temperature of 20-25^{o}C was attained by natural heat loss, and measurements were done.

5.2.2 Materials used

Tables 4-2 (see chapter 4) and 5-1 summarise the five different types of concrete used in this study, which were selected from among the commonly used concretes in Japan. The names of the specimens were coded to portray the cement type, water-binder ratio and type of curing. The type of curing adopted after placement was 28 days in mould. The prismatic specimens were measuring 150 mm x 150 mm x 75 mm. For this study, 21 prismatic specimens were prepared in total for each concrete type. Six has embedded moisture sensors to monitor the moisture during redistribution. Three prismatic specimens were used to determine the volume of permeable pore void as per

ASTM C642 and the PSD was calculated from the average (see Chapter 4, Section 4.3.3.3 for details of PSD calculation) while 12 prismatic specimens were used for SWAT and double chamber air permeability tests.

Table 5-1 Fresh and hardened properties of concrete

Specimen name	Air content (%)	Slump (cm)	Initial temperature (°C)	Volume of permeable pore voids (%)	Compressive Strength (MPa)	
					28 days	90 days
N40-28D	5.6	13.5	22	7.64	41.9	49.1
N50-28D	4.9	14	22	8.42	39.2	44.9
N60-28D	4.3	12.5	22	9.21	27.6	33.9
BB50-28D	3.5	12.5	21	8.8.5	30.6	44.1
FA41-28D	3.8	11.5	22	8.18	40.2	45.7

5.2.3 Measurements and testing

Measurements were conducted after obtaining moisture equilibrium as explained in two sub-sections above. As earlier mentioned, the specimens were first allowed to cool down in a closed chamber to a temperature between 20 to 25°C (to eliminate the influence of temperature on the values of the surface moisture testers) before the sealing materials were removed. The following measurements were sequentially conducted, and the obtained values recorded:

i. Internal moisture distribution by HI-800 (see Chapter 3, Section 3.2.4.1 and Table 3-3 in Chapter 3) for specimens with embedded moisture sensors
ii. Mass of the specimen by AND GX-10K balance with a sensitivity of 0.01g
iii. Moisture content by HI-100 for specimens without embedded moisture sensors (see Chapter 4, Section 4.3.3.1 and Table 3-3 in Chapter 3 for details of HI-100)

iv. Moisture content by HI-520-2 for specimens without embedded moisture sensors (see Chapter 4, Section 4.3.3.1 and Table 3-3 in Chapter 3 for details of HI-520-2)

v. Moisture content by CMEX II for specimens without embedded moisture sensors (see Table 3-3 in Chapter 3 for details of CMEX II)

vi. SWAT on 3 specimens without embedded moisture sensors (see Chapter, Section 2.6.2 for details of SWAT)

vii. Double chamber air permeability tests on 3 specimens without embedded moisture sensors (see Chapter, Section 2.6.4 for details of double chamber air permeability test)

PSD at each measurement time was deduced through the volumes of permeable pore voids as per the ASTM C642 from the mean value of 3 prismatic specimens (see Chapter 4, Section 4.3.3.3 for details of PSD calculation).

5.3 Results and discussions

Figure 5-2 shows the drying and redistribution curves. Internal moisture distribution was monitored at regular intervals until it reached equilibrium and redistribution time was recorded. The mass change was noted and PSD was calculated with equation 4-4, defined as a percentage of pore voids.

It can be noticed that while the moisture redistribution time varied with the type of cement and water-to-binder content, it was similar for OPC concretes when saturation was above 80% PSD, as it refers to the emptying of the large capillary pores. For all the concrete types, moisture redistribution time rapidly increased in multiple orders as drying time increased, revealing that; as drying of the pore water approaches the smaller pores, even much longer time is required for the movement of pore water in smaller pores during redistribution.

5.3.1 Effects of desorption and absorption processes

5.3.1.1 Influence of desorption and absorption processes on SWAT

The result of the ongoing experimental investigation of the rate of water absorption measured by SWAT at different percentage saturation degrees of permeable pore voids obtained through desorption (wet-to-dry) process and absorption (dry-to-wet) process is shown in Figure 5-3.

Although the results shown in Figure 5-3 have not yet covered Contrary to the expectation, the resulting trend shows no visible effects of desorption and absorption processes on the rate of surface water absorption by SWAT. Significant moisture hysteresis that occurs between desorption and sorption over RH range and the well-documented influence of moisture history on equilibrium moisture content [2]–[4] does not seemingly affect the rate of water absorption measured by SWAT. A possible explanation might be the elimination of the ink-bottle effect by preconditioning the entire concrete volume to moisture equilibrium [5] before SWAT measurement.

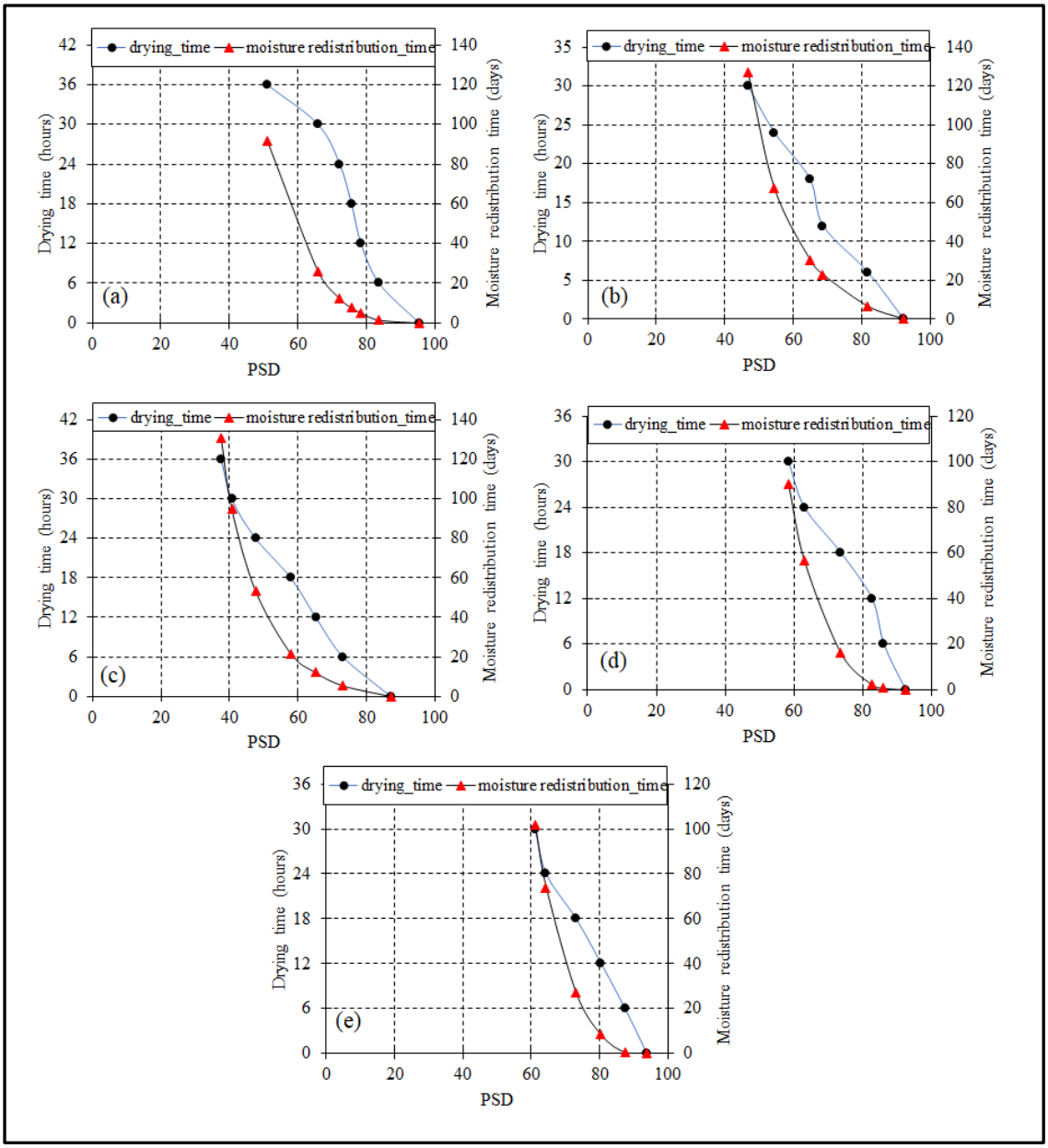

Figure 5-2 Drying and redistribution curves (a) N40-28D (b) N50-28D (c) N60-28D (d) BB50-28D (e) FA41-28D

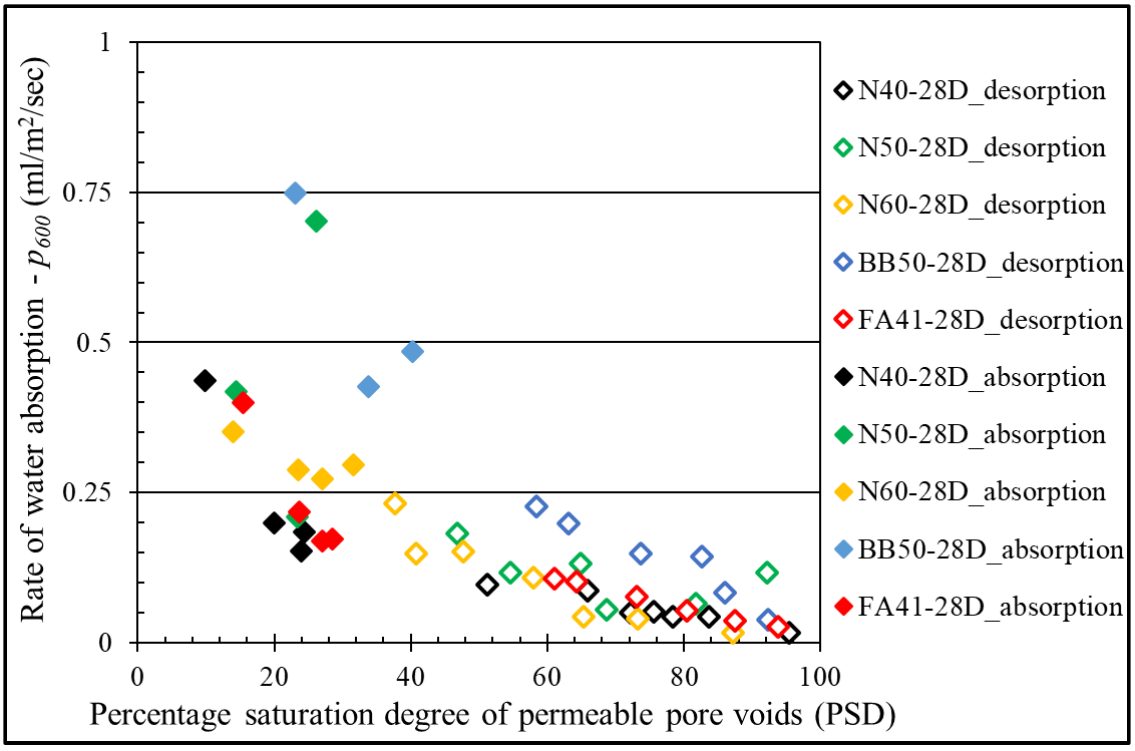

Figure 5-3 Rate of surface water absorption- p_{600} for desorption (wet-to-dry) process and absorption (dry-to-wet) process preconditioned concretes at different percentage saturation degrees of permeable pore voids

5.3.1.2 Influence of desorption and absorption processes on air permeability

It is defining and clear that the coefficient of air permeability- kT value is not affected by the path of preconditioning applied to obtain a particular pore void saturation of concrete expressed in PSD as shown in Figure 5-4.

Although the PSD range for each preconditioning path does not yet cover the entire pore void saturation degrees, the trend can be seen from Figure 5-5 that the kT values against the PSDs for the same concrete mix obtained through desorption and absorption preconditioning processes follow the same linear approximation line. For both preconditioning processes and in all concrete types, kT values increase linearly with a decrease in the PSD. The trend is more pronounced for the N60-28D concrete

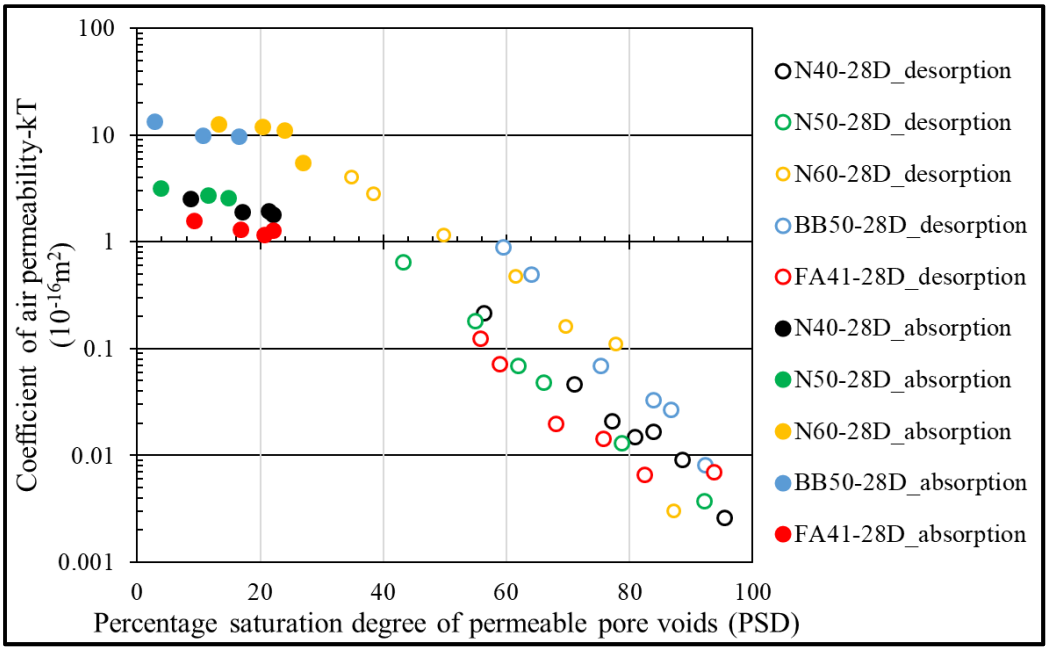

Figure 5-4 Coefficient of air permeability-*kT* for desorption (wet-to-dry) process and absorption (dry-to-wet) process preconditioned concretes at different percentage saturation degrees of permeable pore voids

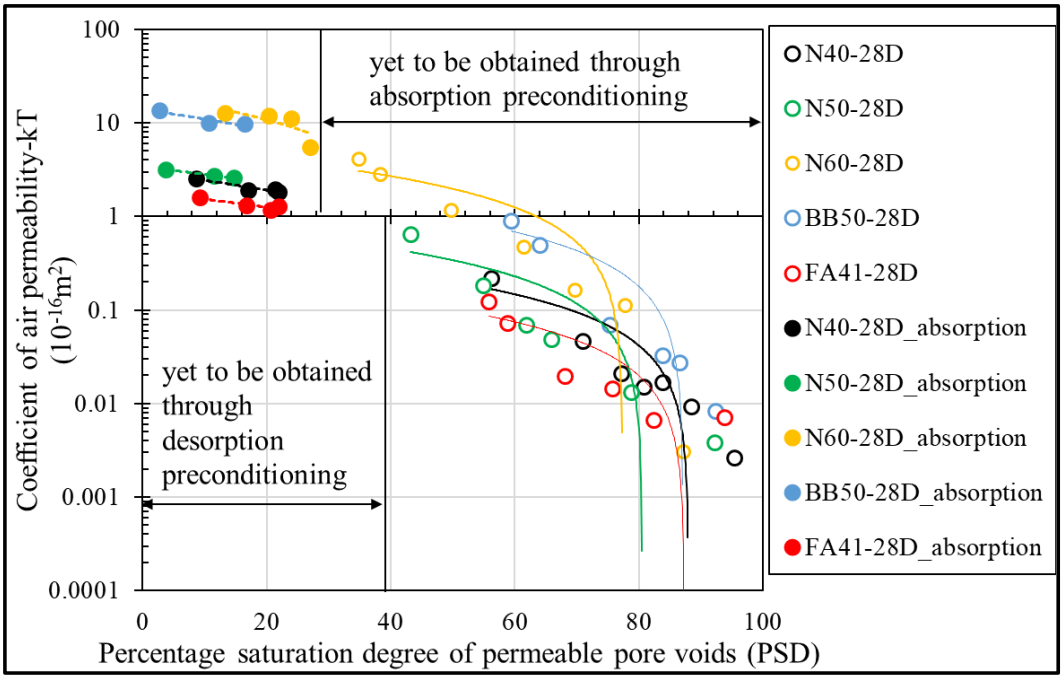

Figure 5-5 Linear approximation line of *kT* values for desorption (wet-to-dry) process and absorption (dry-to-wet) process preconditioned concretes at different percentage saturation degrees of permeable pore voids

5.3.1.3 Influence of desorption and absorption processes on kett HI-100

Figure 5-6 shows HI-100 count values against PSD for equilibrium moisture content by desorption and absorption condition processes for five different concrete types (N40-28D, N50-28D, N60-28D, BB50-28D and FA41-28D). It can be noticed that the influence of moisture history on equilibrium moisture content was not significant on the plot of HI-100 count values against the saturation degree of permeable pore voids-PSD for equilibrium moisture content by desorption and absorption condition processes. Also, the moisture contents (in count values) obtained from both desorption and absorption processes are convergent and similar between 30 % PSD to 40% PSD, which is the intersection for the moisture contents obtained from the two pre-conditioning processes. The negligible effects showing in the difference between the independent approximation lines and the common approximation and non-convergent of points in Figure 5-6 may be an indication of different ionic concentrations in the pore water of the 5 kinds of concrete in the plot since kett HI-100 is an electric resistance-based moisture meter, which is affected by the ionic concentration of pore water [6].

Furthermore, the test results in Figures 5-7 and 5-8 indicated a good coherence on the equilibrium moisture contents from the preconditioning processes. Both the rate of water absorption (Figure 5-7) and the coefficient of air permeability (Figure 5-8) showed good correlations with HI-100 count values.

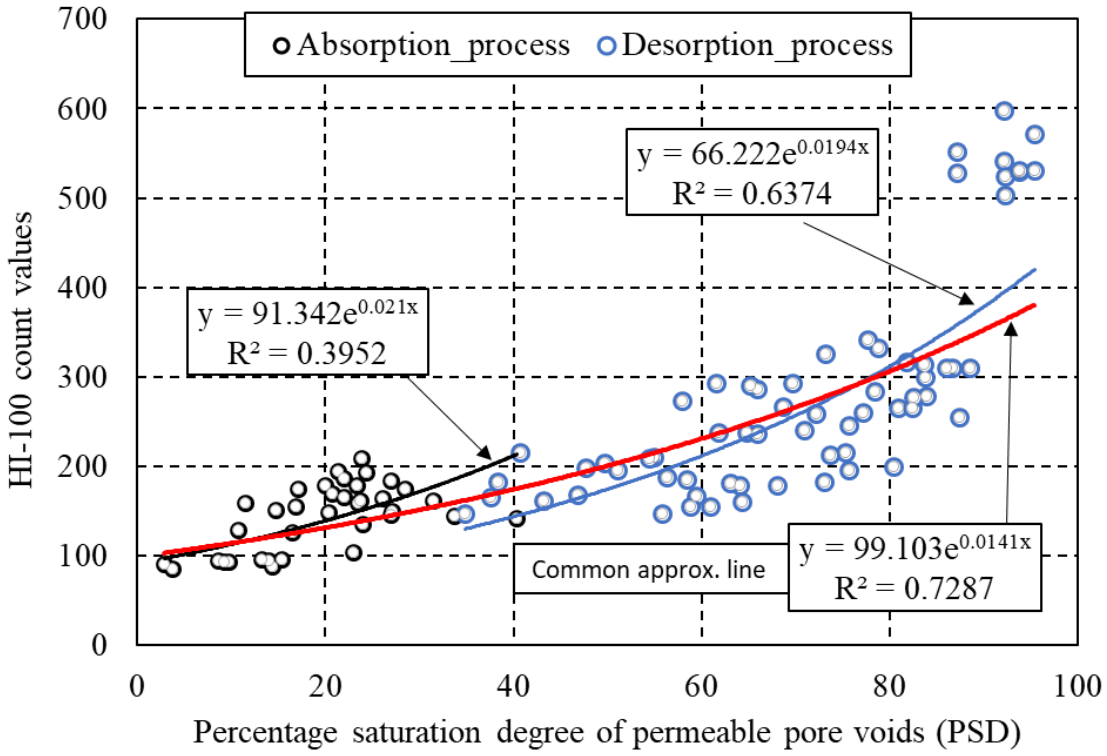

Figure 5-6 HI-100 count values against PSD for equilibrium moisture content by desorption and absorption condition processes

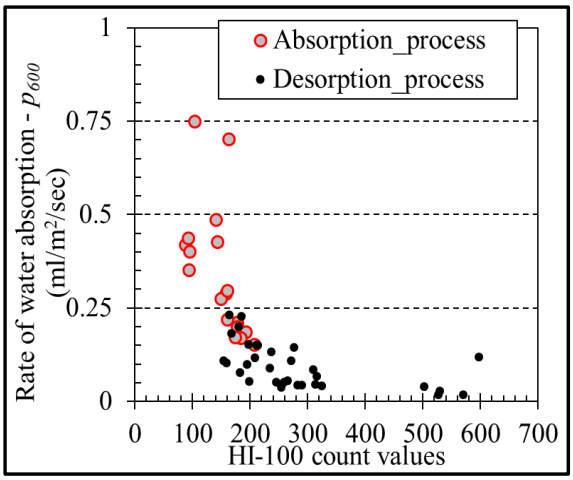

Figure 5-7 P_{600} against moisture content by HI-100 moisture meter

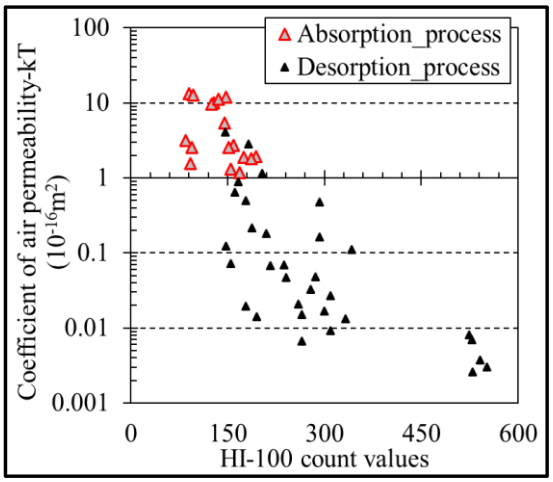

Figure 5-8 kT values against moisture content by HI-100 moisture meter

5.3.1.4 Influence of desorption and absorption processes on kett HI-520-2

Similar to Figure 5-6, the equilibrium moisture content by HI-520-2 (in %) obtained through desorption and absorption condition processes for five different concrete types (N40-28D, N50-28D, N60-28D, BB50-28D and FA41-28D) is shown in Figure 5-9. As could be noticed, desorption and absorption processes do not affect the moisture measured by HI-520-2. Furthermore, a good correlation is obtained between the rate of water absorption measured by SWAT and the equilibrium moisture contents as shown in Figure 5-10. Also, Figure 5-11 showed a good relationship between the coefficient of air permeability and the equilibrium moisture contents.

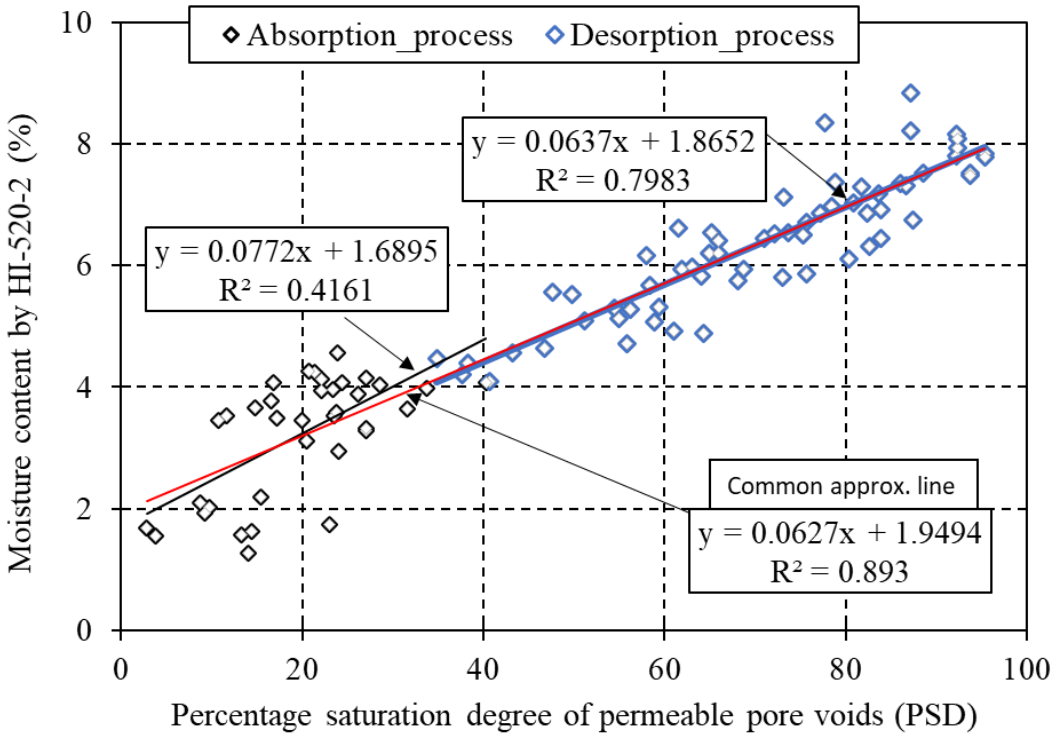

Figure 5-9 HI-520-2 moisture content against PSD for equilibrium moisture content by desorption and absorption condition processes

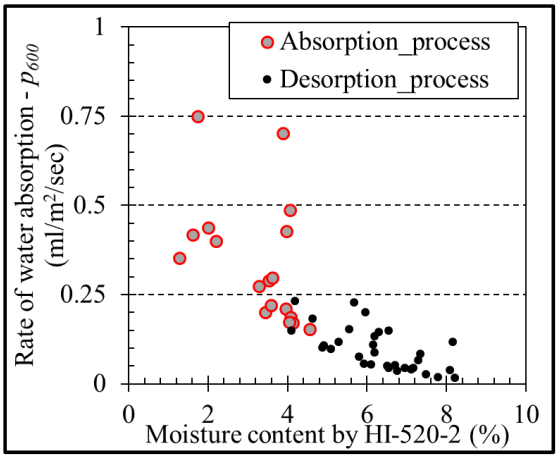

Figure 5-10 P_{600} against moisture content by HI-520-2 moisture meter

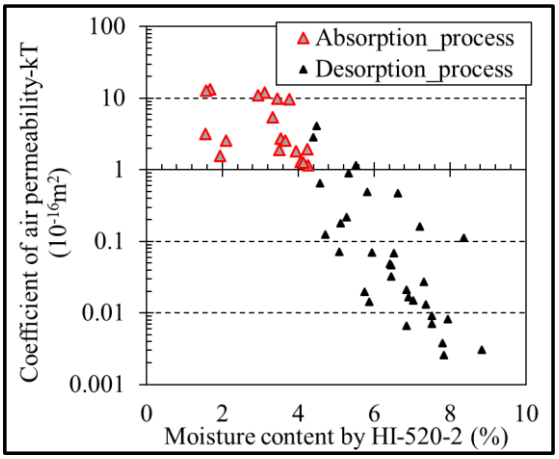

Figure 5-11 kT values against moisture content by HI-520-2 moisture meter

5.3.1.5 Influence of desorption and absorption processes on CMEX II

As can be noticed in Figure 5-12, CMEX II moisture meter is not effective in detecting the moisture contents of concrete towards the two extremes of pore void saturation, below 18% PSD and above 88% PSD. This resulted in poor relationships between the rate of water absorption and CMEX II moisture content, the coefficient of air permeability and CMEX II moisture content shown in Figure 5-13 and Figure 5-14 respectively. In reality, extreme dryness of covercrete (below 20% PSD) might not be observed- particularly in non-dessert areas, but covercrete could be saturated up to 88% PSD and above after rainfall and remain same for several hours. Nonetheless, no significant influence of the desorption and absorption processes was noticed on equilibrium moisture content measured by CMEX II.

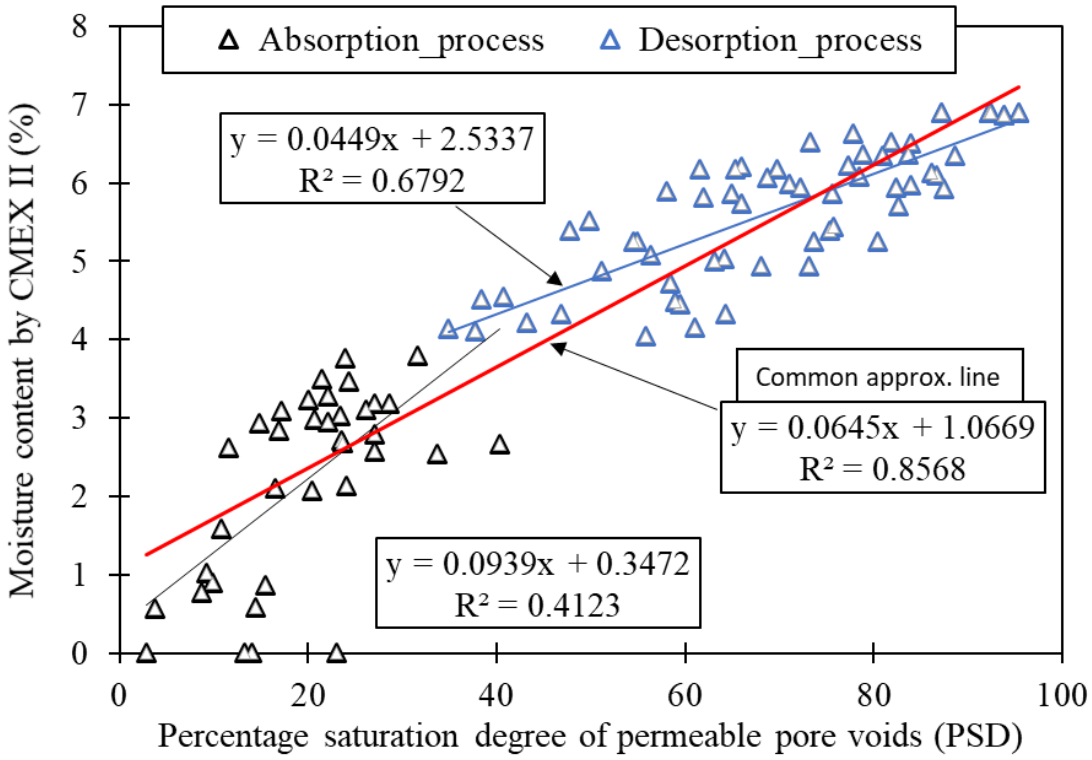

Figure 5-12 CMEX II moisture content against PSD for equilibrium moisture content by desorption and absorption condition processes

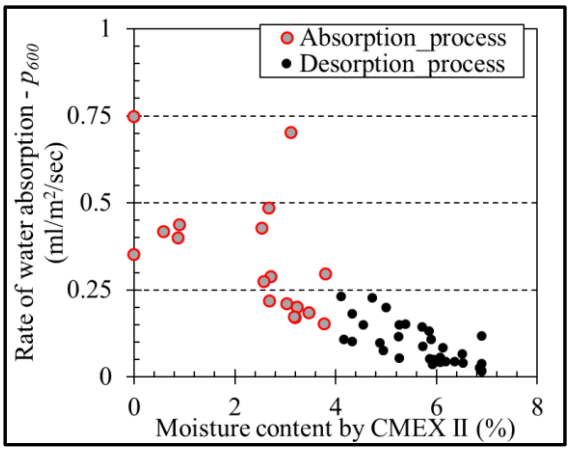

Figure 5-13 P_{600} against moisture content by CMEX II moisture meter

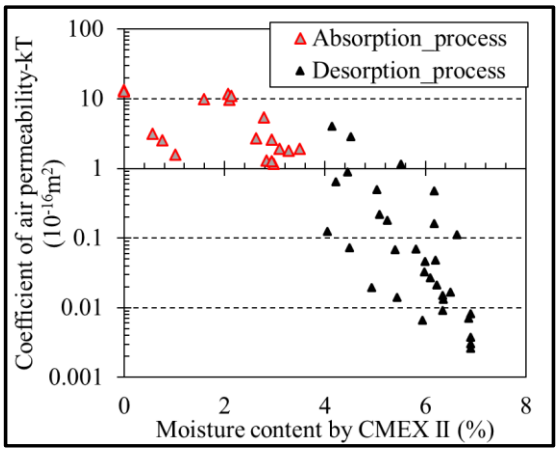

Figure 5-14 kT values against moisture content by CMEX II moisture meter

5.4 Summary of findings

To study the influence of hysteresis on SWAT, double chamber air permeability test and surface moisture meters, five types of concrete were preconditioned to moisture equilibrium at several percentage saturation degrees of permeable pore voids (PSDs) through desorption and absorption processes. Based on the experimental results and the analysis of the data, the following findings have been made:

- There is no influence of hysteresis on the rate of water absorption, p_{600} by SWAT for OPC concrete with w/c contents, 40%, 50% and 60%, ground granulated blast furnace slag cement concrete (50% w/c content) and OPC/fly ash concrete (w/b 41.6%). For the same PSD, the rate of water absorption was similar for specimens from the desorption-preconditioned and absorption-preconditioned processes.
- There is no influence of hysteresis on air permeability, *kT* values by double chamber air permeability test for OPC concrete with w/c contents, 40%, 50% and 60%, ground granulated blast furnace slag cement concrete (50% w/c content) and OPC/fly ash concrete (w/b 41.6%). For the same PSD, the *kT* value was similar for specimens from the desorption-preconditioned and absorption-preconditioned processes.
- For the same PSD, moisture content from HI-100 was similar for specimens from the desorption-preconditioned and absorption-preconditioned processes. The result was similar for HI-520-2 and CMEX II moisture meters respectively. It is summarized that there was no significant effect of hysteresis on moisture contents measured by HI-100, HI-520-2 and CMEX II.

The findings in this present study revealed that there is no significant influence of hysteresis on SWAT, *kT* values and surface moisture contents for 5 types of concretes preconditioned to moisture equilibrium. The reason might be related to a previous study by [5] which explained that preconditioning concrete to moisture equilibrium eliminates the ink-bottle effects (shown to be the major cause of hysteresis [2], [3]), thus different

results might be obtained for concretes with internal moisture gradient. Nonetheless, the present study findings verify SWAT as a simple non-destructive quality evaluation method.

References

[1] C. Antón, M. A. Climent, G. de Vera, I. Sánchez, and C. Andrade, 'An Improved Procedure for Obtaining and Maintaining Well Characterized Partial Water Saturation States on Concrete Samples to be used for Mass Transport Tests', *Materials and Structures*, vol. 46, no. 8, pp. 1389–1400, Aug. 2013, doi: 10.1617/s11527-012-9981-4.

[2] K. Maekawa, A. Pimanmas, and H. Okamura, *Nonlinear Mechanics of Reinforced Concrete*. London; New York: Spon Press, 2003.

[3] K. Maekawa, T. Ishida, and T. Kishi, *Multi-scale Modeling of Structural Concrete*. London ; New York: Taylor & Francis, 2009.

[4] T. Ishida, K. Maekawa, and T. Kishi, 'Enhanced Modeling of Moisture Equilibrium and Transport in Cementitious Materials under Arbitrary Temperature and Relative Humidity History', *Cement and Concrete Research*, vol. 37, no. 4, pp. 565–578, Apr. 2007, doi: 10.1016/j.cemconres.2006.11.015.

[5] P. Rucker-Gramm and R. E. Beddoe, 'Effect of Moisture Content of Concrete on Water Uptake', *Cement and Concrete Research*, vol. 40, no. 1, pp. 102–108, Jan. 2010, doi: 10.1016/j.cemconres.2009.09.001.

[6] E. William and J. S. Erik, 'Electrical Resistivity of Concrete', Directorate of Public Roads, Norwegian Road Research Laboratory, Jun. 1995.

Chapter 6

Investigation on the Correlation between Surface Water Absorption Test (SWAT) and JSCE Sorptivity Test

6.1 Introduction

It is general knowledge that the durability of concrete depends largely on the resistance of concrete against the penetration of both liquid and gaseous deleterious substances[1]. The water absorption resistance of concrete has been the most common and the simplest index for durability assessment.

It has long been confirmed that the short-term water penetration depth of concrete has an approximately linear relationship with the square root of immersion time. Although many methods and test standards have previously been utilized to evaluate the water penetration rate of concrete, most of them are destructive and remain inapplicable in field investigations, evaluations and grading of RC structures. Recently in 2018, JSCE G-582 was established as a test standard for determining the water penetration rate coefficient of concrete subjected to water in short-term. This paper evaluates the relationship between the experimental results of JSCE-G 582 test standard and the results of the Surface Water Absorption Test (SWAT) method.

The coefficient of surface water absorption, *CSWA*, for quality evaluation by SWAT is newly introduced in this study and compared with JSCE-G 582 test results. Furthermore, conventional SWAT indices like p_{600} and total absorption amount are also compared with JSCE-G 582 test results. In this paper, the applicability of SWAT is evaluated for evaluating water absorption resistance in a short time.

6.2 Investigation method

6.2.1 JSCE-G 582 test standard

The 2018 JSCE G-582 described in 2.5.3 was applied to determine the water penetration rate coefficient of the concretes.

6.2.2 SWAT

SWAT described in 2.6.2 was applied in investigating the water penetration resistance of the concretes.

6.2.3 Coefficient of water absorption

Sorptivity is often determined from the gradient of the straight line obtained by plotting the cumulative water absorption per unit area against the square root of time[1]. It is often observed that the straight lines hardly pass through the origin, either with a negative intercept or with a positive intercept. Reasons for negative intercepts have been attributed to the dense surface layer and a slight delay in the start of timing, while for the positive intercept, a slightly early start of timing [1], [2].

The approach to the coefficient of water absorption by SWAT is the same with sorptivity, which is the slope from a linear regression obtained by plotting the cumulative water absorption per unit area against the square root of time. Modifications are applied to linear regression lines when intercepts at the origin are seen, as noted [1] that one-dimensional water absorption data usually produce an intercept at $t = 0$. Thus, the general equation defining one-dimensional water absorption is more correctly written as:

$$i = St^{1/2} + B \qquad [5\text{-}1]$$

where i: cumulative absorbed volume of water per unit area of supply surface, S: sorptivity, t: time and B accounts for the negative or positive intercept.

6.3 Experimental programme

6.3.1 Materials used

Concrete specimens were prepared with ordinary Portland cement (OPC), ground granulated blast furnace slag cement (JIS type B slag cement) and JIS type II fly ash (FA) as 20% by weight of OPC replacing fine aggregate. Tables 4-2 and 5-2 (in chapter 4 and chapter 5 respectively) show the concrete mix proportion and fresh properties of the concrete. For each of the concrete mix designs, 15 cylindrical specimens (ϕ100 mm × 200 mm) were prepared among which 9 specimens were used for JSCE-G 582 and 6 specimens were used for compressive strength tests. 3 prismatic specimens (100 mm × 100 mm × 75 mm) were prepared for SWAT.

The concrete specimens were named as OPC_40 for OPC concrete 40% W/C, as OPC_50 for OPC concrete 50% W/C, as OPC-60 for OPC concrete 60% W/C, as BB_50 for BB cement concrete 50% W/C and as FA_50 for OPC plus FA concrete 41.6% W/B.

After casting, the specimens were sealed and kept in a controlled environment with a temperature of 20ºC and relative humidity of 60% for 28 days before demolding. Thereafter, the specimens were further left in the same controlled environment at the same temperature and humidity until 60 days after casting before test preparations and actual tests were conducted.

6.3.2 Sample preparations and test methods

6.3.2.1 Conditioning for JSCE-G 582 test

For each mix design, 9 cylindrical specimens were prepared for JSCE-G 582 test for water penetration rate coefficients. The steps for sample preparations were per JSCE-G 582 2018 test method. To reduce the time for the preparation of the specimens, the drying time adopted in this study was 28 days drying at a temperature of 40 ± 2ºC and relative humidity of 30 ± 5%. Aluminum tape and epoxy resin were used for sealing the lateral sides and the surface that was not exposed by cutting.

The moisture penetration tests were also conducted following JSCE-G 582 2018 standard. The spacers used were point ended (Figure 6-1) to ensure that they do not occupy up to 10% of the surface area of the specimen. For each specimen, 4 spacers were placed as illustrated in Figure 6-2. The measurements were conducted at 5 hours, 24 hours and 48 hours respectively. For each measurement time, 3 specimens were measured for each of the concrete mix designs. The immersion was done in a controlled room of 20 ± 2°C temperature and relative humidity of 60 ± 5%. The steps for measurements were as follows:

The specimen was split into two halves with a compressive strength testing machine. The water penetration depths were taken at five locations, L1-L5, from one half of the split specimen with a vernier caliper. The recorded measurements close to the edges (sealed sides) of the specimen were taken at a distance, 20 mm from the edge of the specimen. The water penetration depths (as shown in Figure 6-4) were determined by spraying a colour-differentiating water dictator, which corresponds to the NDIS 3423 method.

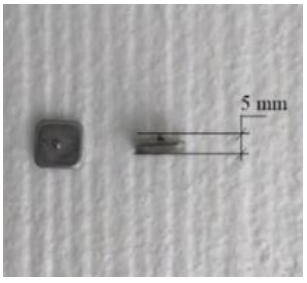

Figure 6-1 Spacer

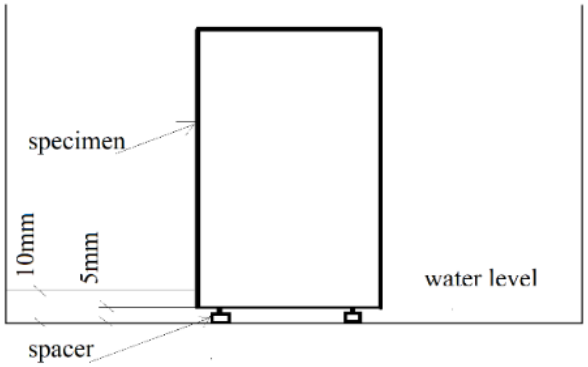

Figure 6-2 Illustration of the placement of the spacers

6.3.2.2 Conditioning for Surface Water Absorption Test

Before cutting and removing the 25 mm thickness from the face of the form-finished-surface of the cylindrical specimens, SWAT was conducted after 60 days of casting. The surface moisture contents were measured by kett HI-100 and recorded

before SWAT. The same measurements were taken at the exposed surface after cutting out the 25 mm. The SWAT measurements on the cylindrical specimens were not utilized in evaluating the correlations between the two test methods. They were conducted to elucidate the influence of surface moisture content on SWAT.

The SWAT conducted on the prismatic specimens were utilized to evaluate the correlation between the two test methods. The prismatic concrete specimens were first exposed to sun drying to reduce the surface moisture content below the threshold for appropriate measurement of SWAT. The threshold value of HI-100 count value of 210 has been previously established by the authors which show sufficient dryness of surface covercrete ensuring accurate covercrete quality evaluation by SWAT [3].

6.3.2.3 Surface moisture content

The surface moisture content of concrete was measured with kett HI-100 moisture tester. The Kett HI-100 surface moisture meter (which is based on the measuring principles of electrical resistivity) results are displaced in percentage (0-6%) or count values (40-990 counts). The count values have been shown to have an inverse linear relationship with electrical resistance. The advantage of this surface moisture meter over others is the ability to measure moisture content up to the depth of 5mm from the surface, which was confirmed by Komatsu et al, where a kett HI-100 revealed a higher correlation with the electric resistivity at the depth of 5 mm from the surface[4]

6.3.2.4 Compressive strength test

The strength development for the concrete specimens was investigated by compressive strength tests at 28 days and 90 days respectively. Results were averaged values from three ϕ100 mm x 200 mm cylindrical specimens.

6.4 Results and discussions

6.4.1 Strength development of concrete

Figure 6-3 shows the compressive strength of the concretes at 28 days and 90 days. It is apparent that the applied curing condition enhanced the hydration which resulted in good strength development of the concretes.

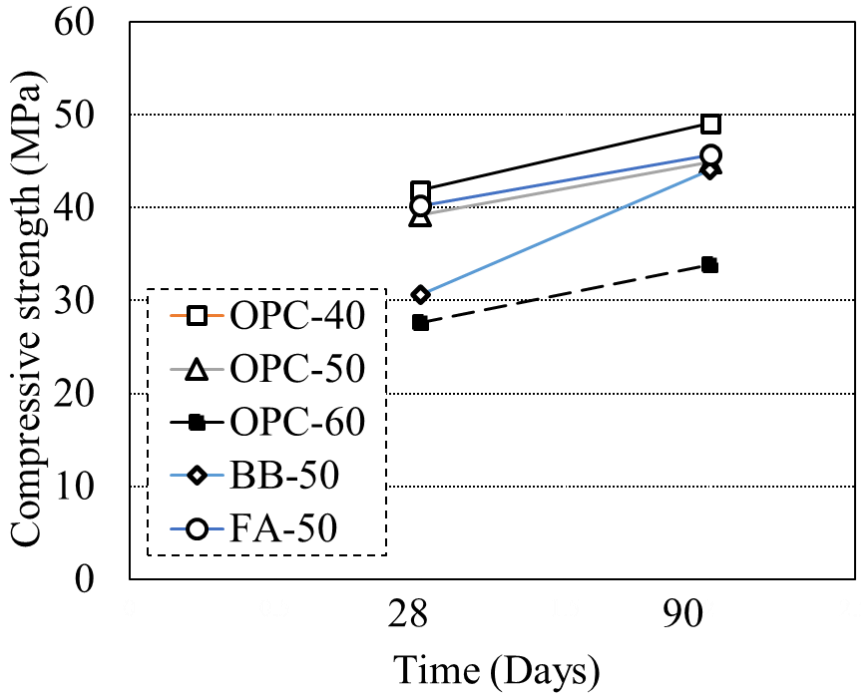

Figure 6-3 Compressive strength of the concrete specimens

6.4.2 Water penetration rate coefficient- *A*

Figure 6-4 shows the waterfront observed by spraying the colour-differentiating water dictator for the measurement of the depths of moisture penetration for the three measurement times.

(a)

(b)

(c)

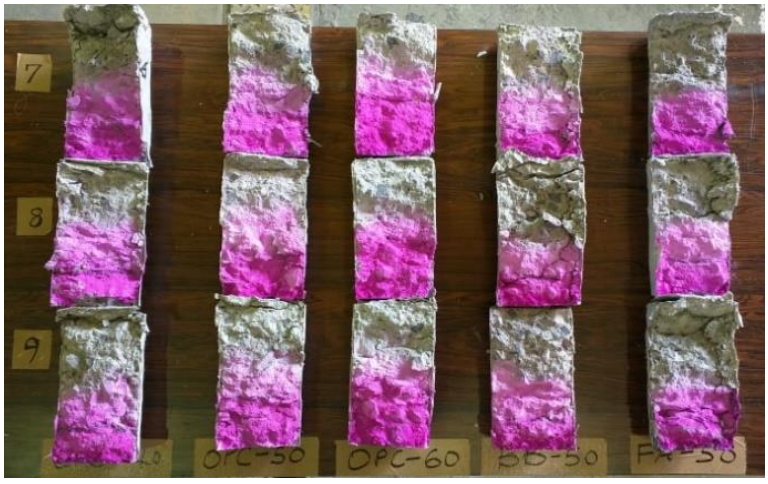

Figure 6-4 (a) 5-hours water penetration depth (b) 24-hours water penetration depth (c) 48-hours water penetration depth

Table 6-2 shows the respective average penetration depths at 5 hours, 24 hours and 48 hours for the concrete specimens, the water penetration rate coefficient-A and the constant- B, obtained from JSCE-G 582 test. Just as expected, the penetration depth increased with immersion time and with the increase in W/C for OPC concretes. It can be inferred that the performances of BB_50 and FA_50 in resistance to moisture penetration were almost the same throughout the measurement. Table 6-1 revealed that the progress of penetration depth of BB concrete between 24 hours and 48 hours was very small compared to those of other concretes. This could be attributed to the discontinuity of pore connections of inside concrete of BB concrete resulting from the continuous hydration. This is evident in its time-dependent strength development shown in Figure 6-3.

Table 6-1 The average moisture penetration depth and the moisture penetration rate coefficients of concrete

Type of concrete	Average Depth of Moisture Penetration (mm)						A: Moisture Penetration Rate Coefficient (mm/$\sqrt{hr}$)	B: Constant
	5 hours		24 hours		48 hours			
	Measured	L=A.$\sqrt{t}$+B	Measured	L=A.$\sqrt{t}$+B	Measured	L=A.$\sqrt{t}$+B		
OPC-40	20.2	21.1	34.7	33.0	42.2	41.8	4.4	11.4
OPC-50	27.2	28.8	47.1	43.9	56.1	55.1	5.6	16.5
OPC-60	30.2	31.4	55.8	54.6	72.0	71.8	8.6	12.5
BB-50	19.4	22.8	34.7	31.7	38.2	38.3	3.3	15.5
FA-50	20.7	22.2	33.5	31.9	39.1	39.1	3.6	14.3

6.4.3 Coefficient of water penetration

From the linear regression of the plot of penetration depth (mm) over the square root of immersion time (in hours) shown in Fig. 6-5, the coefficient of water penetration was deduced and its relationship with the moisture penetration rate coefficient-A by JSCE-G 582 2018 as explained in equation (1) is shown in Fig. 6-6. A good correlation exists between the two indices, proving that the slope from the regression line is a good index.

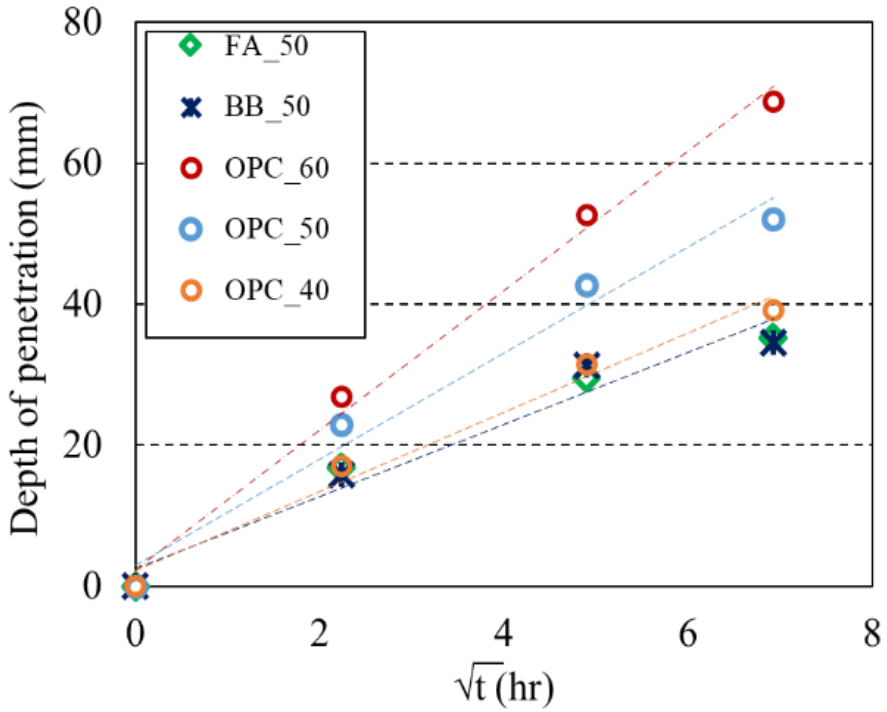

Figure 6-5 Linear regression of penetration depth over the square root of immersion

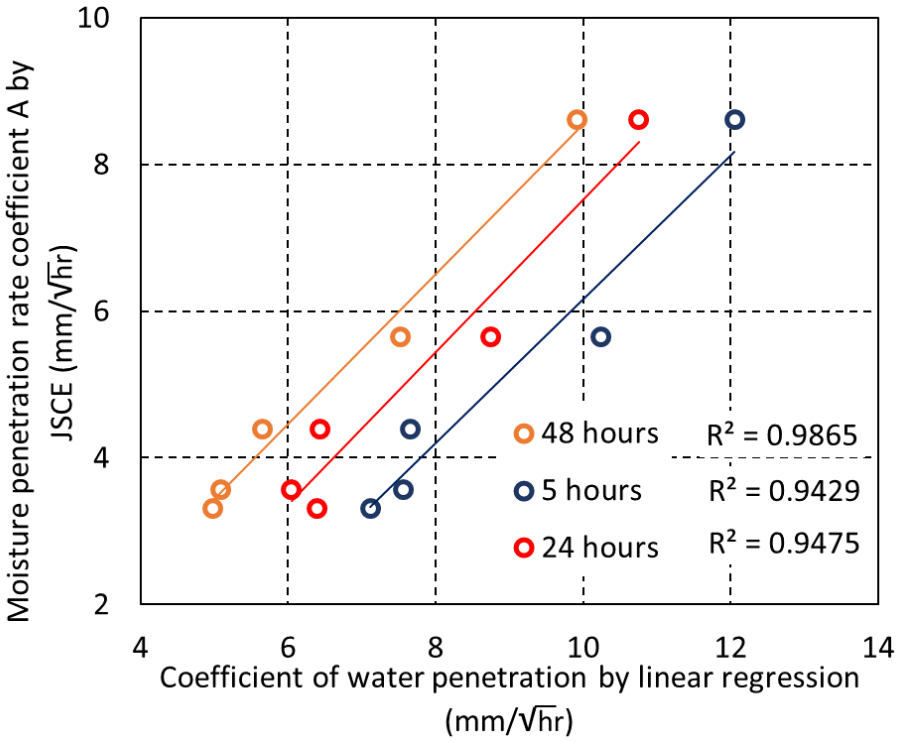

Figure 6-6 Moisture penetration rate, A versus coefficient of water penetration

5.4.4 Coefficient of surface water absorption- CSWA

Figure 6-7 shows the SWAT result (p_{600}) against the surface moisture content for the cylindrical specimens measured at 60 days. The moisture content estimated from the count values obtained from HI-100 moisture meter was much higher than the threshold value proposed by the authors even after 60 days of casting in this research. Threshold value is the maximum moisture content (210 count value of HI-100 moisture meter) beyond which the moisture content of concrete adversely affects the appropriate quality evaluation of covercrete. SWAT was conducted for these relatively wet concretes, whose results did not represent the actual evaluation of the covercrete quality of the concrete[3].

On the other hand, in Figure 6-8 (from prismatic specimens), SWAT result (p_{600}) shows much higher values than in Figure 6-7 due to lower HI-100 count values. It is thought that the results of SWAT in Figure 6-8 with HI-100 count values lower than the threshold value of 210 exhibits the actual covercrete quality. Another clear indication of the accuracy of the evaluation is the visible effect of W/C in OPC concretes.

The coefficients of surface water absorption by SWAT (CSWA) were deduced from the linear regression shown in Figure 6-9. CSWA was obtained by dividing the cumulative water absorption (in ml/m^2) at 600 seconds (after the starting of SWAT measurement) by the square root of the measurement time (in seconds). Intercept C explained in equation 3 is taken as zero. Figure 6-10 shows the relationship between p_{600} and CSWA at different measurement timings. It can be seen that a good correlation exists between the two indices. A new index of SWAT, CSWA can effectively be applied in the reduction of SWAT measurement time for the evaluation of covercrete quality of existing RC structures

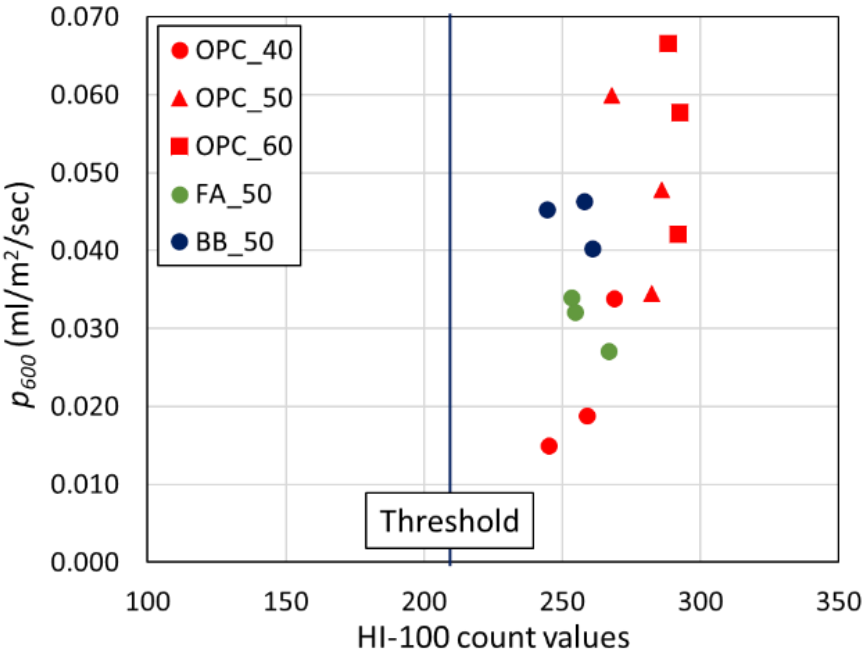

Figure 6-7 p_{600} versus HI-100 count values of the cylindrical specimens after 60 days of casting

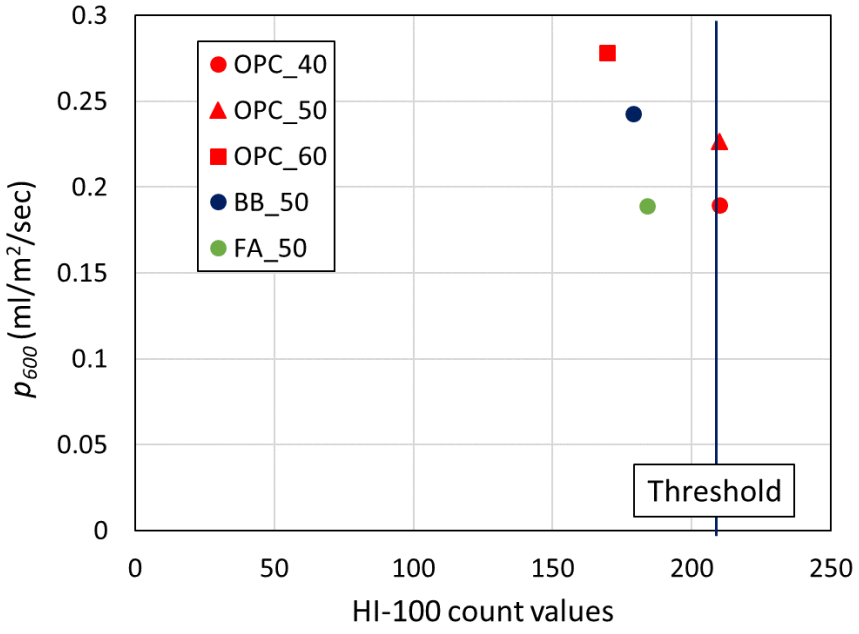

Figure 6-8 p_{600} versus HI-100 count values of the prismatic specimens

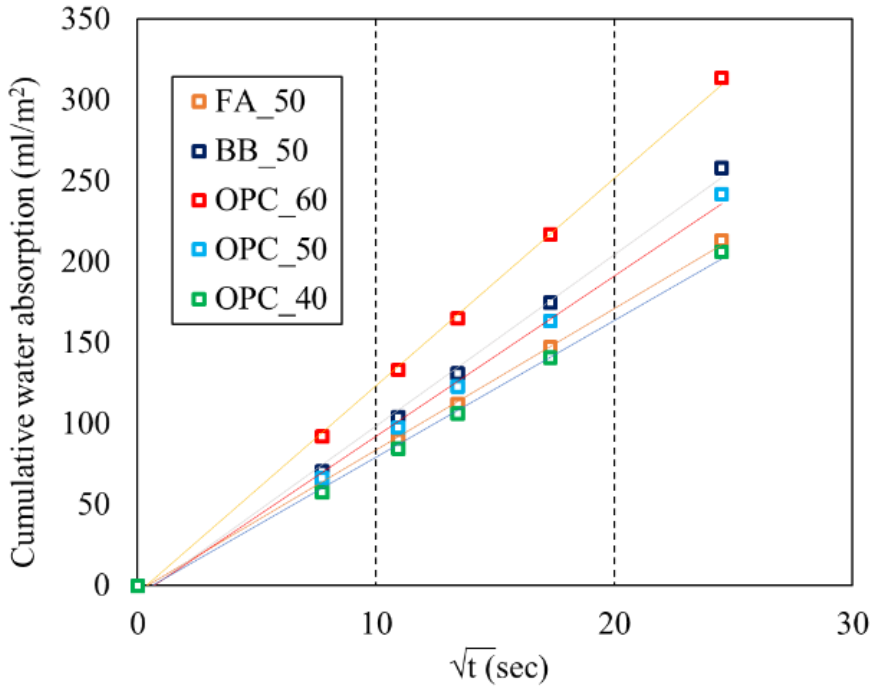

Figure 6-9 Linear regression of cumulative water absorption by SWAT

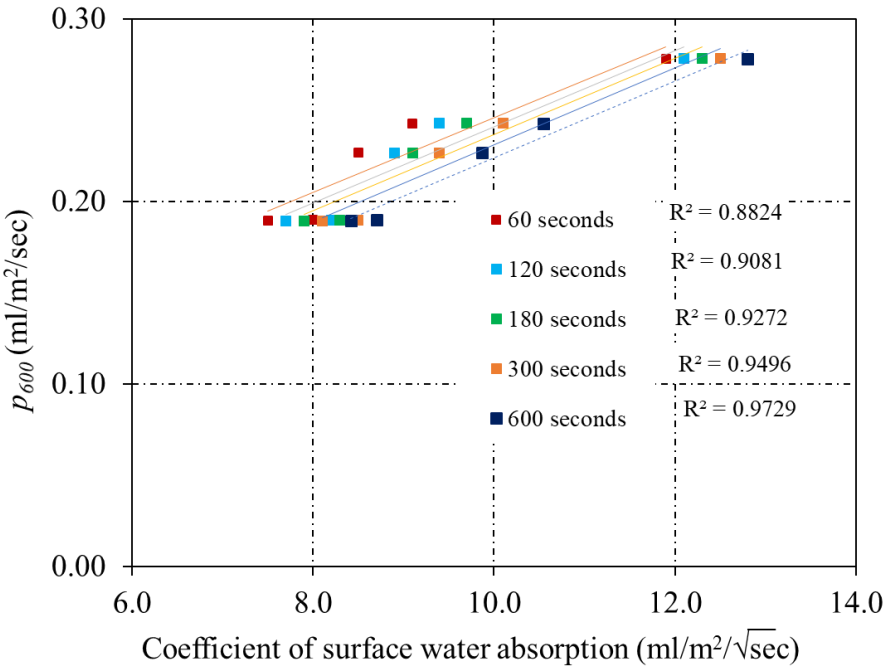

Figure 6-10 Relationship between p_{600} and coefficient of surface water absorption

6.4.5 Relationship between the two test methods

In the case of SWAT, concrete quality is evaluated by measuring the resistance against water absorption in 10 minutes. In this research, SWAT was conducted before removing 25mm thickness from the bottom surface of cylindrical specimens, therefore coarse aggregate was not exposed. On the other hand, in JSCE-G 582 test, 25 mm thickness of concrete was removed from the bottom surface before conditioning and subsequent measurement thereby included the direct influence of exposed aggregate on water absorption. Furthermore, JSCE-G 582 requires long-term drying of specimens to achieve almost steady weight and also requires destructive tests until 48 hours after starting water penetration. Due to the destructive nature of the JSCE-G test result, it can not be applied for the evaluation of covercrete quality of actual structures.

Figure 6-11 shows the relationship between the coefficient of surface water absorption- *CSWA* from SWAT results and the coefficient of water penetration from JSCE-G 582 test results. From this figure, it is shown that the moisture coefficient of water penetration by the JSCE-G 582 test and *CSWA* are correlated with a correlation coefficient of 0.78. A high p-value of 0.12 can be seen from the result. Similarly, Figure 6-12 is showing, the cumulative water absorption from SWAT against the depth of penetration from the JSCE-G 582 test, where a correlation exists with a correlation coefficient of 0.80. A similar p-value of 0.11 was revealed.

SWAT and JSCE-G 582 results have good correlation, however, the number of data is limited at present, and further investigation is necessary. Especially, BB concrete is showing much higher resistance against water absorption in JSCE method than in SWAT, which might be related to the denseness of inner concrete where SWAT is not sensitive.

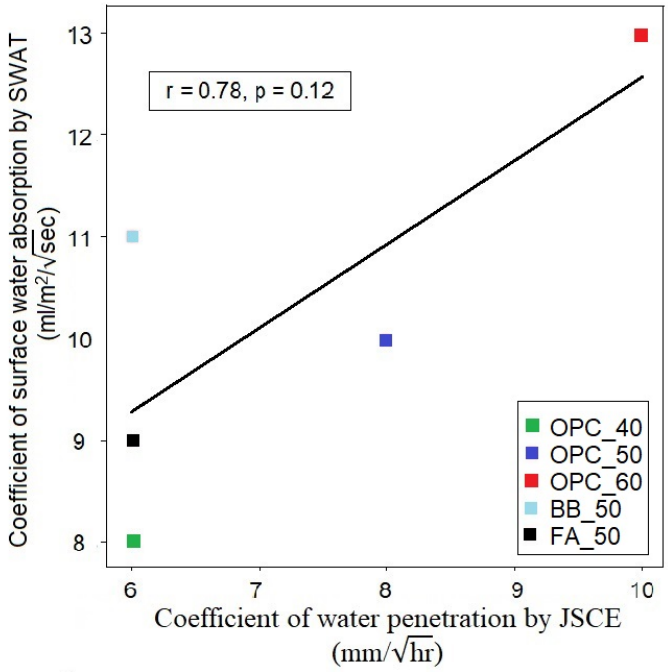

Figure 6-11 Correlations between *CSWA* and coefficient of water penetration by JSCE

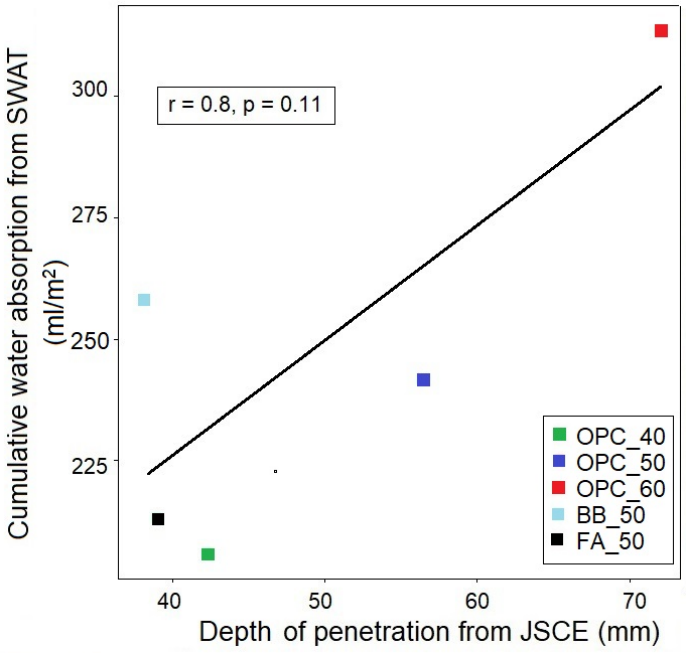

Figure 6-12 Correlations between cumulative water absorption from SWAT and depth of penetration from JSCE-G 582

6.5 Summary of findings

This study investigated the correlations between SWAT and the JSCE-G 582 test standard, and proposed a new SWAT quality grading index, by utilizing concrete mixtures with varying cement types (OPC, BB and FA) and W/B content (40%, 41.6%, 50% and 60%). The following conclusions can be drawn:

- A correlation exists between the coefficient of surface water absorption-*CSWA* by SWAT and the coefficient of water penetration by JSCE-G 582 test with a correlation coefficient of 0.78. Similarly, a correlation exists between the cumulative water absorption from SWAT and the depth of penetration from the JSCE-G 582 with a correlation coefficient of 0.80. This implies that any of the two indices from SWAT could effectively be applied to evaluate the resistance of concrete to moisture penetration without going through the destructive and rigorous process of calculating the moisture penetration rate. However, the number of data is quite limited, so further investigation is necessary.
- The coefficient of water penetration from JSCE-G 582 which was obtained from the slope by linear regression has a good linear relationship with the moisture penetration rate coefficient obtained by JSCE-G 582 calculation formula, A.
- Compared to other concretes, BB concrete showed much higher resistance against water absorption in JSCE method than in SWAT, which might be related to the denseness of inner concrete where SWAT is not sensitive.

References

[1] M. A. Wilson, M. A. Carter, and W. D. Hoff, 'British Standard and RILEM Water Absorption Tests: A Critical Evaluation', *Mat. Struct.*, vol. 32, no. 8, pp. 571–578, Oct. 1999, doi: 10.1007/BF02480491.

[2] R. J. Gummerson, C. Hall, and W. D. Hoff, 'Water Movement in Porous Building Materia.ls--II. Hydraulic Suction and Sorptlvlty of Brick and Other Masonry Materials', *Building and Environment* vol. 15 pp. 101-108, 1980.

[3] R. N. Uwazuruonye and P. A. Hosoda, 'Degree of saturation of permeable pore space at covercrete and its effects on Surface Water Absorption Test (SWAT)', *International Conference on Innovative Materials for Sustainable Civil Engineering(IMSCE),* Nanjing, China, 2019, p. 17.

[4] S. Komatsu, R. Tajima, and A. Hosoda, 'Proposal of Quality Evaluation Method for Upper Surface of Concrete Slab with Surface Water Absorption Test', *Concrete Research and Technology*, vol. 29, no. 0, pp. 33–40, 2018, doi: 10.3151/crt.29.33.

Chapter 7

Conclusions

7.1 General

This research was aimed at elucidating the effects of saturation degree of pore voids on nondestructive test assessment of concrete quality when applying durability indicators such as water absorption, air permeability and electrical resistivity. Systematic laboratory investigations were conducted, appraised by numerical simulations and the applicability of the results to quality evaluation of real concrete structures was verified. The set objectives necessary for achieving the aim follows thus:

- To establish a simplified method for preconditioning of concrete specimens to obtain uniform moisture conditions throughout the volume of the specimens.
- To propose an absolute measure and expression of moisture contents of concrete that relates to the volume of permeable pore voids, experimentally investigate its effects on resistance to water absorption of concrete utilizing Surface Water Absorption Test (SWAT), and the effects on electrical resistivity while verifying the same by numerical simulation. By this means, propose the threshold/edge values of moisture contents of concrete before starting SWAT for appropriate NDT assessment of resistance to water penetration of the covercrete.
- To verify the application of the proposed threshold/edge moisture contents for field durability assessment of covercrete quality and propose the most appropriate surface moisture meter to be used in combination of SWAT during field assessment of covercrete quality.
- To investigate the effects of moisture hysteresis on SWAT, air permeability and surface moisture contents.
- With the application of the threshold/edge moisture contents and the surface moisture meter, investigate the relationship between SWAT and JSCE-G 582

sorptivity test and establish a new NDT concrete quality grading index (via SWAT) that correlates with the destructive sorptivity test gradation.

7.2 Establishing a Simplified Method for Preconditioning of Concrete Specimen to Obtain Uniform Moisture Condition

The current section was tailored towards establishing a simplified method to obtain equilibrium moisture distribution throughout the volume of an experimental concrete specimen applying a preconditioning temperature that lest affects the microstructure and the transport characteristics of the concrete. Based on the results of the present experimental work which utilized 150 mm x 150 mm x 75 mm ninety-day old prismatic concrete specimens (ordinary Portland cement with 0.4%, 0.50% and 0.60 % water-to-cement ratio and ground granulated blast furnace slag cement-JIS type B slag cement with 0.50% water-to-cement ratio), it is concluded that the proposed steps could be used to obtain equilibrium moisture distribution throughout the volume of concrete specimens at many water saturation degrees of pore voids. At preconditioning temperature of 40^{o}C, the combination of vinyl electric insulation tape and polythene sheet as sealing materials could be used to obtain equilibrium moisture distribution in concrete specimens. The steps involve a desorption process as follows: saturate the permeable pore voids by total immersion into water, seal the lateral sides with vinyl electric insulation tape, dry at 40^{o}C to the desired weight, seal the two remaining surfaces with a layer of polythene sheet and return to 40^{o}C temperature until equilibrium moisture distribution is attained.

7.3 Percentage Saturation Degree of Permeable Pore Voids (PSD) and its Effects on SWAT and Electrical Resistivity

A new form of measurement and expression of moisture content of concrete-percentage saturation degree of permeable pore voids (PSD), which relates directly to the volume of permeable pore voids in absolute terms, was proposed and its effect on the

Surface Water Absorption Test (SWAT) and electrical resistivity were investigated. Conclusions are drawn as follows:

- There is over-estimation of moisture content of concrete when the moisture contents were measured without referencing the permeable pore voids of the concrete.
- For accurate and absolute measurement of moisture content of concrete, it is necessary to consider the percentage volume of permeable pore voids of the concrete. The boiling process is necessary for obtaining the accurate volume of permeable pore voids of concrete.
- Count values obtained from Kett HI-100 surface moisture meter, which are directly related to the electric resistance of covercrete, showed good correlations with PSD of concrete. Kett HI-100 may be utilized for detecting PSD of concrete to check whether concrete is sufficiently dried for appropriate measurement of SWAT.
- Similar to Kett HI-100, surface moisture tester, Kett HI-520-2 results showed good correlations with PSD of concrete and may also be utilized to obtain the PSD at the covercrete.
- For accurate covercrete quality evaluation when utilizing SWAT, the threshold and edge PSD should be within region B, i.e the common plateau range for all the specimens. The threshold PSD is 21% and the edge PSD is 45%PSD. For kett HI-100, the threshold and edge PSDs are 135 count values and 210 count values respectively. Similarly, the threshold and edge PSDs for kett HI-520-2 obtained from the linear function are 3.0% and 4.1% respectively. The SWAT results obtained when the surface moisture content of concrete is within this PSD range conforms with the graduation of covercrete quality shown in Table 1.

7.4 Effects of Hysteresis on SWAT, Air Permeability and Surface Moisture Contents

To study the influence of hysteresis on SWAT, double chamber air permeability test and surface moisture content, five types of concrete were preconditioned to moisture equilibrium at several percentage saturation degrees of permeable pore voids (PSDs) through desorption and absorption processes. Based on the experimental results and the analysis of the data, the following conclusions are drawn:

- There is no influence of hysteresis on the rate of water absorption, p_{600} by SWAT for OPC concrete with w/c contents, 40%, 50% and 60%, ground granulated blast furnace slag cement concrete (50% w/c content) and OPC/fly ash concrete (w/b 41.6%). For the same PSD, the rate of water absorption was similar for specimens from the desorption-preconditioned and absorption-preconditioned processes.
- There is no influence of hysteresis on air permeability, *kT* values by double chamber air permeability test for OPC concrete with w/c contents, 40%, 50% and 60%, ground granulated blast furnace slag cement concrete (50% w/c content) and OPC/fly ash concrete (w/b 41.6%). For the same PSD, the *kT* value was similar for specimens from the desorption-preconditioned and absorption-preconditioned processes.
- For the same PSD, moisture content from HI-100 was similar for specimens from the desorption-preconditioned and absorption-preconditioned processes. The result was similar for HI-520-2 and CMEX II moisture meters respectively. It is summarized that there was no significant effect of hysteresis on moisture contents measured by HI-100, HI-520-2 and CMEX II.

The findings in this present study revealed that there is no significant influence of hysteresis on SWAT, *kT* values and surface moisture contents for 5 types of concretes preconditioned to moisture equilibrium. The reason might be that preconditioning concrete to moisture equilibrium eliminated the ink-bottle effects, which has been known to cause the hysteresis loop. Thus different results might be obtained for concretes with

internal moisture gradient. Nonetheless, the present study findings verified SWAT as a simple non-destructive quality evaluation method.

7.5 Investigation of the Correlations between SWAT and JSCE Sorptivity Test

The present section centered on verifying the practical application of the threshold percentage saturation degree of permeable pore voids (threshold PSD) for quality assessment and grading of concrete. A correlative investigation of concrete's resistance to water penetration between results of the non-destructive SWAT (measured within the threshold PSD initial moisture content of unconditioned specimens) and a destructive JSCE-G 582 test standard was conducted. Also, it propounded a new SWAT quality grading index, by utilizing concrete mixtures with varying cement types (OPC, BB and FA) and W/B content (40%, 41.6%, 50% and 60%). The following conclusions can be drawn:

- A correlation exists between the coefficient of surface water absorption-*CSWA* by SWAT and the coefficient of water penetration by JSCE-G 582 test with a correlation coefficient of 0.78. Similarly, a correlation exists between the cumulative water absorption from SWAT and the depth of penetration from the JSCE-G 582 with a correlation coefficient of 0.80. This implies that any of the two indices from SWAT could effectively be applied to evaluate the resistance of concrete to moisture penetration without going through the destructive and rigorous process of calculating the moisture penetration rate. However, the number of data is quite limited, so further investigation is necessary.
- The coefficient of water penetration from JSCE-G 582 which was obtained from the slope by linear regression has a good linear relationship with the moisture penetration rate coefficient obtained by JSCE-G 582 calculation formula, A.
- Compared to other concretes, BB concrete showed much higher resistance against water absorption in JSCE method than in SWAT, which might be related to the denseness of inner concrete where SWAT is not sensitive

7.6 Recommendation for Further Research

1. The verification of the proposed pore void saturation degree threshold in this research covered a range of mix variables and simulated environmental exposures, but the scenarios were by no means exhaustive. Future work could investigate a wider range of conditions (e.g. concrete structures at different ages of production, concrete structures after exposure to freezing and thaw, concrete structures with different aggregate volume fractions) for a more comprehensive understanding of the characteristics of the combined influence of pore void saturation and pore size distribution on nondestructive tests assessment and transport properties in general.
2. Extensive numerical investigations to consider the influence of concrete temperature, environmental temperature and measurement time on the proposed threshold and plateau range is recommended for a better understanding with regards to the degree of saturation of pore voids.